UCL INSTITUTE OF CARDIOVASCULAR SCIENCE

UCL

Systemic amyloidosis by Cardiovascular Magnetic Resonance

Dr Marianna Fontana

PhD Thesis

UCL

2015

1. CONTENTS

1.1 CHAPTERS

1. Contents 2

1.1 Chapters 2

1.2 Figures 6

1.3 Tables 9

2. Abbreviations 10

3. Declaration 14

4. Acknowledgements 15

5. Abstract 16

6. Introduction 19

6.1 What is amyloid 19

6.2 Primary AL amyloidosis 20

6.3 Hereditary Transthyretin-Related Amyloidosis 21

6.4 Wild type transthyretin amyloidosis 21

6.5 Diagnosis and evaluation of cardiac amyloidosis 22

6.6 Amyloid Treatments 43

7. Research Aims 49

8. Material and Methods 50

8.1 Ethical Approval 50

8.2 Patients 50

8.3 Cardiovascular magnetic resonance protocol 53

8.4 Blood pressure and 12 lead ECG 56

8.5 Blood tests 57

8.6 Six minute walking test (6MWT) 57

7.8 Echocardiography 57

7.10 DPD scintigraphy 58

7.11 Statistical analysis 58

9. Results: Comparison of T1 mapping techniques for ECV quantification 60

9.1 Introduction 60

9.2 Hypothesis 61

9.3 Materials and Methods 61

9.4 Results 64

9.5 Discussion 66

10. Results: Native Myocardial T1 mapping in Transthyretin Amyloidosis 69

10.1 Introduction 69

10.2 Hypothesis 70
10.3 Materials and Methods 70
10.4 Results 75
10.5 Discussion 80
11. Results: Myocyte Response in AL and ATTR Cardiac Amyloidosis 85
11.1 Introduction 85
11.2 Hypothesis 86
11.3 Material and Methods 86
11.4 Results 90
11.5 Discussion 96
12. Results: Prognostic Value of Late Gadolinium Enhancement Cardiovascular Magnetic Resonance in Cardiac Amyloidosis 99
12.1 Introduction 99
12.2 Method 101
12.3 Results 105
12.4 Discussion 111
13. Discussion and Conclusion 117
13.1 Background and Hypotheses Explored: 117
13.2 Refining Clinical Applicability of ECV measurement 118

13.3 Native T1 in ATTR amyloidosis 119

13.4 Differential myocyte response in AL and ATTR cardiac amyloidosis 120

13.5 Prognostic value of LGE 121

13.6 Clinical Insights and Potential 121

13.7 Conclusion: 125

14. Publications 126

14.1 Prizes 126

14.2 Papers 127

14.3 Oral Presentations: 130

15. Bibliography 131

1.2 FIGURES

Figure 1. ECG of a patient with cardiac AL Amyloidosis. 23

Figure 2. Transthoracic echocardiogram with speckle tracking. 25

Figure 3. ^{99m}Tc-DPD scan in ATTR cardiac amyloidosis. 28

Figure 4. Extracardiac findings in patients with cardiac amyloidosis. 30

Figure 5. Left ventricular remodelling phenotypes in cardiac amyloidosis. 31

Figure 6. Late gadolinium enhancement. 35

Figure 7. T1 maps, LGE and ECV maps of a patient with aortic stenosis and a patients with cardiac amyloidosis. 38

Figure 8. Kaplan Meier survival curves for native T1 and ECV in AL amyloidosis. 42

Figure 9. CPHPC, SAP and anti-SAP antibody. 48

Figure 10. Native T1 measurement example. 62

Figure 11. Sh-MOLLI and multibreath-hold ECV correlation and Bland-Altman. 64

Figure 12. Extracellular volume (ECV) against collagen volume fraction (CVF%). 65

Figure 13. Bland-Altman: T1 values using FLASH-IR and ShMOLLI. 66

Figure 14 Examples of ROIs in ShMOLLI. 74

Figure 15. Characteristic examples from CMR scans. 76

Figure 16. Native T1 in healthy volunteers, mutation carriers, HCM, definite AL and definite ATTR. 77

Figure 17. ROC curve for native T1. 78

Figure 18. Native T1 and DPD grade. 79

Figure 19. Examples of ROIs in ShMOLLI. 89

Figure 20. Characteristic example CMRs in AL, ATTR patients and healthy volunteer. 91

Figure 21. Native T1 and ECV in healthy volunteers, definite AL and definite ATTR. 92

Figure 22. LV mass indexed, ECV, Total Amyloid Volume, Total Cell Volume in healthy volunteers, definite AL and definite ATTR. 93

Figure 23. ECV and Total Cell Volume in AL and ATTR patients divided according to the degree of cardiac involvement. 94

Figure 24. Characteristic PSIR LGE patterns in 3 AL and 3 ATTR patients. 103

Figure 25. Characteristic CMRs in 4 different patients. 104

Figure 26. Two patients with MAG and PSIR LGE reconstruction images. 107

Figure 27. LGE patterns correlation with amyloid burden. 108

Figure 28. Kaplan Meier curves for late gadolinium enhancement. 110

Figure 29. Hypothesized cardiac amyloid progression across time. 114

1.3 TABLES

Table 1. Multibreath-old T1 and ShMOLLI T1 in normal subjects and disease groups. 64

Table 2. Baseline characteristics of patients and healthy controls. 73

Table 3. Correlations between T1 and cardiac function, biomarkers, ECG and 6 MWT in ATTR and AL patients. 80

Table 4. Baseline characteristics of patients and healthy controls. 88

Table 5. Correlations between native T1 and ECV with cardiac function, biomarkers, ECG and 6 MWT. 95

Table 6. Main Clinical Characteristics, echocardiographic and ECG findings in patients with AL and ATTR amyloidosis according to the LGE pattern. 106

Table 7. CMR findings in patients with AL and ATTR amyloidosis according to the LGE pattern. 109

2. ABBREVIATIONS

6MWT	6 Minute Walking Test
AA	Amyloid (serum amyloid A)
ACE-i	Angiotensin Converting Enzyme inhibitor
AF	Atrial Fibrillation
AFD	Anderson Fabry's disease
AHA	American Heart Association
AL	Amyloid Light-chain
ANOVA	Analysis of Variance
ANP	Atrial Natriuretic Peptide
ApoA1	Apolipoprotein A1
ARB	Angiotensin Receptor Blocker
AS	Aortic stenosis
ASCT	Autologous Stem Cell Transplant
ATTR	Amyloid Transthyretin
AV	Atrioventricular
AVR	Aortic Valve Replacement
BCS	British Cardiovascular Society
BHF	British Heart Foundation
BNP	Brain Natriuretic Peptide
BP	Blood Pressure
CI	Confidence Intervals
CMR	Cardiovascular Magnetic Resonance
CPHPC	R-1-[6-[R-2-carboxy-pyrrolidin-1-yl]-6-oxo-hexanoyl] pyrrolidine-2-carboxylic acid
CR	Complete (light chain) Response
CSF	Cerebrospinal Fluid
CT	Computed Tomography
CTD	Cyclophosphamide, Thalidomide (and) Dexamethasone
CVD	Cyclophosphamide, Velcade (and) Dexamethasone

DCM	Dilated Cardiomyopathy
DNA	Deoxyribonucleic Acid
DOTA	1,4,7,10-tetraazacyclododecane-1,4,7,10-tetraacetic acid
DPD	3,3-diphosphono-1,2-propanodicarboxylic acid
ECG	Electrocardiogram
ECOG	Eastern Cooperative Oncology Group
ECV	Extracellular Volume
EF	Ejection Fraction
eGFR	Estimated Glomerular Filtration Rate
EMG	Electromyogram
EQ-CMR	Equilibrium (contrast) Cardiovascular Magnetic Resonance
FAP	Familial Amyloid Polyneuropathy
FISP	Fast Imaging with Steady State Precession
FLASH	(IR) Fast Low Angle Shot (Inversion Recovery)
FOV	Field of View
GAGS	Glycosaminoglycans
GE	General Electric
GI	Gastrointestinal
GSK	Glaxo Smith Kline
HCM	Hypertrophic Cardiomyopathy
HR	Hazard Ratio
IBM	International Business Machine (Corporation)
ICC	Intraclass Correlation Coefficient
ICD	Implantable Cardioverter Defibrillator
IQ	Interquartile (range)
IVRT	Isovolumic Relaxation Time
KM	Kaplan Meier
LA	Left Atrium
LAA	Left Atrial Area
LBBB	Left Bundle Branch Block

LGE	Late Gadolinium Enhancement
Ln	Natural logarithm
LV	Left Ventricle
LVEDV(i)	Left Ventricular End Diastolic Volume (indexed)
LVESV(i)	Left Ventricular End Systolic Volume (indexed)
LVH	Left Ventricular Hypertrophy
MAPSE	Mitral Annular Plane Systolic Excursion
MGUS	Monoclonal Gammopathy (of) Undetermined Significance
MI	Myocardial Infarction
MOLLI	Modified Look Locker Inversion (recovery)
MRI	Magnetic Resonance Imaging
msec	Milliseconds
mV	Millivolts
NAC	National Amyloidosis Centre
NHS	National Health Service
NNE	Nearest Neighbour Estimator
NT-proBNP	Nitrogen-Terminal Brain Natriuretic Peptide
NYHA	New York Heart Association
PET	Positron Emission Tomography
PR	Partial (light chain) Response
PSIR	Phase Sensitive Inversion Recovery
RF	Radiofrequency
RNA	Ribonucleic acid
ROC	Receiver Operating Characteristic
ROI	Region of Interest
RV	Right Ventricle
SAA	Serum Amyloid A
SAP	Serum Amyloid P
SASHA	Saturation-recovery Single-shot Acquisition
SCMR	Society (for) Cardiovascular Magnetic Resonance

SD	Standard Deviation
ShMOLLI	Shortened Modified Look Locker Inversion (recovery)
SPECT	Single Photon Emission Computed Tomography
SPSS	Statistical Package (for the) Social Sciences
SSA	Senile Systemic Amyloidosis
SSFP	Steady State Free Precession
TAPSE	Tricuspid Annular Plane Systolic Excursion
TD	Trigger delay
TDI	Tissue Doppler Imaging
TE	Echo Time
TI	Inversion Time
TNF	Tumour Necrosis Factor
TR	Repeat Time
TTR	Transthyretin
VIF	Variance Inflation Factor
VT	Ventricular Tachycardia

3. DECLARATION

I, Marianna Fontana, confirm that the work presented in this thesis is my own. Where information has been derived from other sources, I confirm that this has been indicated in the thesis

Signature: 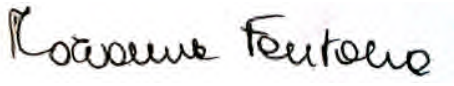

(electronically signed)

Name: **Marianna Fontana** Date: 05th October 2015

4. ACKNOWLEDGEMENTS

This work is funded by a 3 year research training fellowship (FS/12/56/29723) from the British Heart Foundation (BHF). Thanks go to my supervisors, Prof James Moon and Prof Philip Hawkins. Thanks to all the consultants and fellows working at the Heart Hospital Imaging Centre and National Amyloidosis Centre. I gratefully acknowledge the contributions of the administrative and nursing staff, histopathologists, geneticists, echocardiographers and radiographers at the National Amyloidosis Centre and the Heart Hospital. A special thank to the patients, without them this would have not be possible.

5. ABSTRACT

Systemic amyloidosis is an infiltrative disorder caused by amyloid deposition in the extracellular space. Two main types of systemic amyloidosis affect the ventricular myocardium, immunoglobulin light chain (AL) and transthyretin (ATTR). These have different natural histories and prognosis but in both, cardiac involvement is the main driver of outcome. For cardiac amyloidosis, Cardiovascular Magnetic Resonance (CMR) with the late gadolinium enhancement (LGE) technique provides sensitivity for early detection but is highly dependent on operator skills and not quantitative - there is no current method of measuring cardiac amyloid burden. A new technique, T1 mapping permits tissue abnormalities to be directly visualised in a simple scan – the colour changes being instantly recognisable, either before contrast (native T1 mapping) or after, when the myocardial extracellular volume (ECV) can be measured. Furthermore, a widely available LGE approach, phase sensitive inversion recovery (PSIR) LGE, being less operator dependent, had potential for improved performance.

At the National Amyloidosis Centre and Heart Hospital collaboration, I explored:

1- The potential of a new, faster T1 mapping sequence (ShMOLLI).
2- The potential of native T1 mapping for diagnosing cardiac ATTR and AL amyloidosis.
3- The inferred pathophysiology of cardiac amyloidosis by characterising amyloid burden, oedema and myocyte response concurrently.
4- The use of the LGE PSIR approach to improve the LGE technique.

In technical development, I showed that ShMOLLI T1 mapping can more accurately and precisely measure the ECV in various heart diseases including amyloid. Compared to the older multibreath-hold technique, more patients were able to perform ShMOLLI (6% unable to do multibreath-hold); the two techniques correlated (r^2=0.89) with little bias (-2.2%) and good agreement (ICC 0.92, p<0.0001) but ShMOLLI ECV correlated better with histological collagen volume fraction (CVF) (r^2= 0.68 vs r^2= 0.59) with a trend to better inter-study reproducibility (95%CI -4.9% to 5.4% vs -6.4% to 7.3% respectively, p=0.21).

I then explored native T1 mapping to detect cardiac infiltration in amyloidosis. For ATTR amyloidosis, T1 was elevated compared to hypertrophic cardiomyopathy (HCM) or normal subjects (1097±43ms vs 1026±64ms vs 967±34ms, both p<0.0001). This elevation was not as high as in AL amyloidosis (AL 1130±68ms, p=0.01). Diagnostic performance was similar for AL and ATTR amyloidosis (vs HCM: AL AUC 0.84 (95%CI 0.76-0.92); ATTR 0.85 (0.77-0.92) P<0.0001). T1 tracked cardiac amyloid burden as determined semi-quantitatively by DPD scintigraphy (p<0.0001). T1 was not elevated in mutation carriers (952±35ms) but was in isolated DPD grade 1 (n=9, 1037±60ms, p=0.001).

I then used T1 mapping with contrast (and without) to measure the ECV and combined this information with myocardial mass and native T1. I could, for the first time, non-invasively measure the amyloid burden (ECV) and myocyte volume ((ECV-1)*LVmass). Both LV $mass_i$ and ECV were markedly elevated in amyloidosis. However, the Total Cell Volume was normal in AL, 47±17 ml/m^2, but elevated in ATTR, 53±12 ml/m^2 (p<0.05). This implies that all the (lesser) LV mass increase in AL is ECV i.e. amyloid,

whereas the (greater) increase in ATTR is mainly extracellular but with an additional 18% intra-cellular increase – likely myocytes, the dominant (by volume) myocardial cell type.

I then revisited the LGE technique in amyloid. This has always been difficult as nulling often seems to fail in amyloid. Using PSIR, a new, potentially more robust LGE approach, I assessed the incremental prognostic value of LGE. 250 prospectively recruited subjects underwent LGE CMR comprising 122 with ATTR amyloid, 9 asymptomatic mutation carriers, and 119 patients with AL amyloidosis. Subjects were followed up for a mean of 24 months. LGE was performed with PSIR and without (magnitude only, MAG-IR). These were compared with ECV with ShMOLLI. PSIR was superior to MAG-IR LGE since PSIR nulled always the tissue (blood or myocardium) with the longest T1 (least gadolinium). LGE was classified into 3 patterns: none, subendocardial and transmural, which were associated with increasing amyloid burden as defined by ECV ($p<0.0001$) with transitions from none to subendocardial LGE at an ECV of 0.40-0.43(AL), 0.39-0.40(ATTR); and to transmural at 0.48-0.55(AL), 0.47-0.59(ATTR). Sixty seven (27%) patients died. Transmural LGE predicted death (HR=5.4, 95%CI: 2.1-13.7,$p<0.0001$) and remained independent after adjusting for NT-proBNP, ejection fraction, stroke volume index, E/E' and LV mass index (HR=4.1, 95%CI: 1.3-13.1,$p<0.05$).

In conclusion, the work in this thesis has enabled a deeper understanding of cardiac amyloidosis, disease processes and stages. Cardiac amyloidosis is not just infiltration, but there appears to be a myocyte response. It has pioneered the clinical use of native T1, ECV and LGE PSIR, new markers that are able to identify and quantify cardiac involvement and give new insights in the pathophysiology of cardiac disease.

6. INTRODUCTION

This chapter is based on the publication below:

Fontana M, Chung R, Hawkins PN, Moon JC. Cardiovascular magnetic resonance for amyloidosis. Heart Fail Rev. 2015 Mar;20(2):133-44.

My contribution was writing the review.

6.1 WHAT IS AMYLOID

Amyloidosis is a group of diseases characterised by the deposition of amyloid in one or more organs. As many as 23 different precursor proteins to the formation of amyloid have been described in man.(1) These may deposit themselves in a fibrillar matrix within selected tissues. Fibril formation is also associated with deposition of other nonfibrillar substances, notably including glycosaminoglycans and serum amyloid P-component amongst others.(2) Fibrils are formed when normally soluble molecules undergo conformational change and mis-fold to become relatively insoluble, resulting in the deposition of nonbranching fibrils in different organs.(3) Amyloid deposition into the heart is the leading cause of death and influences therapeutic choices.(4)

Amyloid deposits can be massive and cardiac or other tissues may become substantially replaced. Amyloid fibrils bind Congo red stain, yielding the pathognomonic apple-green birefringence under cross-polarized light microscopy that remains the gold standard for identifying amyloid deposits. Further staining with immunohistochemistry is performed to subtype into the 2 main types which affect ventricular myocardium, AL and

ATTR amyloidosis, the latter comprising two forms, wild type or genetically variant – both forms of transthyretin.

6.2 PRIMARY AL AMYLOIDOSIS

Primary AL amyloidosis occurs most often in the setting of a plasma cell dyscrasia, in which circulating amyloidogenic light chains deposit within extracellular space of different organs causing damage.

Cardiac AL amyloidosis may be rapidly progressive. Low QRS voltages, particularly in the limb leads are common. Thickening of the left ventricular wall is typically mild to moderate, and is rarely greater than 18mm, even in advanced disease. Cardiac AL amyloid deposition is accompanied by marked elevation of the brain natriuretic peptide (BNP/NT-proBNP) and cardiac troponins, even at an early stage. The right heart failure is often exacerbated by the co-presence of nephrotic syndrome in 30-50% of cases.(5) The hypoalbuminaemia of nephrotic syndrome is itself exacerbated by concomitant liver disease. Hypotension can be present not only because of a “low-output” state, but also because of associated autonomic neuropathy.

Involvement of the heart is the commonest cause of death in AL amyloidosis, and a major determinant of prognosis: without cardiac involvement, AL amyloidosis has a median survival of around 4 years (6) but with, (e.g. elevated BNP and cardiac Troponin - Mayo stage III disease) (7) It is 6-8 months.

Like all cardiac amyloid, treatment to arrest amyloid deposition may halt disease progression and improve blood biomarkers, but echocardiography, CMR and ECG changes rarely revert.

6.3 Hereditary Transthyretin-Related Amyloidosis

TTR is a small tetramer synthesised in the liver that transports thyroxine and retinol.(8) Myocardial infiltration can be severe, causing overt heart failure. A sensorimotor/autonomic neuropathy frequently co-exists(9).Over 100 mutations are recognised and each mutation can display variable penetrance.(9) For example, the substitution of isoleucine for valine at the position 122 (V122I) occurs in up to 4% of Afro-Caribbeans in London causing eventual cardiac amyloidosis in an unknown proportion.(10) Echocardiography shows restrictive left ventricular features usually with preserved systolic function.(10) This is often mistaken for hypertensive heart disease. In around half of African-Caribbean patients with heart failure the ejection fraction is normal (11) and early evidence suggests that this may be due to undiagnosed cardiac amyloid. Imaging features of ATTR are not known to specify the amyloid subtype (although see DPD scanning, and my CMR results, later), but patients with ATTR typically have fewer symptoms and better survival than AL amyloid patients. (11)

6.4 Wild type transthyretin amyloidosis

Non-hereditary TTR-related amyloidosis is commonly referred to as Senile Systemic Amyloidosis (SSA) owing to its late age of onset (after the seventh decade of life) or wild type transthyretin amyloidosis. Wild-type TTR amyloid deposits are found at

autopsy in about 25% of individuals older than 80 years, but their clinical significance is not clear.(12-14) Epidemiological studies assessing the prevalence of wild type TTR deposits leading to the clinical syndrome of SSA have not been performed. SSA is a predominant cardiac disease often preceding heart failure by 3-5 years.(15) There is a strong male predominance, and like hereditary ATTR, it is often misdiagnosed as hypertensive heart disease.(16) The natural history remains poorly understood, but studies suggest a median survival of about 7 years from presentation. (12,13)The true incidence of SSA is probably underestimated, a gap that is being filled by recent advances in CMR to improve detection of cardiac amyloid – for example, until 2001, it accounted for 0.5% of all patients seen at the UK amyloidosis centre, but now accounts of 7% of 1100 cases with amyloidosis seen since end of 2009 (unpublished data).

6.5 DIAGNOSIS AND EVALUATION OF CARDIAC AMYLOIDOSIS

6.5.1 ELECTROCARDIOGRAPHY (ECG):

Low QRS voltages (all limb leads <5 mm in height) with poor R wave progression in the chest leads (pseudoinfarction pattern) occur in up to 50% of patients with cardiac AL amyloidosis.(17) The combination of low ECG voltage with increased wall thickness is highly suspicious for cardiac amyloidosis (see figure 1), but voltage criteria for left ventricular hypertrophy (LVH) can occur.(18,19). The mechanisms are poorly understood, but a possible hypothesis links low voltages with the myocyte loss associated with amyloid infiltration (see my results).

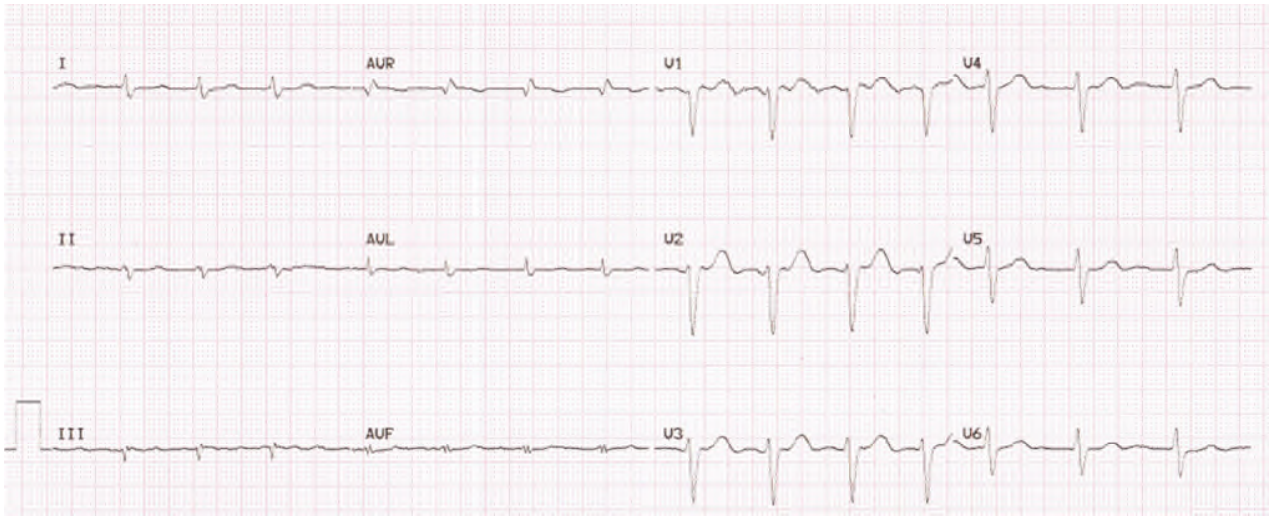

Figure 1. ECG of a patient with cardiac AL Amyloidosis.

Small QRS voltages (defined as <5mm height) in the limb leads.

Other findings include various degrees of AV blocks and intraventricuar blocks (more frequent in ATTR than AL): first degree atrioventricular (AV) block (21%), nonspecific intraventricular conduction delay (16%), second or third degree AV block (3%); (18) left (LBBB) and right bundle branch block can also occur.(20) Rhythm disturbances are frequent as well including AF/flutter (20%) and ventricular tachycardia (VT) (5%).ECG patterns can provide clues to differentiate between AL and ATTR amyloidosis: LBBB is seen in 40% of patients with wild type ATTR but is rare in AL (4%), while typical low QRS voltages are seen in 40% wild type ATTR vs 60% AL.(4)

There has been little recent study of ECG correlation with cardiac biomarkers, treatment toxicity and mortality. Progressive ECG changes may be useful in assessing silent cardiac progression.(21) Changes in ECG abnormalities after treatment in AL amyloidosis remain poorly studied, but can occur – more often, little improvement is seen. Holter ECG monitoring identifies asymptomatic arrhythmias in >75% of cardiac AL patients

(mainly supraventricular tachyarrhythmias and some non-sustained VT), but the prognostic significance is unknown.(22)

6.5.2 ECHOCARDIOGRAPHY

Echocardiography is the first line imaging modality where the suspicion of cardiac amyloidosis is raised. Findings are only characteristic in advanced disease when the study is performed by experienced operators, but harder to detect earlier on and have prognostic and diagnostic significance.(23-25) Typical findings include concentric LVH with right ventricular (RV) involvement, poor biventricular long axis function with mildly reduced ejection fraction (EF) (26,27), valvular and interatrial septal thickening.[4] Diastolic dysfunction is the earliest echocardiographic abnormality, may occur before cardiac symptoms develop but the specificity of these findings is poor (28,29).

Advanced echocardiographic techniques are beginning to reveal more about the underlying pathology and functional abnormalities, such as the twisting and untwisting cardiac motion that may be augmented through compensatory mechanisms before reversing to impairment later in the course of the disease.(30,31) Strain and strain rate imaging, derived from speckle tracking (see figure 2), may improve the specificity of echocardiographic findings, helping differentiate cardiac amyloidosis from hypertrophic cardiomyopathy.(32,33). Typically, there is much greater restriction of basal than apical movement. Mean LV basal strain is an independent predictor of both cardiac and overall deaths.(34)

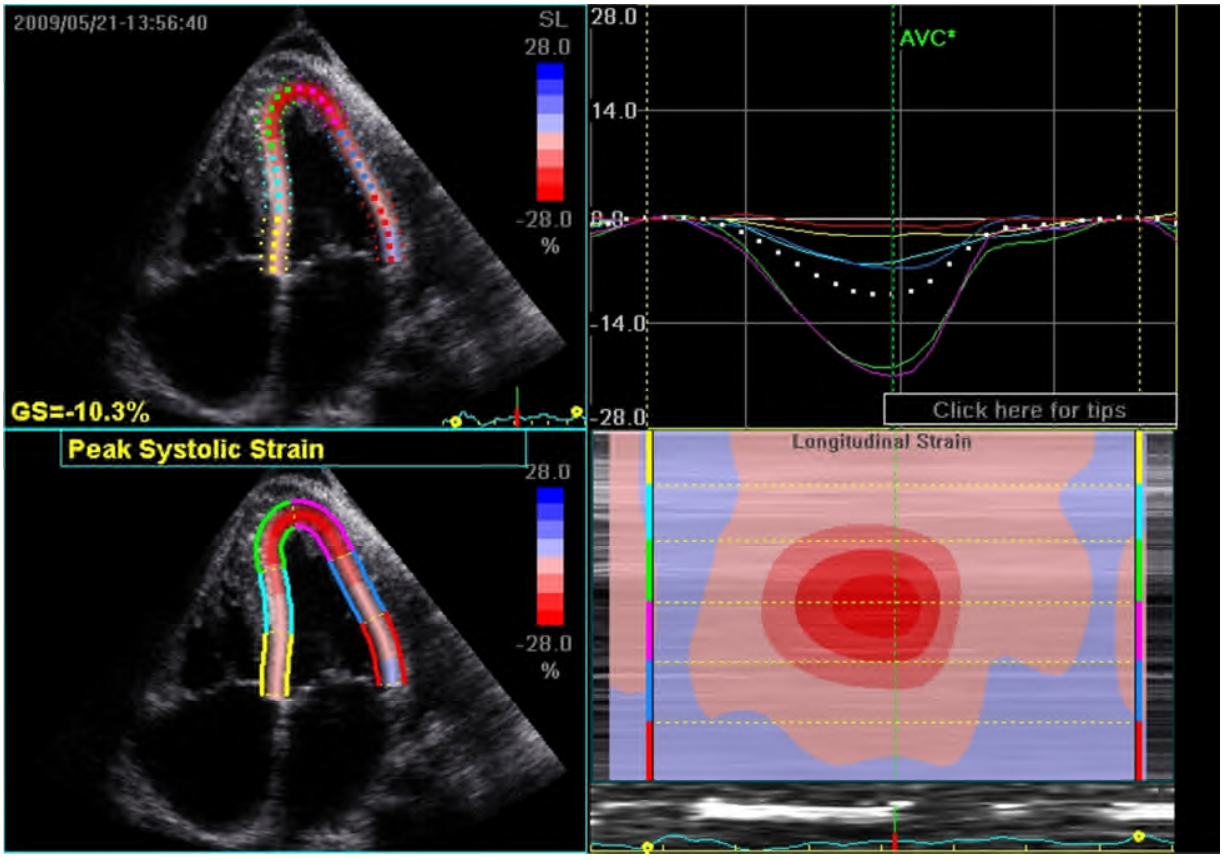

Figure 2. Transthoracic echocardiogram with speckle tracking.

The red and yellow lines represent longitudinal motion in the basal segments while the purple and green lines are apical motion. This shows loss of longitudinal ventricular contraction at the base compared to apex.

6.5.3 Cardiac Biomarkers

Measurements of brain natriuretic peptides (BNP/NT-proBNP) and cardiac troponins are informative in AL amyloidosis, where most study has occurred to date. Their value in ATTR amyloidosis is yet to be determined. Brain natriuretic peptides are cleared by the kidneys (BNP also partially cleared by the liver), confounding the evaluation of patients with kidney involvement. Elevated NT-proBNP levels in systemic AL amyloidosis are a sensitive marker of cardiac involvement, with a cut-off >152pmol/L being associated

with higher mortality (72% vs 7.6% per year).(35) Abnormal NT-proBNP is predictive of clinically significant cardiac involvement developing in future.(36)

Increased troponin is a marker of poor prognosis (37) but the mechanism remains unclear.(37) Indeed more recently, high-sensitivity Troponin T has been shown to correlate with morbidity and mortality after patients with renal impairment were excluded.(38) High-sensitivity Troponin is abnormal in more than 90% of cardiac AL patients (39) and the combination of brain natriuretic peptides plus troponin measurements are used to stage and risk-stratify patients with AL amyloidosis at diagnosis.(7,40)

Interestingly, the concentration of brain natriuretic peptides in AL amyloidosis may fall dramatically within weeks following chemotherapy that substantially reduces the production of amyloidogenic light chains.(41) The basis for this very rapid phenomenon, which is not mirrored by changes on echocardiography or CMR remains uncertain, but a substantial fall is associated with improved outcomes.(42) An early transient increase in brain natriuretic peptides may occur after treatment with the immunomodulatory drugs thalidomide and lenalidomide, which are frequently used in the management of AL amyloidosis (see later), but the significance and cause is unclear.(43,44)

6.5.4 RADIONUCLIDE IMAGING

Serum amyloid P component (SAP) scintigraphy uses purified human SAP radiolabelled with ^{123}I, which is injected into patients. The tracer localises to target organs rich in amyloid and an image captured with a gamma camera. SAP scans enable visceral amyloid deposits, including those in the liver, kidneys, spleen, adrenal glands and bones

to be imaged serially in a specific and qualitative manner.(45) It does not adequately image the heart and thus has no role in assessing cardiac amyloidosis.

Numerous case reports over the past 30 years have indicated that various commonly used diphosphonate bone seeking radionuclide tracers occasionally localise to cardiac amyloid, and this approach has now been investigated systematically and now used routinely in clinical practice. Technetium-labelled 3,3-diphosphono-1,2-propanodicarboxylic acid bone scanning agent (^{99m}Tc-DPD), a particular tracer that has been little used of late for bone scintigraphy, appears to localise to cardiac amyloid deposits very sensitively, especially in patients with ATTR type (figure 3), where it has become the gold standard imaging test for cardiac ATTR amyloid. Indeed, asymptomatic cardiac ATTR deposits can be identified through ^{99m}Tc-DPD scintigraphy at an early stage when echocardiography, serum cardiac biomarkers and perhaps even CMR remain normal. [82]

Uptake of ^{99m}Tc-DPD occurs in fewer (about one third) of patients with cardiac AL amyloidosis at lower grade. ^{99m}Tc-DPD-SPECT-CT can help to distinguish the two types.(46) The sensitivity of DPD scintigraphy for detecting cardiac amyloidosis of ATTR type would appear to have considerable potential for diagnosis and screening.(47) Early work using N-[methyl-(11)C]2-(4'-methylamino-phenyl)-6-hydroxybenzothiazole ((11)C-PIB) PET imaging for cardiac amyloidosis is promising.(48) Currently, because of the much lower sensitivity of DPD scintigraphy in AL compared with ATTR amyloidosis, a multimodality imaging approach is adopted using radionuclide scintigraphy, along with echocardiography and cardiac MRI as described below.

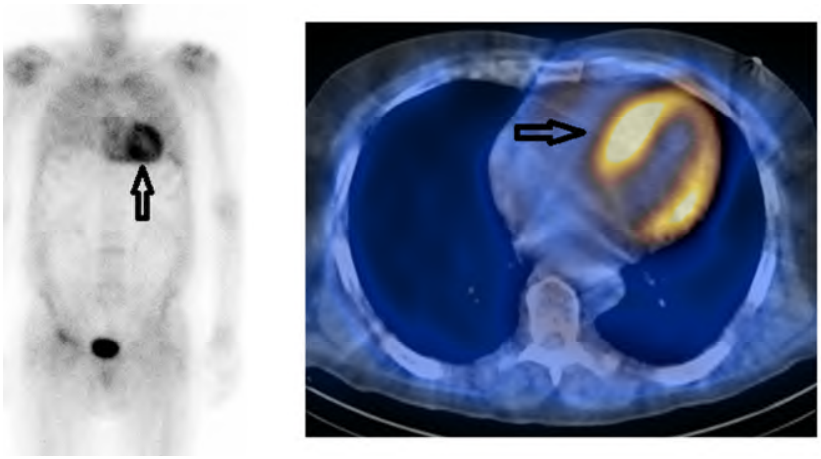

Figure 3. ^{99m}Tc-DPD scan in ATTR cardiac amyloidosis.

A positive ^{99m}Tc-DPD scan for ATTR cardiac amyloidosis (left), showing uptake in the heart (arrow) and reduced bone uptake. The right hand panel showed a fused CT/SPECT image showing myocardial uptake with greater uptake in the septum.

6.5.5 CARDIAC MRI

CMR uses a superconducting magnet with ECG gating to investigate the heart, gaining insight into the extra cardiac anatomy, cardiac structure, function and specific characterisations of myocardial tissue. As a test, it may have high sensitivity and specificity, but the diagnostic yield and importance of findings depends on the pre-test probability. Advanced cardiac amyloidosis is easy to detect by any technique: the detection of earlier cardiac involvement and their differentials from other phenocopies or genocopies may be harder. CMR, like other tests should therefore be interpreted in the clinical context. Specific differentials or disease processes that may raise diagnostic problems and confounders are co-morbidities (age, renal failure, diabetes, hypertension); whether there is another cardiomyopathy such as HCM or dual pathology, eg aortic stenosis and wild type ATTR amyloidosis.

Extracardiac anatomy: Cardiac amyloidosis is frequently associated with other abnormalities. Pleural effusions are common, as is ascites in advanced disease (Figure 4). Effusions and ascites when there is apparently good cardiac function (normal ejection fraction) are signs of heart failure with preserved ejection fraction (HFpEF) - one cause of which is amyloidosis. However, by the time patients are referred for CMR, many have frequently started heart failure treatment and may occasionally have ascites without pleural effusions (figure 4). Nephrotic syndrome, from renal involvement in AL amyloidosis, is yet another manifestation. Patchy lung changes are not infrequently seen, but many patients are elderly, and CMR is not adequate to diagnose lung infiltration (figure 4). Occasionally the presence of increased gas in the bowel or dilated oesophagus from autonomic dysfunction can be seen. Similarly, liver changes are occasionally seen – fatty liver with its featureless hypovascular appearance is an occasional finding in patients with known AL amyloidosis (figure 4).

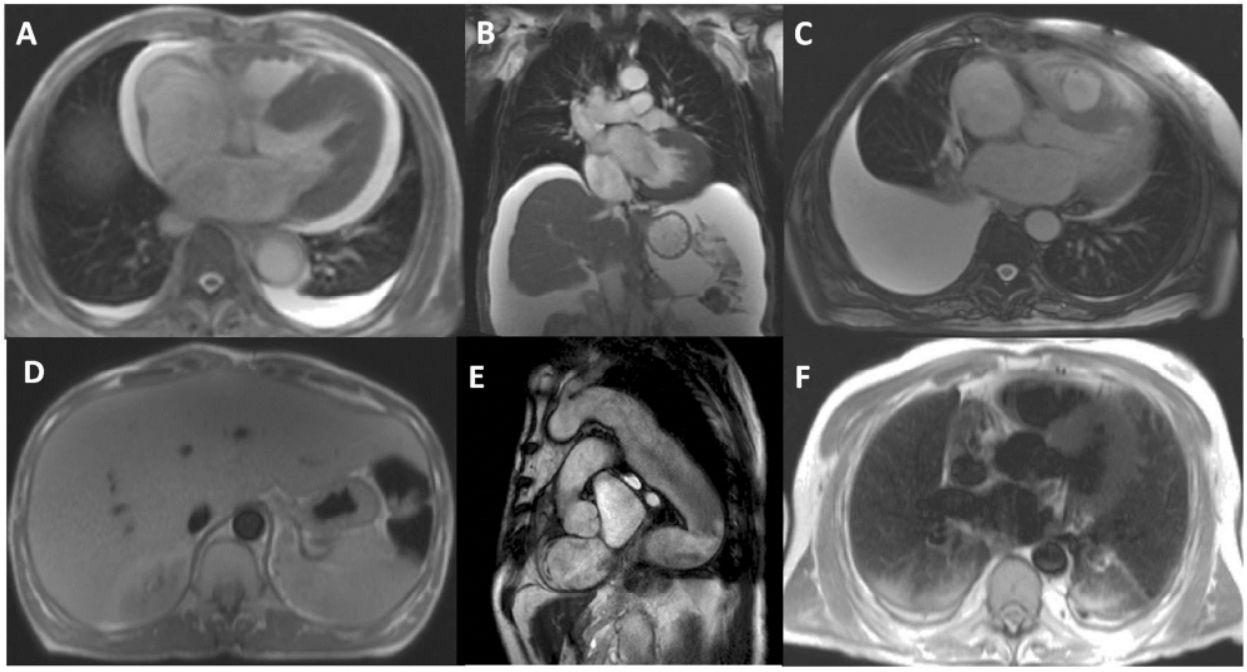

Figure 4. Extracardiac findings in patients with cardiac amyloidosis.

Panel a: pleural and pericardial effusions. Panel b: ascites without pleural effusions. Panel c: Right pleural effusion. Panel d: lardaceous fatty liver with its featureless hypovascular appearance. Panel e: tortuous and dilated thoracic aorta, frequently seen in hypertension, one of the main differentials. Panel f: patchy lung changes (non-specific by CMR).

Morphology, function and anatomy: Traditionally cardiac amyloidosis has been thought to be characterized by concentric and symmetric hypertrophy of the left ventricle as opposed to apical or asymmetric wall thickening in HCM (figure 5). However, recent work documents concentric LVH in 59% of patients with cardiac amyloidosis, as well as eccentric LVH or concentric remodelling in 33% and normal geometry in the remaining 8% (49). Cardiac amyloidosis may present with both symmetric and asymmetric, concentric and eccentric hypertrophy (Figure 5). Hypertrophy may be disproportionately greater than in hypertension (e.g. greater than ~17 mm) and is more prominent in ATTR than AL amyloid. RV involvement with hypertrophy is frequent - the RV end systolic thickness may

be up to 1 cm. A few cases have been observed with a dilated cardiomyopathy phenotype (again with classical tissue characterisation findings) (figure 5), and occasionally patients have outflow tract obstruction. Thus, although many cases are characteristic, the full range of morphological findings in amyloid is broad.

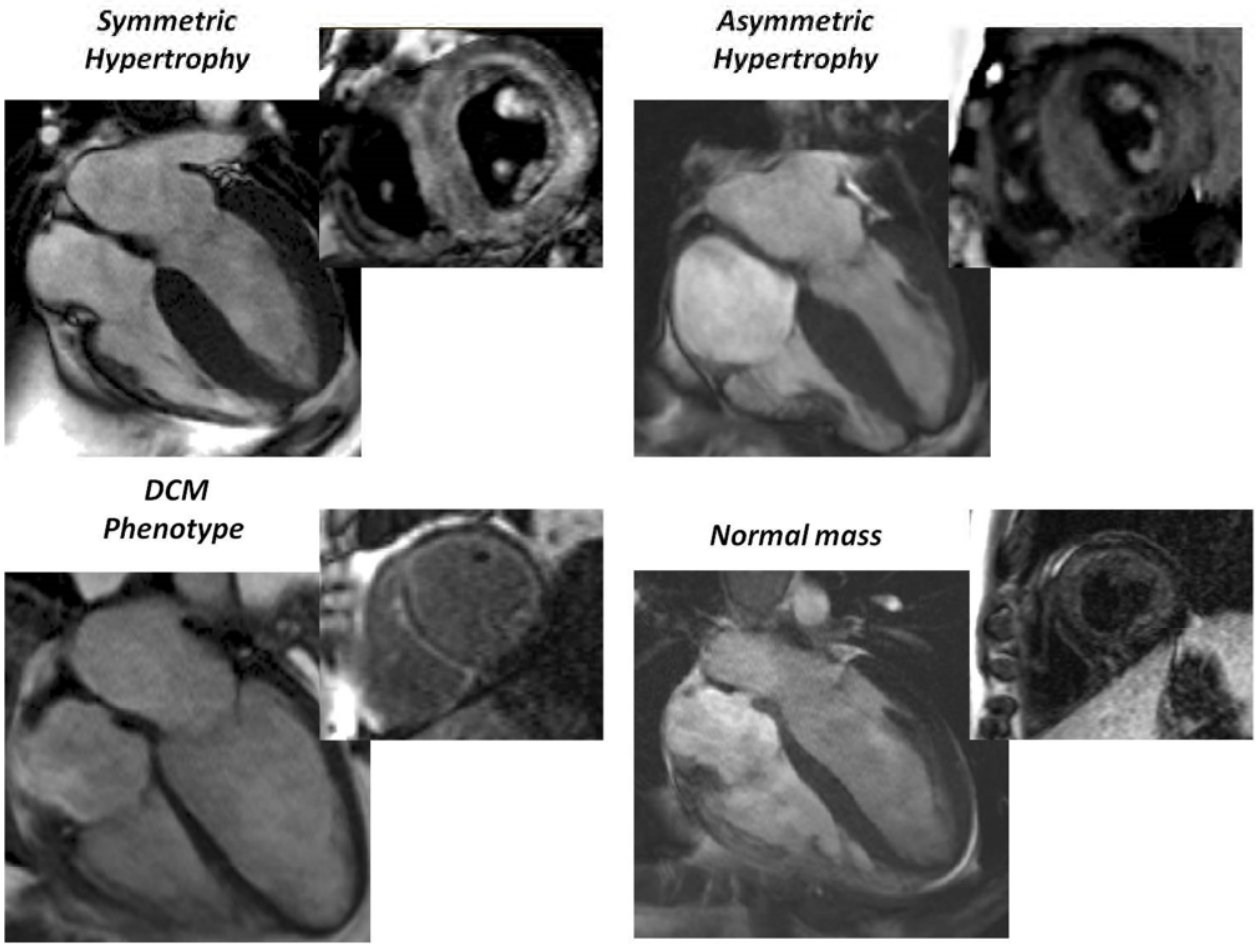

Figure 5. Left ventricular remodelling phenotypes in cardiac amyloidosis.

For each pattern there is an example of a cine four chamber view and a short axis late gadolinium enhancement. Left upper panel: symmetric hypertrophy, traditionally considered the characteristic pattern. Right upper panel: asymmetric hypertrophy, recently proven to be highly prevalent in cardiac amyloidosis. Left lower panel: dilated cardiomyopathy phenotype (rare-described in few cases). Right lower panel: no left ventricular hypertrophy with late gad features of amyloidosis, a less uncommon finding that is hard to detect without tissue characterisation.

Traditional markers such as ejection fraction may be normal even into the late phase of disease because it is a poor measure of systolic function in patients with concentric remodelling. Long axis function (typically biventricular) reduces early, mainly at the level of the basal segments. The reduction, in many cases to effectively zero longitudinal function, is associated with small cavity size, decreased stroke volume and reduced cardiac output (50). The indexed stroke volume, usually severely reduced, is therefore a better measure of systolic function than the ejection fraction, and we would recommend scrutinising it in reports of possible cardiac amyloid.

CMR is less adept than echocardiography for diastolic function assessment. Valvular disease in cardiac amyloidosis seems no more prevalent than in other people of similar age. Atrial infiltration definitely occurs, but CMR shows that much of the apparent atrial thickening in amyloidosis is interatrial fat. In later phases, atrial fibrillation, particularly coarse or flutter-like fibrillation may be observed and thrombi may be seen in the left atrial appendage. The severe reduction in the atrial contraction characteristic of later stages is often associated with signs of very slow flow (“smoke”) in the left atrium and also occurs in patients in sinus rhythm.

Serial imaging studies provide additional insight into the time course of amyloidosis. Swiftly changing cardiac hypertrophy is not common in cardiomyopathy in adult life (although late onset HCM is well known), but rapid changes over months in wall thickness and function, should place AL amyloidosis high on the differential list. Although CMR-based morphological and functional assessment is probably more accurate than with echocardiography alone (with the important exception of diastolic dysfunction and strain

measurement) (34), these features are nonspecific and vary in prevalence until late phases of disease. Thus, in high pre-test probability scenarios, the absence of these morphological and functional markers does not fully exclude cardiac amyloidosis (49).

Tissue characterisation: A key advantage of CMR is its unique ability to give information about the tissue composition by "myocardial tissue characterization". Healthy and pathological myocardium may differ because of "intrinsic contrast" (without the use of gadolinium) - signal difference from the myocardium as pathology changes the myocardial T1, T2 and T2*. Alternatively, the addition of an extrinsic gadolinium-based contrast agent Gd-DTPA (gadolinium diethylenetriamine penta-acetic acid) may reveal "extrinsic contrast" properties as in the LGE. The gadolinium component alters the CMR signal and the chelator makes it inert and determines the *in vivo* properties of the whole, determining the tracer behaviour (51). These purely extracellular agents are small enough to pass across the vascular wall into the extracellular space, yet are large enough to not penetrate myocardial cells with intact membranes. It accumulates passively in the gaps between cells through post-bolus tracer kinetics and the increased volume of distribution (interstitial expansion) in hydrated 'scar' tissue or in areas of amyloid deposition (52). After gadolinium, in normal tissue, the whole myocardium will have a diffuse lowering of T1. In scar/focal amyloid there will be areas where the T1 is regionally detectably lower, the basis of the LGE technique for qualitative detection of focal fibrosis (e.g. myocardial infarction). In diffuse infiltration, the whole myocardium will have substantially lower T1 – which was a problem until the development of the extracellular volume (ECV) technique.

The typical" amyloid LGE pattern" is global subendocardial LGE in a non-coronary artery territory distribution with a dark blood pool, but this can vary. (53) Patterns vary in different series:(52,54-57) some find mainly localised enhancement; others diffuse transmural or patchy LGE (53,58,59) (figure 5 and 6). Thus, despite there being a "typical LGE pattern" in amyloid, current research suggests a more variable LGE pattern. Recent studies separating ATTR from AL are more informative. LGE (when classical) can be virtually pathognomonic and significantly more specific and sensitive than echo or CMR functional assessment. This can even be an apparently early finding – some patients are seen where the classical LGE appearance is present without hypertrophy (figure 5).

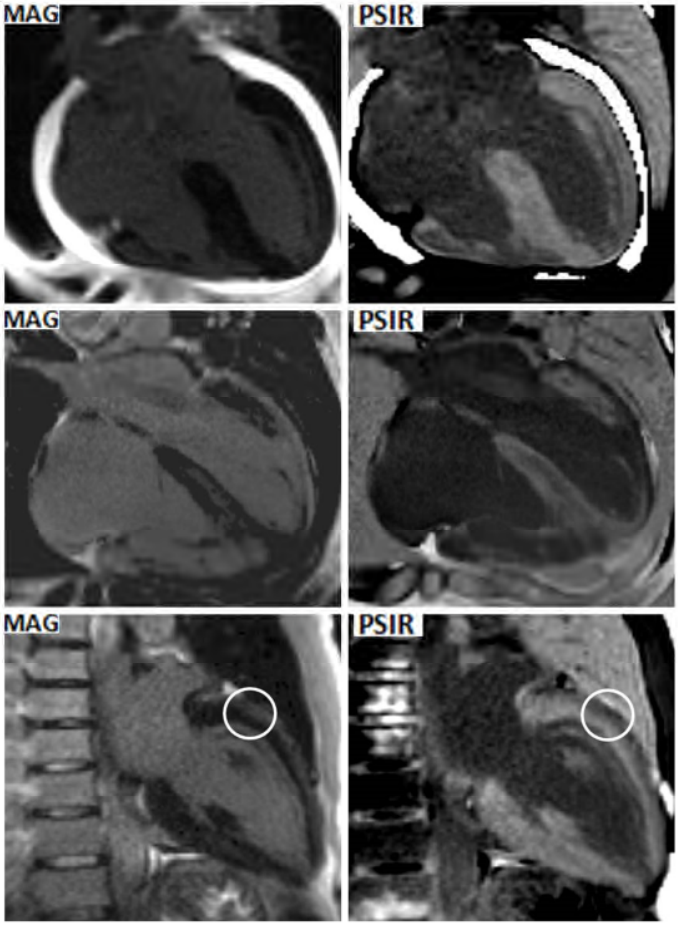

Figure 6. Late gadolinium enhancement.

LGE with magnitude (MAG) reconstruction (left panels) and LGE with phase sensitive inversion recovery reconstruction (PSIR) (right panels). There is discordance between magnitude and PSIR reconstruction in the three examples. ECV mapping (not shown) can arbitrate – the areas of the highest ECV are the ones that should show LGE and PSIR always gets this right. Upper panels: the MAG looks normal; the PSIR shows transmural LGE, concordant with an ECV here of >0.5, not shown. Middle panels: the MAG (patchy more apical LGE) is a mirror of the PSIR (more apical). Lower panels: the MAG (subepicardial LGE, circle) is a mirror image of the true PSIR pattern.

The traditional LGE technique is a difference test for focal lowering of T1Infiltrative diseases, especially amyloid, that affect the entire myocardium may have no remote regions of normal myocardium. This exposes a pitfall of the traditional approach in that the operator determining the optimal null-point for the myocardium may erroneously choose to

null the abnormal and not the normal myocardium. This can result in a serious risk of false negative examinations (when the entire myocardium is involved but could appear as normal) or “wrong” LGE patterns (i.e. mirror image of the true pattern, with mid-myocardial patterns becoming subendocardial and *vice versa*), potentially contributing to the variable LGE patterns described (figure 6).

The relatively new approach of Phase Sensitive Inversion Recovery (PSIR) sequence (60), now available from almost all the CMR manufacturers, could reduce the need for a optimal null point setting, making LGE in cardiac amyloidosis far easier and operator-independent (Figure 4). This approach is likely to improve the diagnostic and prognostic performance on “true” LGE patterns of cardiac amyloidosis, with the potential to reduce heterogeneity in the patterns reported (Figure6). I explore this later (chapter 11)

However the use of gadolinium is relatively contraindicated in patients with severe renal failure (estimated glomerular filtration rate, eGFR, <30 ml/min - a relatively common finding in patients with systemic AL amyloidosis). LGE in non-ischaemic cardiomyopathy, especially amyloid, is not easy to quantify so it is not reliable for following up changes over time. Newer T1 mapping techniques may overcome these limitations.

T1 mapping is a new technique where direct quantitative signal from the myocardium is measured, either pre-contrast (native T1) or post-contrast. Each pixel in the image is coded in colour, reflecting the absolute value of T1 (Figure 7). Native myocardial T1 mapping therefore measures myocardial intrinsic signal and T1 “maps” in a single breath-hold (61). Pathology changes native T1. Reduced T1 is uncommon,

occurring only in iron overload (62) and fat infiltration such as Fabry disease (FD] (63) (64). Increases in native T1 occurs: modestly in diffuse fibrosis, more in scar and substantially in amyloid and oedema – with good signal to noise ratio (figure 7). Native myocardial T1 mapping is associated in single centre studies with a high diagnostic accuracy for cardiac amyloidosis for AL when compared against patients with LVH from different causes such as aortic stenosis (63,65) (Figure 7). This may find clinical utility particularly when gadolinium contrast is contraindicated. In AL amyloidosis, T1 tracks markers of systolic and diastolic function, mass and prognostic markers (66). T1 is an early disease marker, being elevated before the onset of LVH, presence of LGE or elevation in blood biomarkers. I explore T1 in ATTR in chapter 11.

There are three problems with native T1 mapping: firstly conceptually, it measures a composite myocardial signal from both interstitium and myocytes. Secondly, it does not differentiate fully the underlying processes – particularly oedema and amyloid (though it is not impossible that that oedema may form part of the spectrum of myocardial amyloid infiltration) and thirdly, different CMR systems and sequences have different normal ranges. Standardization is only now starting – but consensus guidelines (67) are now available. Normal T1s are higher when measured at 3T (68), with different sequences ("SASHA" compared to other techniques), and typically with newer variants of mapping compared to older ones (69). Current recommendations are for normal reference ranges to be defined locally, but this may change over time.

The use of gadolinium-chelated contrast agents adds another dimension to CMR tissue characterization with T1 mapping. Post-contrast T1 may be lower in cardiac disease

suggesting increased myocardial interstitial space. However, care is needed as the disease may have altered body composition (a higher percentage of body fat and, thus, a greater contrast dose per unit of total body extra-cellular water), reduced renal function, or altered haematocrit. The fraction of tissue that is interstitial space is referred to as the extracellular volume (ECV). It can be calculated from the ratio of signal change in blood and myocardium after contrast administration and the blood contrast volume of distribution (equal to one minus haematocrit) (figure 7).

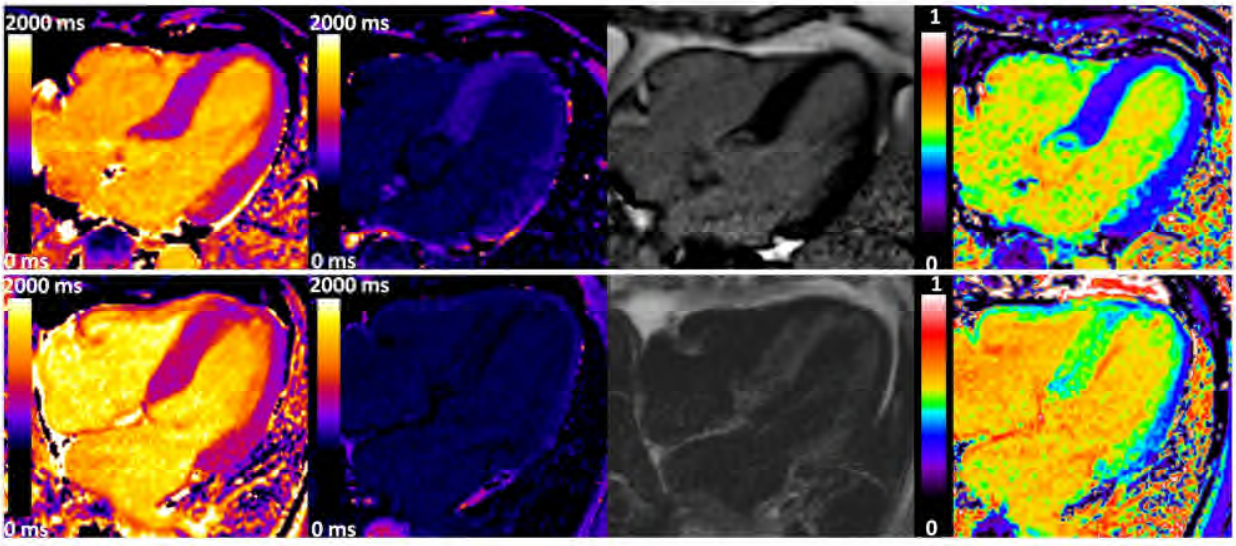

Figure 7. T1 maps, LGE and ECV maps of a patient with aortic stenosis and a patients with cardiac amyloidosis.

A patient with left ventricular hypertrophy from aortic stenosis (upper panels) and cardiac amyloidosis (lower panels). From left to right: T1 maps pre-contrast (left), post-contrast centre left, LGE centre right and extracellular volume (ECV) maps right. In the patient with cardiac amyloidosis on the ECV maps there is evidence of massive interstitial volume expansion with ECV elevation.

Amyloidosis is the exemplar of interstitial disease, and this is reflected by massive ECV elevation in the patients with definite AL cardiac amyloidosis (65,70). ECV is

elevated also in AL patients where conventional clinical testing and LGE suggested no cardiac involvement, highlighting a potential role as early disease marker (65).

ECV appears to be more robust between centres and approaches, being a ratio of change compared to T1. Furthermore high global ECVs can become very specific: fibrosis cannot achieve remote (non-infarct) ECVs of above ~0.4, implying that an ECV value greater than ~0.4 in remote myocardium become highly specific, with the only other differential being global oedema – a newly reported but not well understood phenomenon. Combined, native T1 mapping and ECV measurement could therefore over time add insight into cardiac amyloidosis at 3 different levels, i.e. infiltration (amyloid burden, ECV), oedema (native T1) and myocyte response (intracellular volume), providing a richer understanding of the pathophysiological mechanism. These hypotheses are derived from my work in chapter 10.

Diagnostic utility: CMR adds value to the certainty of probable amyloidosis patients. In the UK, where CMR is a well-developed national service, it has impacted referral patterns with a large national increase in the identification of patients with ATTR cardiac amyloidosis, particularly wild type, constraining resources in existing amyloid centres. Prospective studies with the aim of comparing the diagnostic accuracy of CMR against other approaches have not been done yet, but there are pointers.

. CMR adds value to the Mayo classification (or its equivalent in ATTR), and LGE can be pathognomonic of amyloidosis (but less so of specific subtype). CMR findings have increased accuracy compared to conventional echocardiographic imaging both in

terms of specificity and sensitivity: for example HCM may share features such as concentric hypertrophy, bi-atrial dilatation, reduced longitudinal function(72,73) and decompensated biventricular restrictive disease (74) but both HCM and amyloid may have unique tissue characterisation findings (54,58,75), but difficulties persist because of the variable pattern of LGE.

Native myocardial T1 can be used to support the diagnosis or exclusion of AL cardiac amyloidosis. This can be done choosing different cut-offs, based on the clinical scenario, with specificity and sensitivity to diagnose or exclude cardiac amyloidosis respectively. Ideally, the native T1 on subjects with end stage renal failure should be known as the comparator (rather than just healthy subjects), but this is not well studied at this time.

CMR methods to distinguish types of cardiac amyloidosis: Structural findings related to hypertrophy and functional characteristics differ according to amyloid sub-type. Transthyretin amyloid usually manifests as disproportionately increased LV mass and interventricular septal thickness, larger atrial area, smaller cavity volumes and lower ejection fraction (within the normal range) than AL amyloid (58), despite similar NYHA class and NT-proBNP levels.

Tissue characteristics can be different in the different amyloid subtypes. The pattern and extent of LGE differs in ATTR and AL amyloidosis, with LGE typically more extensive in ATTR than AL patients, but (chapter 11), this may be a survivor bias – with transmural LGE in AL associated with swift death. RV LGE appears to be present in most ATTR

amyloid cases, but in only a majority with AL amyloid. A semi-quantitative LGE score combined with age and myocardial wall thickness had a reported sensitivity of 87% and specificity of 96% for distinguishing ATTR from AL amyloid (58). Caveats to this score were the non-standardized approach used in the validation cohort of a retrospective study, use of different contrast agents, doses, acquisition times and LGE sequences which are all factors that have the potential to affect LGE patterns.

Prognostic ability: Presence of LGE is predictive of prognosis in virtually all the cardiac pathologies, except for amyloidosis where studies have conflicting results and have been small and in AL only with non-standardized LGE approaches (52,54,55,76). As discussed above, the LGE can be problematic in amyloid with global infiltration and altered wash-in and wash-out kinetics. Specifically, patients exhibiting the most advanced interstitial infiltration can occasionally be portrayed as having no LGE (figure 6) – a misclassification that profoundly confounds prognostic studies. PSIR-LGE approach has the potential to shed light on this, clarifying the role of LGE in the stratification of patients with AL and ATTR cardiac amyloidosis.

Measurement of native myocardial T1 and ECV aids risk-stratifying patients with AL cardiac amyloidosis (77) (Figure 8).

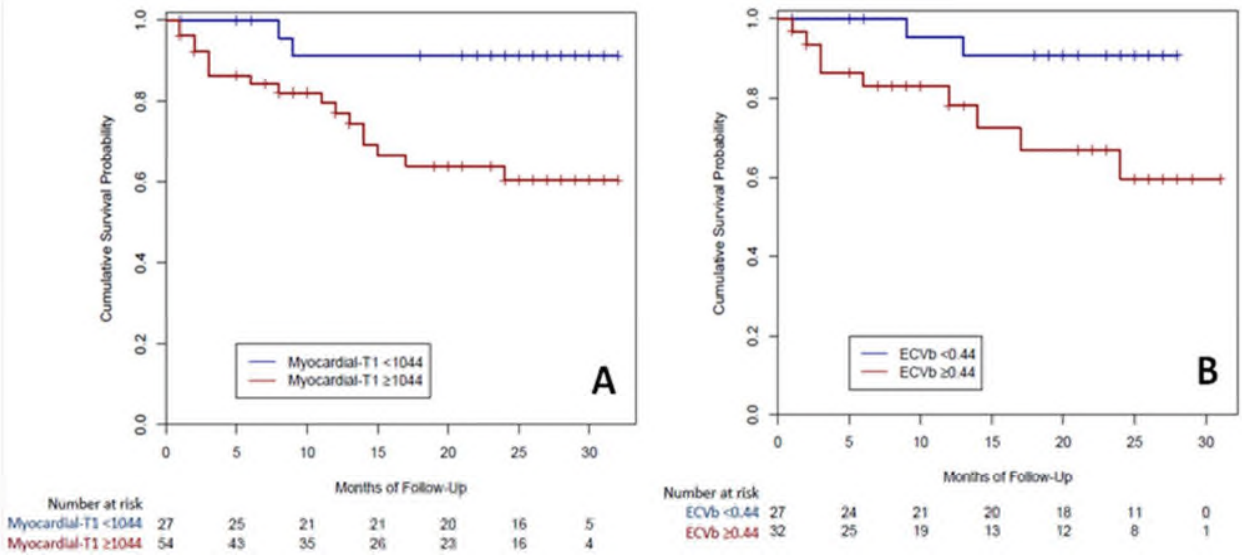

Figure 8. Kaplan Meier survival curves for native T1 and ECV in AL amyloidosis.

(A) Native myocardial T1 and (B)Extracellular volume (ECV_b). Adapted from Banypersad SM *et al.(77)*

This probably adds incremental value over and above existing clinical markers, although the published multivariable analyses are somewhat strained. More certainly, T1 and ECV add value when conventional parameters are confounded – e.g. blood biomarkers in renal failure, mild LVH in hypertension. Incremental value appears present regardless of treatment status and whether newly presenting or under established follow-up; ATTR amyloidosis data is awaited. The use of these biomarkers to guide or tailor therapy and monitor response has not been explored yet.

Surrogate endpoints in drug development: Disease tracking is a fundamental step for drug development – the detection of biological effect (beneficial and off target) and dose ranging. No imaging modality has been shown to track changes over time in patients with cardiac amyloidosis, particularly away from “end-stage” diseases, but T1 mapping has

high potential. LV mass changes are a poor target endpoint as mass consists of myocyte volume (beneficial) and infiltration volume (adverse), and changes over time are not large compared to measurement error. Changes in function (stroke volume index rather than EF) have similar problems, with the additional confounder of deterioration in function associated with occurrence of atrial fibrillation rather than disease progression. T1 mapping, has the potential to track structural changes over time at 3 different levels, i.e. infiltration (amyloid burden, ECV), possibly oedema (native T1) and myocyte response (intracellular volume), providing a richer understanding of the pathophysiological of the response to treatment (78,79) – hypotheses from chapter 10. ECV quantification has however been considered sufficiently robust to be used (by my centre, myself leading) in several early phase drug development studies.

6.6 AMYLOID TREATMENTS

Cardiac amyloidosis in general has a poor prognosis, but this differs according to amyloid type, and availability and response to therapy. Treatment may be "amyloid-specific" or "non amyloid-specific" as detailed below:

6.6.1 AMYLOID NON-SPECIFIC TREATMENTS

Heart failure treatment – Standard heart failure therapy may be of limited benefit or even detrimental in cardiac amyloidosis. There is scanty evidence for the use (or not) of ACE-i, ARBs and β blockers. These may be poorly tolerated, worsen postural hypotension or renal function (ACE/ARBs). Restrictive cardiomyopathy leads to a heart-rate dependent cardiac output in some cases and such patients may find difficulty in

tolerating beta-blockers. Digitalis and calcium channel blockers may be selectively concentrated in amyloidotic tissue and are relatively contraindicated on grounds of increased toxicity (80-82) especially the latter, which can lead to rapid worsening.

Device therapy – Pacemakers or implantable cardioverter-defibrillators (ICDs) may not prevent sudden cardiac death, since this is thought to often be due to electromechanical dissociation.(83,84) In the absence of evidence, pacing indications remain within current standard guidelines. High defibrillator thresholds may be encountered and the benefits of such devices remain uncertain.(83) (85,86) Biventricular pacing appears to play little role. (87)

Cardiac transplantation – Cardiac transplantation has played a disappointingly small role, due to the multisystem nature of amyloidosis, advanced age, treatment related complications, and rapid disease progression. As a result, only a few dozen cardiac transplants have ever been performed for amyloidosis. However, the long-term outcome can be good in highly-selected patients with AL amyloidosis.(88) Cardiac transplantation followed by successful peripheral blood autologous stem cell transplant (ASCT) was associated with better survival in selected patients as reported (89) from most major amyloidosis units in the UK,(88) France,(90) Germany(91) and the USA.(92) For variant ATTR, combined cardiac and liver transplantation has been performed in a few dozen cases throughout the world.(88,89,93,94)

6.6.2 AMYLOID SPECIFIC TREATMENTS

Reducing amyloid fibril precursor protein production – Treatment is currently based on the concept of reducing the supply of the respective amyloid fibril precursor protein.

In AL amyloidosis, therapy is directed towards the clonal plasma cells. Achieving a haematological response in AL amyloidosis translates into improved overall survival and complete haematologic responses (CR; defined as a normal ratio of κ to λ FLC in the serum and negative serum and urine immunofixation) and very good partial haematologic responses (VGPR; defined as difference in level of involved and uninvolved FLC [dFLC] <40 mg/l) are associated with the best clinical outcomes(42,95). A new paradigm for the treatment of AL amyloidosis has been proposed in which the underlying haematologic disorder and the end-organ damage should be monitored using FLC assays and cardiac biomarkers, respectively, to optimize therapy and minimize toxicity.(96) Treatment regimens for AL amyloidosis are administered by haematologists and were adapted from regimens that were developed for multiple myeloma, although most patients with AL amyloidosis have a low-grade plasma cell dyscrasia and small clonal burden. Treatment for AL amyloidosis is based on age, regimen toxicities and cardiac involvement that currently is based on Troponin and brain natriuretic peptide levels (97). Outcomes in patients with AL amyloidosis have improved following the introduction of effective chemotherapy regimens.

Currently, the treatment regimens that are most widely used to treat AL amyloidosis include combinations that contain bortezomib (cyclophosphamide, bortezomib and

dexamethasone), melphalan (melphalan and dexamethasone), thalidomide (cyclophosphamide, thalidomide and dexamethasone) and lenalidomide (lenalidomide and dexamethasone). High-dose melphalan in combination with autologous stem cell transplantation is associated with excellent clinical outcomes,(98,99) but rigorous selection of suitable patients is required owing to the excessive risk of treatment-related mortality in certain individuals with AL amyloidosis, particularly those with substantial cardiac or autonomic nerve involvement.(100)

ATTR is produced almost exclusively in the liver. Liver transplantation has been used as a treatment for variant ATTR for 20 years, to remove genetically variant TTR from the plasma. Although this is a successful approach in ATTR Val30Met, it has had disappointing results in patients with other ATTR variants which often involve the heart. The procedure commonly results in progressive cardiac amyloidosis through on-going accumulation of wild-type TTR on the existing template of variant TTR amyloid.(101) The role of liver transplantation in non-Val30Met associated hereditary TTR amyloidosis thus remains very uncertain. Exercise training post-surgery can be helpful however.(102)

ATTR amyloidosis has lately become a focus for novel drug developments aimed at reducing production of TTR through silencing RNA and antisense oligonucleotide therapies (103) (104,105).

Inhibition of amyloid formation – Amyloid fibril formation involves massive conformational transformation of the respective precursor protein into a completely different form with a predominantly β-pleated sheet structure. The hypothesis that this

conversion might be inhibited by stabilising the fibril precursor protein through specific binding to a pharmaceutical product has lately been explored in ATTR amyloidosis. A key step in TTR amyloid fibril formation is the dissociation of the normal TTR tetramer into a monomeric species that can auto-aggregate into a misfolded form. *In vitro* studies identified that diflunisal, a non-steroidal anti-inflammatory analgesic bound by TTR in plasma, enhances the stability of the normal soluble structure of the protein.(106,107) Preliminary clinical data showed that diflunisal may reduce the rate of neurological impairment and preserve quality of life in patients with FAP.(108)

Tafamidis is a compound without anti-inflammatory analgesic properties that has a similar mechanism of action. Tafamidis has been licensed for neuropathic ATTR but its role in cardiac amyloidosis remains uncertain.(109) Higher affinity 'superstabilizers' are also in development.(110)

Targeting Amyloid Deposits – Amyloid deposits are remarkably stable, but the body evidently has some limited capacity to remove them. Following treatment that prevents the production of new amyloid, e.g. successful chemotherapy in AL type, amyloid deposits are gradually mobilised in the majority of patients, though at different rates in different organs and between individuals. Unfortunately clearance of amyloid is especially slow in the heart, and echocardiographic evidence of improvement is rare, even over years.

The challenge of developing a therapeutic monoclonal antibody that is reactive with all types of amyloidosis is currently being addressed by targeting SAP, since this is a universal constituent of all amyloid deposits and an excellent immunogen. Anti-SAP

antibody treatment is clinically feasible because circulating human SAP can be depleted in patients by the bis-d-proline compound CPHPC, thereby enabling injected anti-SAP antibodies to reach residual SAP in the amyloid deposits (Figure 9).(111) The unprecedented capacity of this novel combined therapy to eliminate amyloid deposits in our phase I study recently published in NEJM is encouraging and seems be applicable to all forms of human systemic and local amyloidosis(112).

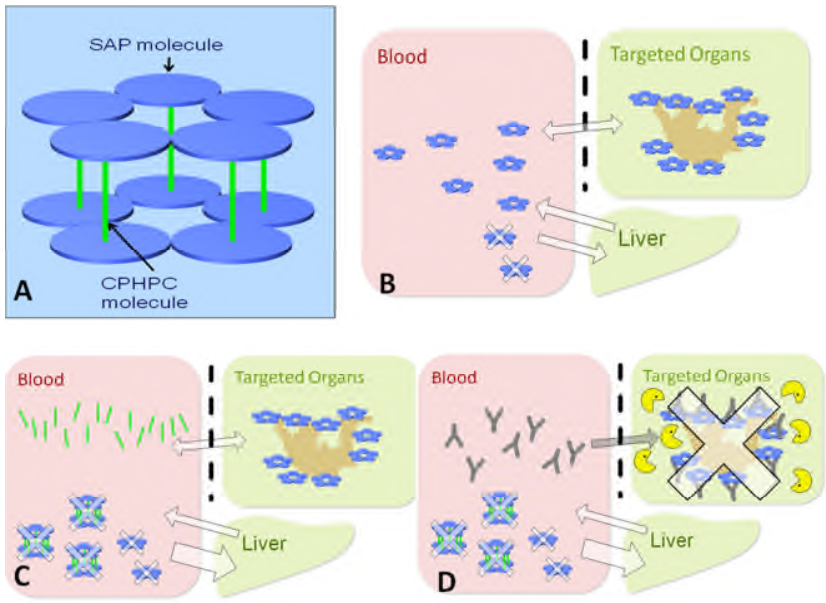

Figure 9. CPHPC, SAP and anti-SAP antibody.

Showing (A) cross-linking of SAP by CPHPC molecule; (B) Circulating SAP in a patient with amyloidosis, showing the normal level of "coating" of amyloidotic organs by SAP and baseline low-level sequestration of circulating SAP by the liver; (C) Addition of CPHPC causing cross-linking of SAP in the blood and subsequent high level excretion of SAP from blood by the liver; (D) Addition of the anti-SAP antibody causing removal of SAP coating from amyloidotic organs, allowing immune system to destroy the amyloid in the target organ. Picture courtesy of Dr Duncan Richards, GSK.

7. RESEARCH AIMS

This thesis investigates the use and development of novel CMR methods to improve the diagnostic accuracy, risk stratification and gain pathophysiology insights in amyloidosis. This thesis is built on the work of others – key methods were developed at Heart Hospital by my colleagues: (a) Dr Andrew Flett (UCL MD (Res), 2012) who designed and validated EQ-CMR (Equilibrium contrast CMR) to measure myocardial fibrosis in aortic stenosis and HCM; (b) Dr. Daniel Sado (UCL MD (Res), 2013) who explored ECV (again for fibrosis) across a variety of cardiac diseases; (c) Dr. Sanjay Banypersad (UCL MD (Res), 2015) who explored ECV (here for amyloid burden) for the investigation of the extracellular space of heart, liver and spleen in AL amyloidosis. My thesis built on these.

My aims were:

1- Methodology: Improve the technique currently used to measure ECV with the use of newer, faster sequences (ShMOLLI) to measure the extracellular volume.
2- To assess the diagnostic accuracy of non-contrast techniques (native T1) to detect cardiac involvement in ATTR amyloidosis.
3- Improve the understanding of the pathophysiology of the disease: understand the myocardial response to amyloid: is there cell hypertrophy or cell loss in response to amyloid infiltration? Is the myocyte response different in AL and ATTR?
4- Deliver a test suitable for use in clinical practice: to explore the potential of a widely available technique (LGE PSIR approach) to improve risk stratification of patients with cardiac amyloidosis.

8. MATERIAL AND METHODS

8.1 ETHICAL APPROVAL

All ethics were approved by the UCL/UCLH Joint Committees on the Ethics of Human Research Committee, and all participants provided written informed consent.

8.2 PATIENTS

PATIENTS WITH AL AND ATTR AMYLOIDOSIS

A total of 250 consecutive patients were scanned from the NAC over the course of 3 years. These patients were usually attending the NAC for a 24 or 32 hour period in order to have ECG, echo, SAP scan and a clinical consultation. All CMR scans were performed at the Heart Hospital and it was therefore necessary to transport patients from the NAC to the Heart Hospital and back in between their other numerous investigations. This was a limitation of the recruitment process.

Patients were categorized as follows:

- AL 119
- ATTR 122
- Mutation carriers 9

Before having their CMR scan, AL patients were sub grouped into their pre-test probability of having cardiac involvement as follows: (113)

Definite cardiac involvement – any of:

- Left ventricular wall thickness of ≥12mm by echocardiography in the absence of any other known cause
- RV free wall thickening co-existing with LV thickening by echocardiography in the absence of systemic or pulmonary hypertension

Possible cardiac involvement – any of:

- LV wall thickening by echocardiography in the presence of hypertension
- RV thickening by echocardiography in the presence of pulmonary hypertension
- Normal wall thickness by echocardiography with diastolic dysfunction and raised serum biomarkers (7)

No suspected involvement

- Normal wall thickness by echocardiography with normal serum biomarkers

Before having their CMR scan, ATTR patients were sub grouped into their pre-test probability of having cardiac involvement as follows:

Definite cardiac involvement – any of:

- cardiac biopsy showing ATTR amyloid;
- non-cardiac biopsy showing ATTR amyloid in association with left ventricular/right ventricular thickening in the absence of other explanatory causes;

- intense DPD uptake in heart (grade 2 or 3 as defined by Perugini *et al)* in the absence of a plasma cell dyscrasia;*(47)*
- non-cardiac biopsy showing presence of ATTR amyloid and LGE consistent with cardiac amyloid - In practice, all had apparent left ventricular hypertrophy (LVH).

Possible cardiac involvement:

- minimal cardiac DPD uptake (grade 1 as defined by Perugini et al(47) in the absence of LVH – in practices, none of these had LVH.

No suspected involvement:

- Normal wall thickness by echocardiography with normal serum biomarkers and no cardiac uptake on DPD.

HEALTHY VOLUNTEERS AND OTHER DISEASE COHORT

65 normal subjects were recruited through advertising within the hospital, university and general practitioner surgeries. All normal subjects had no history or symptoms of cardiovascular disease or diabetes. Four subjects had been prescribed statin therapy for hypercholesterolaemia (primary cardiovascular prevention), but no other normal subject was taking any cardiovascular medication. All subjects had a normal blood pressure, 12 lead electrocardiogram and clinical CMR scan.

Patients with HCM (n=46) or aortic stenosis (AS) (n=18) were prospectively recruited from tertiary clinical and research departments at the Heart Hospital or the National Amyloidosis Centre, Royal Free Hospital.

These scans (healthy individuals, HCM and AS) were performed and reported by Dr. Daniel Sado, Dr. Viviana Maestrini and Dr Steve White as a comparator group for ECV studies within our group.

8.3 CARDIOVASCULAR MAGNETIC RESONANCE PROTOCOL

All scans were performed on a 1.5 Tesla Siemens™ Avanto scanner and images always acquired during breath-hold at end expiration.

PILOT IMAGES:

All studies started with single shot pilot images with the following settings: repeat time (TR): 3.39ms, echo time (TE): 1.7ms, slice thickness, 5mm, field of view (FOV) 360 x 360mm, read matrix 256 and flip angle 60^{o}.

CINE IMAGES:

After piloting, steady state free precession (SSFP) cine imaging was then undertaken, firstly in the long axis planes with a short axis cut through the aortic valve. A standard LV short axis stack was then acquired using a slice thickness of 7mm with a gap of 3mm. Retrospective ECG gating was used with 25 phases. Typical fast imaging with steady state precession (FISP) imaging parameters were TE: 1.6ms, TR: 3.2 ms, in plane pixel size 2.3 x 1.4mm, slice thickness 7mm, flip angle 60°. These settings were optimised accordingly if the subject was unable to breath-hold, or had an arrhythmia etc..

T1 AND ECV MEASUREMENT

T1 measurement pre-contrast was performed using:

(a) FLASH-IR (in 100 subjects, 50 healthy volunteers and 50 patients, see chapter number 8) at increasing inversion times from 140 to 800ms (or 900ms if patient heart rate permitted), “multibreath-hold technique”.

(b) ShMOLLI T1 mapping “single breath-hold technique”, (in all patients). After a bolus of Gadoterate meglumine, (0.1 mmol/kg, gadolinium-DOTA, marketed as Dotarem © Guerbet S.A. France) and standard LGE imaging, at 15-minute post bolus, an infusion at a rate of 0.0011 mmol/kg/min contrast (equivalent to 0.1 mmol/kg over 90 minutes) was given. The patient was typically removed from the scanner at this time. At between 45 minutes and 80 minutes post bolus, the patient was returned to the scanner, still with the infusion, and the T1 measurement repeated using both multi and single breath-hold techniques. Separate regions of interest (ROIs) were placed in all available images and recovery curve was reconstructed by fitting the relaxation formula to ROI averages. Heart rate correction was used for the multibreath-hold technique (9). In the ShMOLLI sequence, T1 maps were generated using previously published algorithm (12). A single ROI was drawn directly in each T1 map at the same location as the multibreath-hold technique and T1 averaged between all pixels. T1 was measured in the basal to mid septum avoiding areas of late gadolinium enhancement, except in myocardial infarction (where the infarct zone was assessed) and amyloid (where the regions was drawn irrespective of the ill-defined

presence/absence of LGE). The blood T1 was assessed in the descending aorta. All the analysis were performed blinded.

A single ROI was drawn directly in the septum in each 4 chamber T1 map performed prior to contrast administration and at equilibrium. A haematocrit was taken in all subjects on the same day. Five different parameters were calculated (114):

1- Native myocardial T1

2- ECV = (1 - haematocrit) x ($\Delta R1_{myocardium}$ / $\Delta R1_{blood}$)

3- ICV= 1 - ECV

4- Total Amyloid Volume = ECV x $LVmass_i$

5- Total Cell Volume = ICV x $LVmass_i$

For test:retest interstudy reproducibility, 10 normal subjects and 7 patients with amyloid underwent repeat scanning, one week apart. The analysis was carried out by a single observer blinded.

LGE IMAGING

Intravenous Gadoterate meglumine (gadolinium-DOTA, marketed as Dotarem® Guerbet, S.A., France) was then administered as a 0.1mmol/kg dose via a pressure injector at a rate of 3ml/sec, with a 25ml normal saline flush. LGE assessment was then undertaken using a FLASH IR sequence. Magnitude reconstruction was available in all patients (MAG-IR) phase sensitive inversion recovery sequences (PSIR) reconstructions the later 43% of patients. Slice thickness 8 mm, TR: 9.8 ms, TE: 4.6ms, α: 21^o, FOV 340 x 220 mm (transverse plane), sampled matrix size 256 x 115-135, 21 *k*–space lines acquired

every other RR interval (21 segments with linear reordered phase encoding), spatial resolution 1.3 x 2.1 x 8 mm, no parallel imaging, pre-saturation bands over CSF and any pleural effusions.

These parameters were optimised according to individual patient characteristics. The TI was manually set to achieve nulling of the myocardium between 300 and 440 ms. When LGE was observed, images were acquired in phase swap and cross cut to ensure artefact elimination. Where the LGE distribution appeared particularly diffuse, a TI scout was used to ascertain the specific parts of myocardium with the highest concentration of gadolinium. If the participant was struggling with the breath-hold, FISP imaging or IR-SSFP imaging (single shot or segmented) was used as an alternative sequence.

8.4 BLOOD PRESSURE AND 12 LEAD ECG

All patients had their blood pressure (BP) measured at the National Amyloidosis Centre on a CareScape™ V100 machine by the nursing staff as part of their routine workup. In the healthy volunteer cohort, BP was measured after their CMR scan by Dr. Daniel Sado and Dr. Viviana Maestrini using a Mindray™ machine.

A 12 lead ECG was performed on all patients at the National Amyloidosis Centre on the same day as the CMR scan, as part of their clinical work up. The ECG was acquired using a calibration of 10 mm/mV and speed of 25 mm/s. Interpretation of the trace was performed by myself. Healthy volunteers followed an identical protocol.

8.5 BLOOD TESTS

All participants had blood tests taken prior to the CMR scan at the National Amyloidosis Centre as part of their clinical workup. This included NT-proBNP and serum free light chain in all cases, with Troponin T in just over half the cases as this is only routinely performed on new patients.

8.6 SIX MINUTE WALKING TEST (6MWT)

This was performed at the Heart Hospital (where the test was originally developed) along a flat corridor in accordance with current guidelines.(115) Patients were asked to walk a 30-metre length of the corridor at their own pace while attempting to cover as much ground as possible in the 6-minute period. Verbal encouragement was given using either of 2 standardised phrases: ‘‘You are doing well’’ or ‘‘Keep up the good walk.’’ At the end of 6 minutes, participants were asked to stop and the distance covered was recorded. Any symptoms were recorded, as was the Borg score (on a scale of 1-10) to assess the degree of breathlessness.(116)

7.8 ECHOCARDIOGRAPHY

In all patients, transthoracic echocardiography was performed at the National Amyloidosis Centre on a Philips® IE33 machine as a part of the routine clinical work up. Echo studies, included tissue doppler just above the mitral valve annulus at the septal and left ventricular lateral wall. Scans were performed and analysed by 2 echocardiographers experienced in scanning patients with cardiac amyloidosis. Accepted markers of diastolic dysfunction i.e. isovolumic relaxation time (IVRT), E-deceleration time and E:E’ ratio were

all measured.(117) Echocardiography was not used to assess left ventricular systolic function for this work, as CMR was seen as the gold standard in this regard.(118)

7.10 DPD SCINTIGRAPHY

Most of the ATTR patients had DPD scans (instead of SAP scans) by the time of their appointment though this was not always possible because of time and scanner limitations on the day. Where performed, Patients were scanned using two General Electric (GE) Medical Systems hybrid SPECT-CT gamma cameras (Infinia Hawkeye 4 and Discovery 670) following administration of 700 MBq of intravenously injected 99mTc-DPD.Three hour (delayed) whole body planar images were acquired followed by a single photon emission computed tomography (SPECT) of the heart with a low-dose, non-contrast CT scan. Gated/non-gated cardiac SPECT reconstruction and SPECT-CT image fusion was performed on the GE Xeleris workstation. Cardiac retention of 99mTc-DPD was visually scored as: Grade 0 - no visible myocardial uptake in both the delayed planar or cardiac SPECT-CT scan; Grade 1 - cardiac uptake on SPECT-CT only or cardiac uptake of less intensity than the accompanying normal bone distribution; Grade 2 – moderate cardiac uptake with some attenuation of bone signal; and Grade 3 – strong cardiac uptake with little or no bone uptake.

7.11 STATISTICAL ANALYSIS

Statistical analysis was performed using IBM SPSS Statistics Version 19 (IBM, Somers, New York) and R programming language (available at http://www.r-project.org/).

All continuous variables were normally distributed (Shapiro-Wilk), other than NT-proBNP and Troponin T which were therefore log transformed; these are presented as mean ± standard deviation (SD) (non-transformed NT-proBNP as median and interquartile range).

Comparisons between groups were performed by 1-way analysis of variance with post-hoc-Bonferroni correction. The chi-square test or Fisher exact test was used to compare discrete data as appropriate. Receiver-operating characteristic (ROC) curve analysis was performed to define the diagnostic accuracy of native T1. Correlations between were assessed using Pearson (*r*) or Spearman's rho.

We used Intraclass Correlation Coefficient (ICC) and Bland-Altman plot to compare ECV values from the two methods. Interstudy reproducibility for ECV was assessed by calculating the ICC and Bland Altman plots. To compare the squared difference of paired ECV measurements Wilcoxon signed rank test was used. To assess the agreement of the assignment of the LGE pattern by two different observes, ICC was calculated.

Survival was evaluated using Cox proportional hazards regression analysis, providing estimated hazard ratios (HR) with 95% confidence intervals (CI) and Kaplan Meier curves. Variables selected *a priori* for the clinical relevance and first explored with univariate Cox regression were entered in the multivariable models. Multivariable models evaluated the independent predictive value of LGE above other clinically and statistically significant covariates. Harrell's C statistic was calculated for the different models.

A p value <0.05 was considered statistically significant.

9. RESULTS: COMPARISON OF T1 MAPPING TECHNIQUES FOR ECV QUANTIFICATION

This chapter is based on the publication below:

Fontana M, White SK, Banypersad SM, Sado DM, Maestrini V, Flett AS, Piechnik SK, Neubauer S, Roberts N, Moon JC. Comparison of T1 mapping techniques for ECV quantification. Histological validation and reproducibility of ShMOLLI versus multibreath-hold T1 quantification equilibrium contrast CMR. J Cardiovasc Magn Reson. 2012;14:88.

My contribution was analysing all the data as first operator, doing the statistical analysis and writing the paper.

9.1 INTRODUCTION

ECV can be measured non-invasively by CMR using pre and post contrast T1 relaxation times of blood and myocardium (the latter at sufficient contrast equilibrium) with correction for the blood volume of distribution via the haematocrit. (119,120) A number of T1 measurement techniques exist including multibreath-hold techniques such fast low angle single shot inversion recovery ("multibreath-hold FLASH-IR"). Here the sequence is performed at increasing inversion times to generate T1 recovery curves and heart rate correction.(121,122) Newer, faster sequences such as MOLLI (Modified Look-Locker Inversion recovery)(123) perform IR measurements in a single breath-hold. A recent evolution of MOLLI, the Shortened-MOLLI (ShMOLLI) (124) improves clinical utility with a shorter breath-hold and immediate map reconstruction directly on the scanner. ECV measurements have been performed and validated using MOLLI for bolus-only protocols. Equilibrium contrast CMR (EQ-CMR) with single breath-hold sequences has not yet been

validated for ECV assessment. ECV mapping with such sequences would be a significant technical advance, being easier for patients with shorter breath-holds (either shorter scans or whole heart coverage) and easier quantification.

9.2 HYPOTHESIS

We hypothesised that ECV mapping using ShMOLLI would be superior to the multibreath-hold FLASH-IR technique. This was assessed in three ways: firstly, to determine any bias in ECV between the two techniques. Secondly, we compared both CMR techniques with histological collagen volume fraction (CVF%). Finally, we assessed the reproducibility of both CMR techniques. For equivalence of contrast conditions between the two techniques, we used the primed infusion technique, equilibrium contrast CMR.

9.3 MATERIALS AND METHODS

CMR PROTOCOL

After ethical approval, subjects underwent CMR as described in the methods. For this study, T1 measurement pre-contrast was performed using (a) FLASH-IR at increasing inversion times from 140 to 800ms (or 900ms if patient heart rate permitted), “multibreath-hold technique”, Figure 10a and (b) ShMOLLI T1 mapping “single breath-hold technique”, Figure 10b. After a bolus of Gadoterate meglumine, (0.1 mmol/kg, gadolinium-DOTA, marketed as Dotarem © Guerbet S.A. France) and standard LGE imaging, at 15-minute post bolus, EQ-CMR was performed as described in the methods. A single ROI was drawn directly in each T1 map at the same location as the multibreath-hold technique and T1 averaged between all pixels (Figure 10b) and ECV was calculated as described in the

methods.

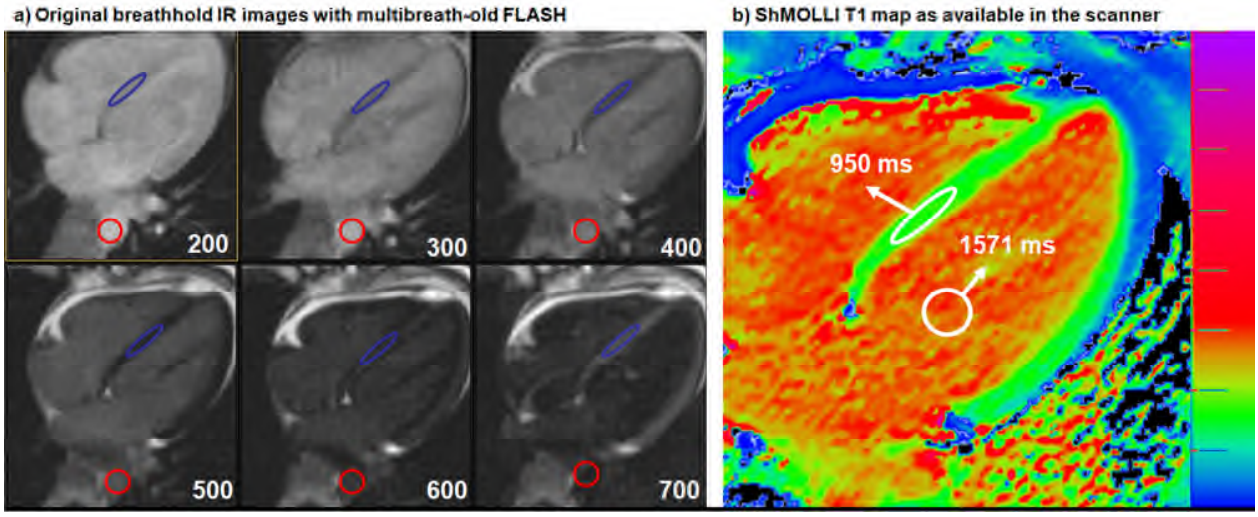

Figure 10. Native T1 measurement example.

Left multiple panels: the multibreath-hold T1 measurement uses up to 7 CMR acquisitions with linearly increasing inversion time. T1 value is reconstructed from fitting average signal intensity from individual image intensity averages. Right single panel: ShMOLLI technique generates T1 map directly on the scanner console using pixelwise calculations based on a single breath-hold experiment. ShMOLLI T1 is calculated as average of all pixels from a region of interest drawn in the myocardium.

PATIENT STUDIES: HEALTHY NORMAL SUBJECTS AND DISEASE GROUPS

Normal subjects (n=50, median age 47±17, 53% male) were recruited. Patients (n=50) were: (1) 12 patients with HCM meeting the diagnostic criteria (average age 52±13, 60% male). (2) 18 patients with severe aortic stenosis waiting for aortic valve replacement (median age: 71±10, 72% male). (3) 20 patients with cardiac AL amyloidosis with disease proven by non-cardiac biopsy and cardiac involvement ascertained through echocardiography, supported by a Mayo clinic classification score of 2 or 3 (average age: 60±10, 75% male). Patients with atrial fibrillation or a contra-indication to contrast CMR examination were excluded.

Histological Validation

24 patients with severe aortic stenosis listed for surgical aortic valve replacement were studied. An intraoperative deep myocardial biopsy (Tru-Cut needle) was taken in aortic stenosis. Samples were stained and analysed for CVF%, as previously described.(121) 6 patients were excluded (2 patients had focal fibrosis detected as LGE in the basal septum; 2 patients had biopsies consisting solely of endocardial fibrosis; in 1 patient multibreath-hold T1 quantification was not performed because the patient was unable to breath-hold; 1 patient had a pulmonary oedema during the scan) leaving 18 patients.

Reproducibility

For test:retest interstudy reproducibility, 10 normal subjects and 7 patients with amyloid underwent repeat scanning, one week apart. The analysis was carried out by a single observer blinded.

Data Analysis and Statistics

Intraclass Correlation Coefficient (ICC) and Bland-Altman plot compared ECV values from the two methods and Interstudy reproducibility. To compare the squared difference of paired ECV measurements Wilcoxon signed rank test was used.

9.4 RESULTS

ECV COMPARISON

No patients failed ShMOLLI acquisition. 6% of patients were unable to perform all the 14 breath-holds required for the multibreath-hold technique. The mean ECV assessed using multibreath-hold T1 quantification and ShMOLLI T1 in normal subjects and disease groups is shown in table 1. ECV by multibreath-hold T1 quantification and by ShMOLLI T1 mapping showed excellent correlation (r^2=0.892) and agreement across disease groups (overall ICC 0.922, 95% CI 0.802 to 0.961, p<0.0001), figure 11a, with little bias on Bland Altman (bias -2.2%, 95%CI -8.9% to 4.6%), figure 11b.

	Multibreath-hold T1 ECV (%)	ShMOLLI ECV (%)
Normal subjects (n=50)	26±3	27±3
HCM (n=12)	28±4	30±3
AS (n=18)	27±6	31±5
Amyloid (n=20)	48±6	52±7

Table 1. Multibreath-old T1 and ShMOLLI T1 in normal subjects and disease groups.

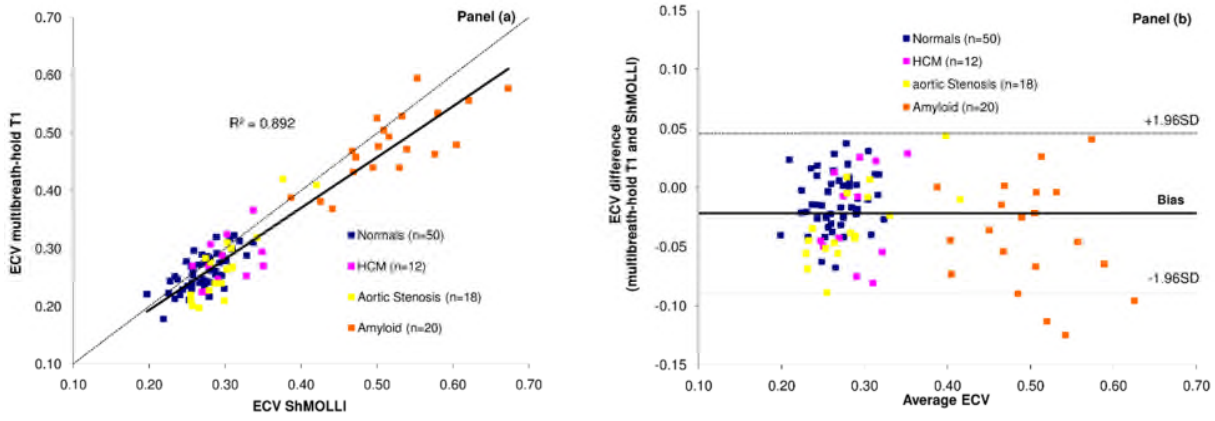

Figure 11. Sh-MOLLI and multibreath-hold ECV correlation and Bland-Altman.

Sh-MOLLI and multibreath-hold ECV correlation in health and disease (panel a) and the same data plotted as a Bland-Altman analysis (panel b), showing little bias.

HISTOLOGICAL VALIDATION

All biopsies were uneventful. The mean histological CVF of the 18 biopsies was 18% ± 8% (range 7% to 40%). There was a strong correlation between histological CVF% and FLASH ECV (r^2= 0.589) but this was stronger with ShMOLLI ECV (r^2= 0.685) (Figure 12).

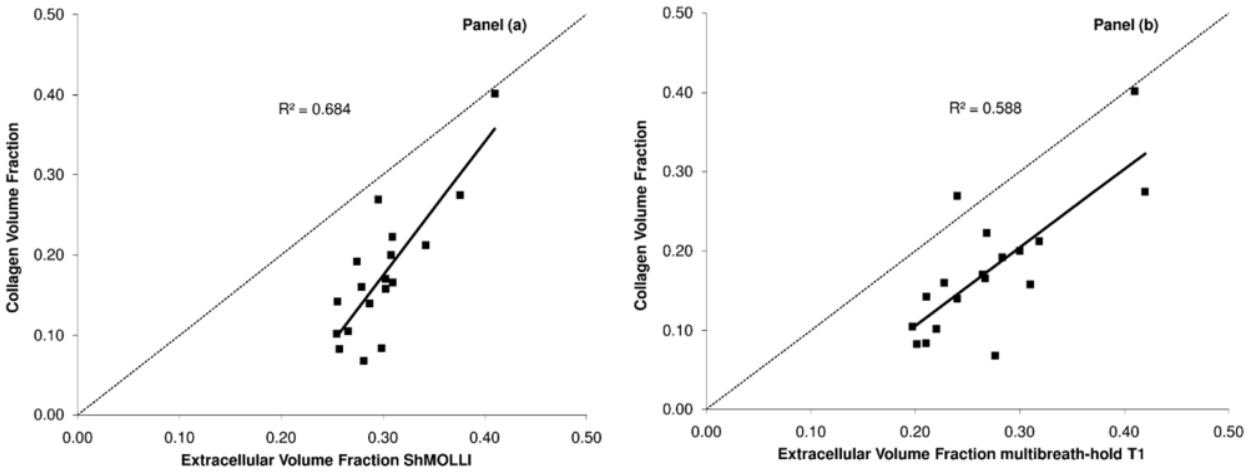

Figure 12. Extracellular volume (ECV) against collagen volume fraction (CVF%).

ECV against histological CVF% (n=18) by ShMOLLI (panel a) and multi-breath-hold (panel b).

INTERSTUDY REPRODUCIBILITY

ShMOLLI ECV was slightly more reproducible than the multibreath-hold ECV, Figure 13, (ICC 982, 95%CI 0.951-0.994 versus ICC 962, 95%CI 0.897-0.987), with narrower confidence intervals (95%CI -4.9% to 5.4% versus 95%CI -6.4% to 7.3% respectively). Neither of these reached statistical significance however , P>0.2.

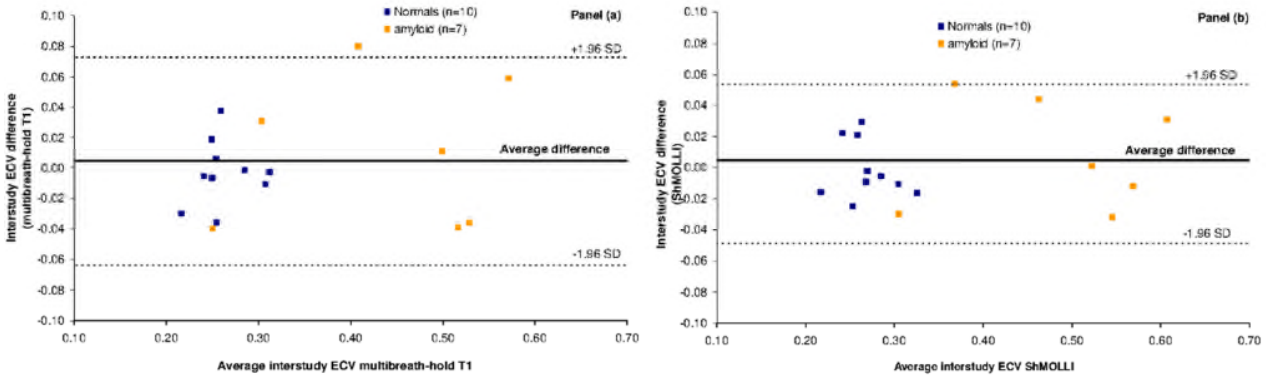

Figure 13. Bland-Altman: T1 values using FLASH-IR and ShMOLLI.

Bland-Altman analysis to express the intrasequence reproducibility of the myocardial T1 values using FLASH-IR (panel a) and ShMOLLI (panel b) in normal subjects (blu square) and amyloid patients (orange square). The limits of agreement are slightly narrower for ShMOLLI than multibreath-hold.

9.5 DISCUSSION

CMR ECV quantification requires accurate and rapid T1 relaxation time calculation. We have found that ShMOLLI compared to multibreath-hold T1 quantification has a greater chance of technical success on all patients, less bias over a wide range of ECV measurements, a higher correlation with histological CVF% as well as better reproducibility. These four findings combine with key advantages of the mapping technique: a single breath-hold per T1 map, simple analysis and the potential for whole heart ECV quantification. Therefore, it is our opinion that T1 mapping technique ShMOLLI is the superior CMR technique for ECV quantification.

T1 mapping by means of the multi-breath-hold technique is one of the most commonly utilised methods for T1 quantification.(121,122) The main advantage of this technique is that it is not vendor specific and it has been heavily optimised by everyday clinical practice

to obtain high resolution LGE images. However it also has a number of limitations. Firstly, in order to map a single cardiac slice, it requires the sequence to be run up to 9 times at increasing inversion times. The average breath-hold time for each sequence is 14 seconds (longer at slower heart rates). If the patient cannot hold their breath for the duration of the sequence, artefact will appear on any one of the images. This may also occur if the patient has an arrhythmia. As each slice takes so many breath-holds to map, this method can not be used clinically for whole heart mapping (i.e. of multiple cardiac slices). Once the images have been obtained, the offline post processing is laborious and the results require heart rate correction for the calculated T1 relaxations times.(121)

We have found that ECV quantification using ShMOLLI improves on several practical aspects compared to multibreath-hold T1 quantification. ShMOLLI imaging is characterised by lower breath-hold failure rate, less bias over a wide range of ECV, a slightly higher correlation with histological collagen volume fraction and slightly better reproducibility, although it does not reach statistical significance. Shorter acquisition times and direct T1 map calculation on the scanner (124) ensures ShMOLLI is quicker to perform and analyse with a potential to provide whole heart ECV quantification. While currently ShMOLLI is (was) vendor specific, its predecessor MOLLI exists for more than one platform (126)(13).

Future techniques for T1 measurement are likely to be based on mapping. Further advances may include higher resolution imaging with reduction of partial volume effects, with that incorporate motion correction and improved capabilities for measuring longer T1s.(127-130) We preferred here to re-iterate the T1 map for maximum accuracy – a step

that will likely be un-necessary in future refinements. Preliminary exploration is being made of combining the two T1 maps into an ECV map using further non-rigid registration.(122)

This study has limitations. We have not presented the phantom work comparing ShMOLLI and FLASH-IR T1 estimation as this was primarily an ECV clinically-orientated paper with many of the likely confounders present only in-vivo and not detectable by phantom work. Histology correlations were lower than previously described.(121) We believe this is primarily due to different population characteristics (the population examined here is older) and to a greater number of surgeons involved in the biopsy arm of this study (with associated reduced homogeneity of samples). Finally, FLASH-IR was compared to a single T1 mapping technique, ShMOLLI. MOLLI, its variants and other T1 mapping techniques were not considered in this study.

As ECV quantification experience increases, technology will advance to become more precise, accurate and automated (see later). This study was the first such paper and demonstrated that single breath-hold ShMOLLI T1 mapping can quantify ECV by EQ-CMR across the spectrum of interstitial expansion, and that it is clinically more straightforward with improvements in reproducibility and histological correlation when compared to the older multibreath-hold FLASH techniques.

10. RESULTS: NATIVE MYOCARDIAL T1 MAPPING IN TRANSTHYRETIN AMYLOIDOSIS

This chapter is based on the publication below:

Fontana M, Banypersad,SM, Treibel TA, Maestrini V, Sado DM, White SK, Pica S, Castelletti S, Piechnik SK, Robson MD , Gilbertson JA, Rowczenio D, Hutt DF, Lachmann HJ, Wechalekar AD, Whelan CJ, Gillmore JD, Hawkins PN, Moon JC. Native myocardial T1 mapping in transthyretin amyloidosis. JACC Cardiovasc Imaging. 2014 Jan 2.

My contribution was recruiting, consenting and performing the scans of all the ATTR patients and 50 % of AL patients. I have analysed all the data as first operator, done the statistical analysis and wrote the paper.

10.1 INTRODUCTION

Cardiac ATTR amyloidosis is a progressive and often fatal disorder that may be greatly under diagnosed and is certainly an underappreciated cause of heart failure in the elderly and specific ethnic populations. ATTR amyloid deposits are present in 8-16% of hearts at autopsy in the over 80 year olds.(131) One particular TTR variant, V122I, which confers susceptibility to amyloid cardiomyopathy has a population prevalence of 3-4% in Afro-Caribbeans(132) and a 10% frequency among individuals of this ethnicity who present with heart failure.(133)

Diagnosing cardiac ATTR amyloidosis is often challenging. A suggestive constellation of ECG, echocardiography and biomarker findings are found mainly in advanced disease, but interpretation may be confounded by common comorbidities such as left ventricular hypertrophy, diabetes, diastolic dysfunction and renal disease.(134-136) The challenging

diagnosis and lack of validated quantitative investigations to monitor the course of the disease pose unique problems at a time when new specific therapies for ATTR amyloidosis are emerging.(137)

New imaging modalities are however showing promise. Technetium-labelled bone scintigraphy tracers, notably 3,3-diphosphono-1,2-propanodicarboxylicacid (DPD), localise strikingly to hearts infiltrated by ATTR amyloid(47) whilst CMR LGE produces a characteristic appearance.(138) However, neither is truly quantitative and both have limitations.(139)

Recently, native myocardial T1 mapping has been shown in cardiac AL amyloid to track disease.(140) Here, we assess this test in patients with ATTR amyloidosis.

10.2 Hypothesis

We hypothesised that the native myocardial T1 would be elevated in this disease, that elevation would correlate with other disease markers (e.g. intensity of DPD uptake), and that T1 elevation would be an early marker of disease.

10.3 Materials and Methods

Amyloidosis patients

A total of 172 individuals were categorized into 3 groups:

ATTR AMYLOID PATIENTS

Eighty-five consecutive, consenting patients with cardiac ATTR amyloidosis (70 male; age 73±10) were recruited. The presence of cardiac amyloid was defined by presence of ATTR amyloid in a myocardial biopsy or positive DPD scintigraphy. Eighty two percent (n=70) had histological proof of ATTR amyloidosis by Congo red and immunohistochemical staining of myocardial (n=30, 35%) or other tissues (n=40, 47%). All patients underwent sequencing of exons 2, 3, and 4 of the *TTR* gene. Before having their CMR scans ATTR patients were sub grouped into their pre-test probability of having cardiac involvement (no, possible and definite cardiac involvement) as described in chapter 7.

TTR GENE CARRIERS

8 *TTR* gene carriers (n=8; 3 male; age 47±6) defined as individuals with pathogenic *TTR* gene mutation but no evidence of disease (no cardiac uptake on 99mTc-DPD scintigraphy and normal echocardiography, CMR, NT-proBNP and Troponin T). This group constituted the non-cardiac involvement group.

AL AMYLOID PATIENTS

79 patients with biopsy proven systemic AL amyloid (55 male; age 62±10), the biopsies being from the myocardium (n=6, 8%) or other tissues (n=73, 92%). Before having their CMR scans AL patients were sub grouped into their pre-test probability of having cardiac involvement (no, possible and definite cardiac involvement) as described in chapter 7. These were compared with 46 patients with hypertrophic cardiomyopathy (HCM) and 52 healthy volunteers:

HYPERTROPHIC CARDIOMYOPATHY (HCM) PATIENTS

46 patients with HCM (n=46; age 50±13, 34 male) fulfilling diagnostic criteria.(141) Seventy-two percent of patients had an asymmetrical septal hypertrophy pattern, with the remainder apical predominant hypertrophy. Sixty percent of patients had LV outflow tract obstruction. Seventy-six percent of patients were found to have LGE in a variety of locations, such as at the right ventricular insertion points or the left ventricular apex.

HEALTHY VOLUNTEERS

52 healthy volunteers (n=52, age 46±15, 17 male) were recruited as described in the methods.

All patients and healthy controls underwent 12-lead ECG. Cardiac amyloid patients/carriers additionally underwent assays of cardiac biomarkers (N-terminal pro-brain natriuretic peptide [NT-proBNP] and Troponin T), echocardiography, a 6-minute walk test where health and patient choice permitted (e.g. arthritis, postural hypotension, neuropathy).The ATTR group also underwent DPD scintigraphy. See chapter 7 for more details on the methods. The baseline characteristics of all patients are provided in Table 2. All ethics were approved by the UCL/UCLH Joint Committees on the Ethics of Human Research Committee.

EXCLUSION CRITERIA

All patients with contraindications to CMR: glomerular filtration rate <30 mL/min, incompatible devices.

	TTR mutation carriers	Possible ATTR	Definite ATTR	Definite AL	HCM	Healthy controls
N	8	9	76	45	46	52
Men/women	3/5	3/6	68/8	33/12	34/12	17/35
Age, yrs	47±6	67±15	73±9	63±9	50±13	46±15
Afro-Caribbean (n)	0	1	24	2	3	1
eGFR, ml/min/1.73 m^2	82±14	82±15	62±19	74±20	66±7	92±16
NT-proBNP, pmol/L	7.5(4.7-9.7)	14(10-85)	286(165-524)	194(160-457)	66(19-114)	-
AF/atrial flutter,%	0	0	33	11	2	0
CMR indices						
EDV_i, ml/m^2	67±13	61±9	70±15	62±16	68±14	73±12
ESV_i, ml/m^2	21±8	20±12	33±15	24±9	17±9	25±7
LVEF, %	69±7	69±15	53±15	61±11	75±8	67±6
SV_i, ml/m^2	46±7	41±6	36±9	38±12	51±9	48±15
LV $mass_i$, g/m^2	60±11	74±18	133±27	101±25	129±42	65±6
LAA_i, cm^2/m^2	13±2	12±3	16±3	14±3	15±5	11±1

Table 2. Baseline characteristics of patients and healthy controls.

AL, light-chain amyloidosis; ATTR, transthyretin amyloidosis; TTR transthyretin protein; eGFR, estimated glomerular filtration rate; NT-proBNP, N-terminal pro-brain natriuretic peptide; AF, atrial fibrillation; CMR, cardiovascular magnetic resonance; EDV_i, end diastolic volume indexed; ESV_i end systolic volume indexed; LVEF, left ventricular ejection fraction; SV_i, stroke volume indexed; LV, left ventricular; LAA_i left atrial area indexed.

CMR PROTOCOL

All subjects underwent standard CMR - see methods, including volumes, LGE and T1 mapping with ShMOLLI. For native T1 mapping, a basal and mid ventricular short-axis and a 4-chamber long-axis were acquired using the shortened modified look-locker inversion recovery (ShMOLLI) sequence after regional shimming (Figure 14).

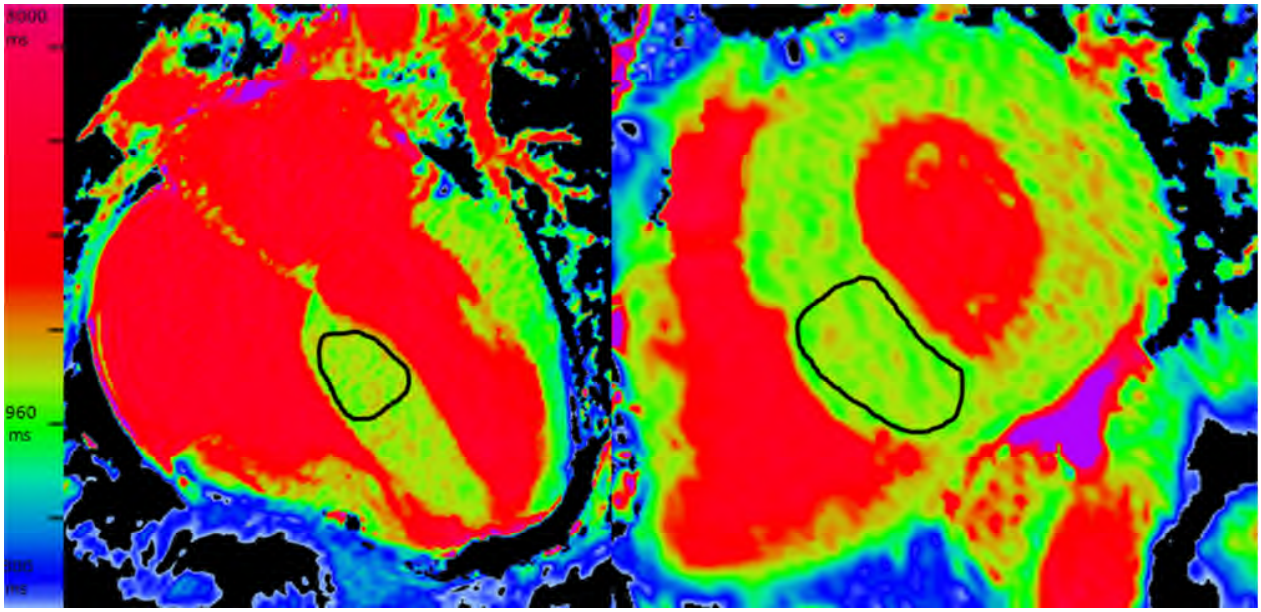

Figure 14 Examples of ROIs in ShMOLLI.

(A) pre-contrast 4 chamber and (B) pre-contrast short axis ShMOLLI image with ROIs drawn in the basal septum of LV for native myocardial T1.

99mTc-DPD SCINTIGRAPHY

Patients were scanned using two General Electric (GE) Medical Systems hybrid SPECT-CT gamma cameras (see chapter 7 for more details). Cardiac retention of 99mTc-DPD was visually scored (see chapter 7 for details)

CMR IMAGE ANALYSIS

For T1 measurements, the basal ventricular short-axis or the 4-chamber ShMOLLI image were manually contoured approximately 2 pixels in (to minimize partial volume effects) from the endocardium and epicardium, and the average T1 value was calculated, figure 14. This was drawn without review of the LGE images. The LGE images were visually analyzed for the presence or absence of enhancement blinded to T1 mapping results. The

presence of LGE was classified as: circumferential in the subendocardium; diffuse circumferential (extend into the epicardial layer); and abnormal contrast handling on T1 scout with no discernible LGE.

STATISTICAL ANALYSIS

See methods.

10.4 RESULTS

Eighty-five patients with ATTR amyloid, 8 *TTR* mutation carriers and 79 patients with AL amyloid were enrolled. These were compared with 52 healthy volunteers and 46 patients with HCM. Baseline characteristics are shown in Table 2. Amyloid patients had the following co-morbidities: treated hypertension (22% ATTR, 15% AL); diabetes (12% ATTR, 3% AL); angiographically confirmed coronary artery disease (13% ATTR, 9%). The echocardiogram was performed within one day of the CMR. The time gap between the DPD and CMR was 26±36 days. Thirty-five ATTR amyloid patients were familial (V122I [n = 18], T60A [n = 6], V30M [n = 2], E54G [n = 2], and all others unique: D38Y,G47V, E89K, I84S,I107F, L12P,S77Y); 50 had SSA. Of the 8 gene carriers, 5 had *TTR* V30M and 3 T60A. Compared to definite cardiac AL patients, definite ATTR amyloid patients had a higher LV mass indexed (133±27 vs 101±25) reduced EF (53±15 vs 61±11). The PR interval and QRS were longer in ATTR (PR 209±54ms vs 185±38ms, QRS 116±28ms vs 106±23ms, both $p<0.05$). NT-proBNP and Troponin T were similar.

T1 Elevation

ATTR T1 was elevated compared to HCM and normals (1097±43ms vs 1026±64ms vs 967±34ms, both p<0.0001), but was not as high as AL (AL 1130±68ms, p=0.01), and was not elevated in mutation carriers (n=952±35ms), figure 15 and 16.

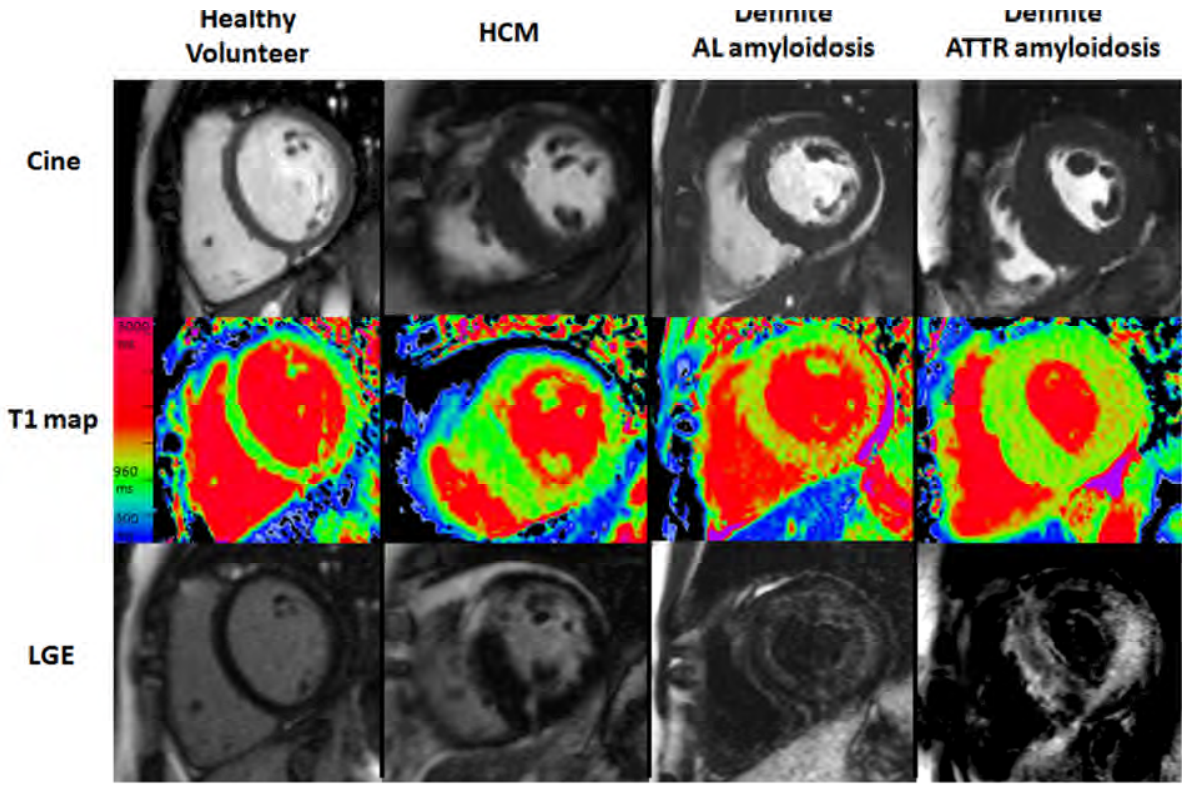

Figure 15. Characteristic examples from CMR scans.

CMR end-diastolic cine still (upper panel); ShMOLLI native T1 map (middle) and late gadolinium enhancement (LGE) images (lower) in (left to right) healthy volunteer, HCM, definite AL and definite ATTR patients.

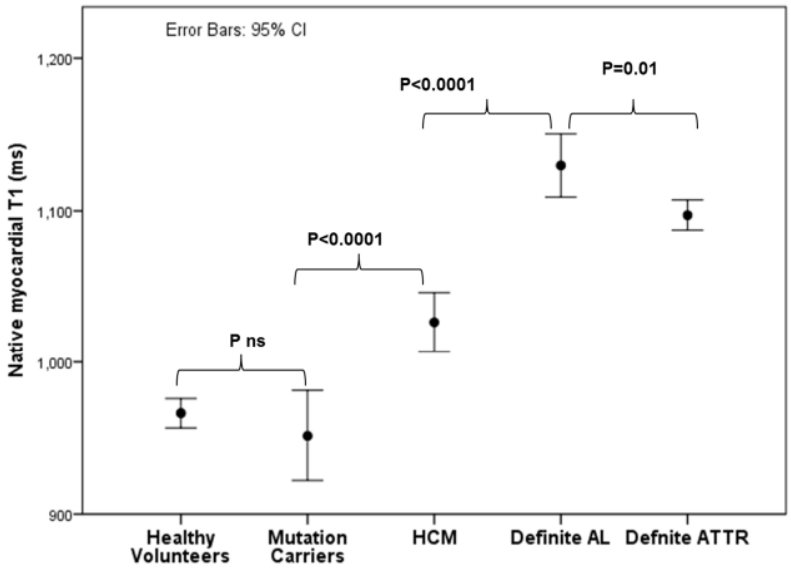

Figure 16. Native T1 in healthy volunteers, mutation carriers, HCM, definite AL and definite ATTR.

Mean native myocardial T1±2 standard error (SE) in healthy controls subjects, gene carriers, patients with definite AL cardiac amyloid and patients with definite ATTR cardiac amyloidosis.

T1 Diagnostic accuracy

ROC curve analysis was performed for the discrimination of possible or definite cardiac amyloid from the meaningful combined differentials of HCM, systemic amyloid without detected cardiac involvement or ATTR mutation positive patients without evidence of cardiac amyloid. Using ROC analysis, ATTR and AL amyloid patients with possible or definite cardiac involvement had an area under the ROC curve of 0.85(95%CI 0.79-0.92).

Example cut-off values to diagnose cardiac amyloid (high specificity) are 1048ms, 1065ms, 1090ms. These have 80%, 85%, 90% specificity and 83%, 74%, 56% sensitivity respectively. Example cut-off values to rule out cardiac amyloid (high sensitivity) are

954ms, 968ms, 1012ms. These have 99%, 98%, 95% sensitivity and 17%, 30%, 58% specificity respectively. Native T1 was similarly accurate for AL and ATTR (AUC 0.84 95%CI 0.76-0.91, AUC 0.85 95%CI 0.77-0.92 respectively), figure 17.

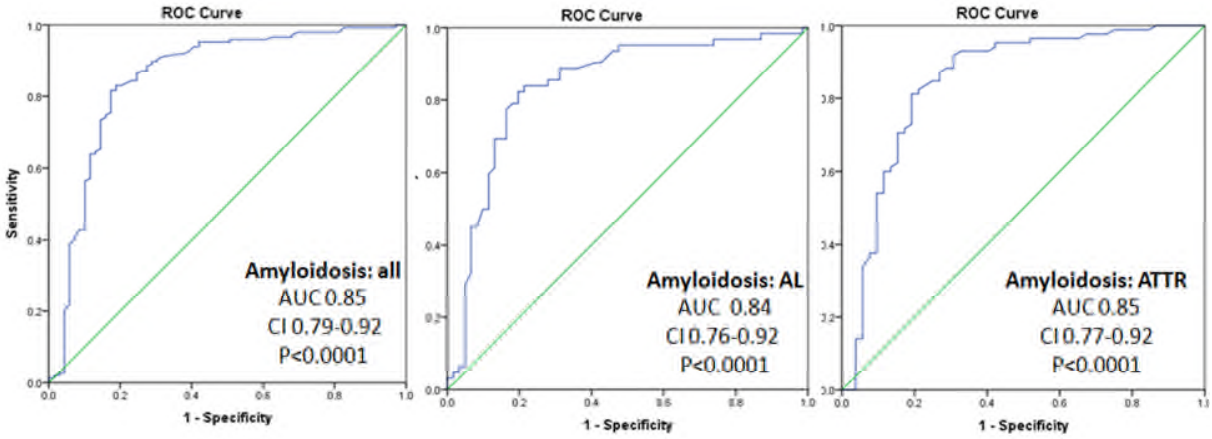

Figure 17. ROC curve for native T1.

Receiver operating characteristic (ROC) curve for the discrimination of possible or definite cardiac amyloid by native myocardial T1 from the clinically significant differentials of HCM; systemic amyloid without detected cardiac involvement or ATTR mutation positive patients without apparent cardiac amyloid for: a) cardiac amyloid, type unspecified (AL and ATTR); b) AL amyloid alone; c) ATTR amyloid alone.AUC= area under the curve.

T1 AND DPD/LGE FINDINGS

T1 increased with increasing cardiac amyloid burden as assessed by bone scintigraphy, ($p<0.0001$ for trend), figure 18. T1 was not elevated in mutation carriers (n=952±35ms) but was in the 9 patients with isolated DPD grade 1 (1037±60ms, $p=0.001$), all of which had no amyloid-like LGE (but one had inferior myocardial infarction, one had RV LGE).

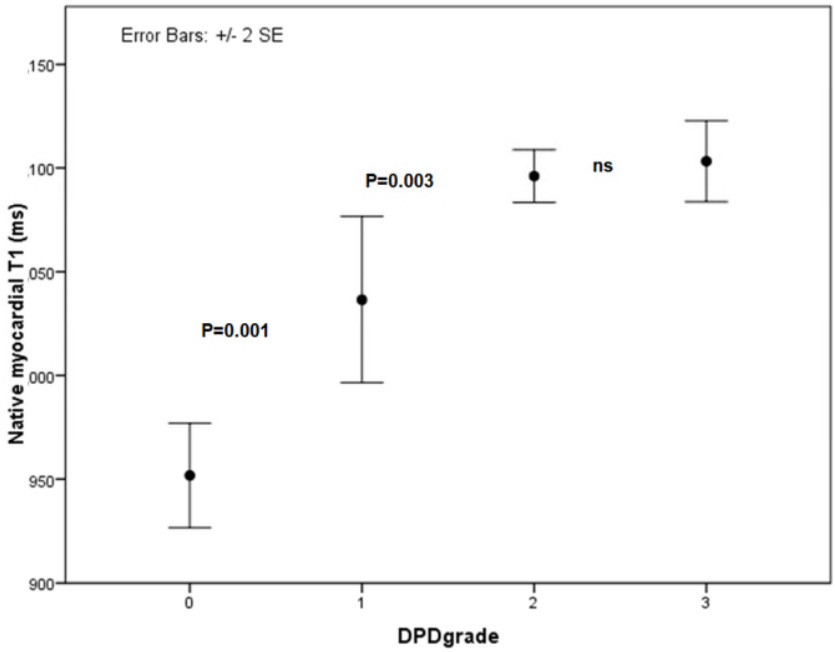

Figure 18. Native T1 and DPD grade.

Mean native myocardial T1±2 standard error (SE) in gene carriers and ATTR patients according to different degrees of uptake on the 99TcDPD scintigraphy.

T1 and Cardiac Function, Blood Biomarkers, ECG and 6 MWT

Correlations were broadly similar for AL and ATTR disease (Table 3). T1 correlated with indices of systolic and diastolic function, indexed LV mass and known prognostic biomarkers both in ATTR and AL amyloid patients. In ATTR patients, T1 correlated with indexed left atrial area, 6 min walking test performance and PR and QRS duration on ECG, whereas in AL patients, T1 correlated with indexed stroke volume, ECG limb lead mean voltage and E deceleration time, table 3.

	ATTR patients (R)	AL patients (R)
LV structure by MRI		
LV $mass_i$, g/m^2	0.62*	0.44*
LA $area_i$,cm^2/m^2	0.31*	0.058
LV systolic function by CMR		
LVEF, %	-0.22*	-0.36*
SV_i,ml/m^2	-0.151	-0.28†
LV diastolic function by echo		
E/E'	0.32*	0.47*
E-deceleration time, ms	-0.106	0.41*
6 minutes walking test	-.32	-0.147
Biomarkers		
NT-proBNP, pmol/L	0.57*	0.56*
Troponin T, pmol/L	0.57*	0.32†
ECG		
PR, ms	0.32†	0.073
QRS, ms	0.26†	0.077
ECG limb lead mean voltage	-0.151	-0.48*

Table 3. Correlations between T1 and cardiac function, biomarkers, ECG and 6 MWT in ATTR and AL patients.

R = Pearson correlation coefficient; AL, light-chain amyloidosis; ATTR, transthyretin amyloidosis; NT-proBNP, N-terminal pro-brain natriuretic peptide; CMR, cardiovascular magnetic resonance; EDV_i, end diastolic volume indexed; ESV_i end systolic volume indexed; LVEF, left ventricular ejection fraction; SV_i, stroke volume indexed; LV, left ventricular; LAA_i left atrial area indexed. * P< 0.01 level; †P<0.05.

10.5 DISCUSSION

In this, the largest ever (at that time – my later studies are larger) CMR study in patients with amyloidosis, we found that native myocardial T1 mapping has a high diagnostic accuracy for cardiac amyloid for both AL and ATTR when compared against HCM, a relevant clinical differential diagnosis. Furthermore, T1 tracks cardiac amyloid burden in both diseases, and is more sensitive for detecting early disease in gene mutation carriers

than LGE imaging. In both amyloid types, T1 tracks markers of systolic and diastolic function, mass and prognostic markers. In ATTR amyloid, T1 additionally correlates with ECG PR and QRS duration and indexed left atrial area whereas in AL type, it correlates with reductions in limb lead voltages. T1 also has functional associations with a reduction in 6 minute walk test in ATTR amyloidosis. Interestingly and perhaps unexpectedly,(143) T1 elevation was lower in ATTR compared to AL type.

Amyloidosis is considered the exemplar of an interstitial disease, the quantity of amyloid in the extracellular space amounting to kilograms overall in some patients and able to constitute the majority of the heart by weight at times.(144)

Our earlier work in AL amyloidosis demonstrated that measurement of myocardial T1 times using ShMOLLI had high diagnostic accuracy (against aortic stenosis) and tracks disease burden.(140) Here, this work is extended to ATTR –and the diagnostic accuracy was tested against hypertrophic cardiomyopathy, a relevant clinical differential. Although T1 was raised in ATTR amyloid, it was not as high as in AL type, a surprising finding given that ventricular wall thickness is greater in ATTR amyloid.(143) T1 mapping measures a composite tissue signal from both cells and the interstitium. The extent and/or distribution of amyloid, plus how it interacts with water or changes in the myocyte signal, could all be implicated in causing the T1 difference. Native myocardial T1 measures a composite signal from both the intracellular and extracellular space. Therefore the less raised T1 value found in patients with ATTR amyloidosis could be due to (amongst others), a lower amyloid burden, less hydration of the amyloid, less collagen associated with amyloid or differential effects on the intracellular signal. Finally AL may have additional processes

occurring, such as oedema from possible light chain toxicity. (9) (145) Further work is needed. Many differences in the biology of ATTR and AL cardiac amyloidosis have been described but are not understood. This study shows specific differences between AL and ATTR in their correlations with other parameters, for example the positive correlations in ATTR amyloid of T1 with left atrial area, PR and QRS duration and negative correlations in AL type of T1 with mean QRS voltage in the limb leads. These findings support the concept of ATTR amyloid being a more purely infiltrative disease but AL having a dual pathology with contributions from interstitial expansion and cell death.

Native myocardial T1 yielded high diagnostic accuracy in ATTR and AL amyloidosis against the common clinical differential diagnosis of HCM. These findings combine a number of key advantages of the mapping technique namely, the absence of need for contrast, a single breath-hold per T1 map, simple analysis and the potential for measurement of whole heart T1.Other investigators have proposed bone scintigraphy using the DPD tracer as the non invasive “gold standard” for diagnosis of cardiac ATTR amyloid.(146) However, this is semi-quantitative and is scored in 4 grades based on visual estimation; although the radiation dose is low, serial follow-up is problematic for gene mutation carriers. Native T1 showed high concordance with DPD scintigraphy and T1 was measured on a continuous scale, a possible advantage. DPD scanning dichotomises mutation carriers into DPD negative or DPD grade 1. T1 was exactly concordant with this dichotomy, with T1 elevation and DPD grade 1 patients having no other abnormalities (no hypertrophy, no biomarker elevation, no amyloid related LGE), suggesting both methods identify the earliest disease expression. These preliminary findings require further

confirmation in larger, particularly multicentre, studies with assessment of diagnostic and prognostic performance. In native T1 measurement, there is the potential for age and gender biases. Some of these biases may be about partial voluming and may have reducing relevance in hypertrophied hearts. The disease biology means that the ATTR and AL populations have a different age of presentation, with ATTR older and more male. The HCM patients and the controls are younger. Data on age dependant changes in T1 are conflicting. A subtle trend in increasing T1 measurement has been detected in the MESA study (r^2=0.021, 5ms/decade in men but not women)(147), but a reduction in T1 with age in women but not men with ShMOLLI(148). Fortunately, most of the effect sizes detected here are large compared to the potential biases, and some of them go in the opposite direction to a confounding bias: for example, the (10 years younger) ALs have more T1 elevation than the ATTR patients by 33ms – the *opposite* way to the age related bias that most experts expect to exist. The ATTRs are 82% male whereas AL is 72% male. A male:female difference in T1 is not found in the over 45s in the Piechnik paper(148), but even if the 24ms difference found in the young males vs females was present, this would make only a ~3ms overall difference, ~10% of the difference found in this paper. Furthermore, ATTR had more hypertension, coronary artery disease and diabetes. All these might be expected to contribute to increase in T1 times in ATTR – the opposite trend to that found, but potentially leading to a possible underestimation of the difference between AL and ATTR patients.

The main limitation of this study is the lack of histological validation of the technique. This is challenging because diagnosis in many patients was secured following biopsy of non-

cardiac sites, and it was not ethical to obtain cardiac biopsies for research given its invasive nature. Furthermore, quantification of amyloid (rather than presence/absence) is challenging in myocardial biopsies due to its often patchy and microscopic distribution. The second limitation is lack of biopsy evidence of amyloid in 18% of ATTR patients. However this cohort of patients was fully characterized with all the other clinical investigative techniques currently available. When combined, these are known to provide high diagnostic accuracy. CMR extracellular volume measurement was not included in this study. No follow-up data are available at this time. T1 mapping is yet to be standardized across manufacturers, although efforts are underway to do this. In our paper we analysed only a single region of interest in the septum. A segmental or whole heart approach should be explored in the future.

In conclusion, native myocardial T1 mapping detects cardiac ATTR amyloid and has similar performance for diagnosis and tracking disease in both ATTR and AL amyloidosis.

The lower T1 elevation in ATTR amyloid, and the specific differences between AL and ATTR correlations with other cardiac findings, may support a concept of ATTR amyloid being a more purely infiltrative disease but AL type having a dual pathology with both interstitial expansion and cell death.

11. RESULTS: MYOCYTE RESPONSE IN AL AND ATTR CARDIAC AMYLOIDOSIS

With the work described in this chapter I won the Early Career Award at SCMR 2014.

This chapter is based on paper below.

Fontana M, Banypersad SM, Tribel TA, Maestrini V, Abdel-Gadir Amna, Lane T, Gilbertson JA, Hutt DF, Lachmann HJ, Whelan CJ, Wechalekar AD, Herrey AS, Gillmore JD, Hawkins PN, Moon JC. Cardiac ATTR and AL amyloid deposits evoke differential myocyte responses: new pathophysiological insights from Cardiovascular Magnetic Resonance. Radiology. 2015 May 21:141744.

My contribution was recruiting, consenting and performing the scans of all the ATTR patients and 60% of AL patients. I have analysed all the data as first operator, done the statistical analysis and wrote the paper.

11.1 INTRODUCTION

The extent or severity of cardiac involvement in amyloidosis can be described by ventricular wall thickness, LV mass and the degree of transmurality of LGE on CMR (4,135,149-151). By these measures, ATTR is morphologically more severe than AL. Other measures, such as diastolic impairment, brain natriuretic peptide and troponin are higher in AL than ATTR (152), and, crucially, the prognosis is much worse in AL. This discordance is not understood (4,135) but has been ascribed to either a direct toxic effect of the amyloid in AL (153) or a faster rate of amyloid deposition in AL than ATTR leading to differences in the resulting myocardial damage. However, *in vivo* tools to assess the differences in the degree of amyloid deposition or myocyte response in ATTR and AL cardiac amyloid have not previously existed, leaving a knowledge gap of disease

pathophysiology that needs to be addressed to ensure optimal early phase clinical testing of the heterogeneous new amyloid therapies now in development (154).

CMR can now measure: 1- Native T1 signal, a composite signal from the interstitium and the cell, sensitive to extracellular amyloid (140), fibrosis (155), and particularly sensitive to myocardial edema, in which elevations may be very high (156); 2- ECV and Intracellular Volume fractions (ICV) (representing the fraction of myocardium, which is amyloid and cells, respectively (144)); 3- Total Amyloid Volume and Total Cell Volume, calculated by multiplying the ECV and ICV by the myocardial volume from cine images. (121,144).

11.2 HYPOTHESIS

We report here studies of these new *in vivo* CMR tools enabling amyloid and myocytes to be characterized and quantified separately, which elucidate substantial differences in the pathogenesis of AL and ATTR amyloidosis.

11.3 MATERIAL AND METHODS

AMYLOIDOSIS PATIENTS

A total of 210 patients were categorized into 3 groups:

AL AMYLOIDOSIS PATIENTS

92 patients with biopsy proven systemic AL amyloid (60 male; age 62±10), with biopsies from the myocardium (n=7, 8%) or other tissues (n=85, 92%). These 92 patients include 50 patients studied previously in an AL only study (144). Before having their CMR scans

ATTR patients were sub grouped into their pre-test probability of having cardiac involvement (no, possible and definite cardiac involvement) as described in chapter 7.

ATTR AMYLOIDOSIS PATIENTS

110 consecutive, consenting patients with cardiac ATTR amyloidosis (94 male; age 71±11) were recruited. The presence of cardiac amyloid was defined by presence of ATTR amyloid in a myocardial biopsy or positive technetium-labelled bone scintigraphy tracers, notably 3,3-diphosphono-1,2-propanodicarboxylicacid (DPD scintigraphy). Seventy percent (n=77) had histological proof of ATTR amyloidosis by Congo red and immunohistochemical staining of myocardial (n=32, 29%) or other tissues (n=45, 41%). All patients underwent sequencing of exons 2, 3, and 4 of the *TTR* gene. Before having their CMR scans AL patients were sub grouped into their pre-test probability of having cardiac involvement (no, possible and definite cardiac involvement) as described in chapter 7.

TTR GENE CARRIERS

8 *TTR* gene carriers (n=8; 3 male; age 47±6) defined as individuals with pathogenic *TTR* gene mutation but no evidence of disease (no cardiac uptake on DPD scintigraphy and normal echocardiography, CMR, N-terminal pro-brain natriuretic peptide [NT-proBNP] and Troponin T). This group constituted the non-cardiac involvement group.

HEALTHY VOLUNTEERS

47 healthy volunteers (n=47, age 45±15, 21 male) were recruited (see chapter 7 for more details). All patients and healthy controls underwent 12-lead ECG. Cardiac amyloid patients/carriers additionally underwent assays of cardiac biomarkers (NT-proBNP and

Troponin T), echocardiography, 6-minute walk test where health and patient choice permitted (e.g. arthritis, postural hypotension, neuropathy). The ATTR group also underwent DPD scintigraphy. The baseline characteristics of all patients are provided in Table 4.

	Definite AL	Definite ATTR	p
N	50	98	
Men/women	35/15	88/10	<0.05
Age, yrs	63±9	73±8	<0.001
eGFR, ml/min/1.73 m^2	74±23	58±19	<0.001
LV structure by CMR			
LV $mass_i$, g/m^2	107±30	134±28	<0.001
LA $area_i$,cm^2/m^2	14±3	17±3	<0.001
LV systolic function by CMR			
LVEF, %	62±11	53±15	<0.001
SV_i,ml/m^2	39±12	36±9	0.1
LV diastolic function by echo			
E/E'	17±9	16±5	0.7
E-deceleration time, ms	170±58	170±63	0.9
6 minutes walking test, meters	278±105	320±122	0.3
Biomarkers			
NT-proBNP, pmol/L	294 (132-518)	193 (350-595)	0.5
Troponin T, pmol/L	0.055 (0.02-0.08)	0.046 (0.06-0.08)	0.1
ECG			
PR, ms	189±43	215±55	<0.05
QRS, ms	106±24	117±27	<0.05

Table 4. Baseline characteristics of patients and healthy controls.

AL, light-chain amyloidosis; ATTR, transthyretin amyloidosis; TTR transthyretin protein; eGFR, estimated glomerular filtration rate; NT-proBNP, N-terminal pro-brain natriuretic peptide; AF, atrial fibrillation; CMR, cardiovascular magnetic resonance; EDV_i, end diastolic volume indexed; ESV_i end systolic volume indexed; LVEF, left ventricular ejection fraction; SV_i, stroke volume indexed; LV, left ventricular; LAA_i left atrial area indexed. * P< 0.01 level; †P<0.05.

EXCLUSION CRITERIA

All patients with contraindications to CMR: glomerular filtration rate <30 mL/min, incompatible devices.

CMR PROTOCOL

CMR included EQ-CMR with standard LGE (+/- PSIR) and T1 mapping using ShMOLLI. Regions of interest drawn without reference to the LGE images (157) (Figure 19). See chapter 7 for more details on the methods.

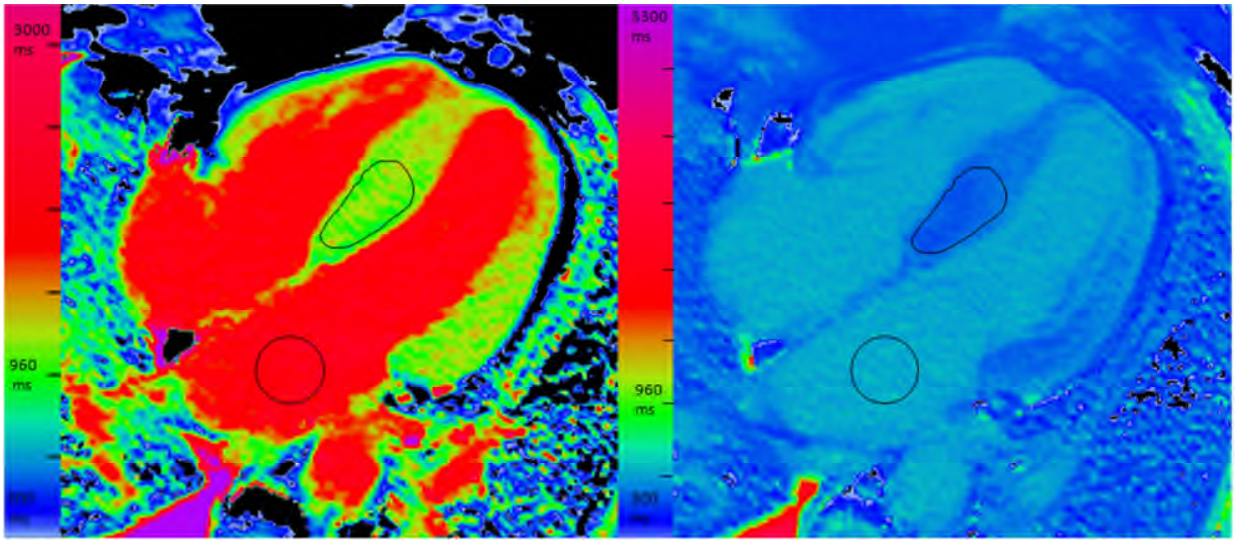

Figure 19. Examples of ROIs in ShMOLLI.

4-chamber ShMOLLI (A) pre-contrast and (B) post-contrast with ROIs drawn in the basal septum.

CMR IMAGE ANALYSIS

A single ROI was drawn directly in the septum in each 4 chamber T1 map performed prior to contrast administration and at equilibrium (Figure 19). A haematocrit was taken in all subjects on the same day. Five different parameters were calculated (114):

1- Native myocardial T1

2- ECV = (1 - haematocrit) x ($\Delta R1_{myocardium}$ / $\Delta R1_{blood}$)

3- ICV= 1 - ECV

4- Total Amyloid Volume = ECV x $LVmass_i$

5- Total Cell Volume = ICV x $LVmass_i$

STATISTICAL ANALYSIS

See methods (chapter 7).

11.4 RESULTS

The baseline characteristics of the 92 AL and 110 ATTR patients are shown in Table 4. Forty-four ATTR amyloidosis patients were familial (V122I [n = 22], T60A [n = 9], V30M [n = 3], E54G [n = 2], S77Y [n = 2] and all others unique: D38Y, G47V, E89K, I84S, I107F, L12P); 66 had senile systemic amyloidosis (SSA). Of the eight gene carriers, five had *TTR* V30M and 3 T60A. As expected, for the definite cardiac involvement AL and ATTR subsets, there were differences in cardiac function and morphology, table 4, with AL showing a lower LV mass indexed (107±30 g/m^2 vs 134±28 g/m^2, p<0.0001) and higher EF (62%±11% vs 53%±14%, p<0.0001). Differences in the ECG were present: the PR interval and QRS were shorter in AL (PR 189±43 ms vs 215±56 ms, QRS 106±24 ms vs 117±28 ms, both p<0.05). NT-proBNP and Troponin T biomarker concentrations were similar.

NATIVE T1, ECV, TOTAL AMYLOID VOLUME AND TOTAL CELL VOLUME IN AL AND ATTR

ECV and T1 were elevated in all types of amyloidosis compared to healthy volunteers (ECV: AL 0.54±0.07, ATTR 0.58±0.06 vs 0.27±0.03, both p<0.0001, T1: AL 1126±70ms, ATTR 1101±46ms vs 968±36ms, both p<0.0001) (Figure 20 and 21).

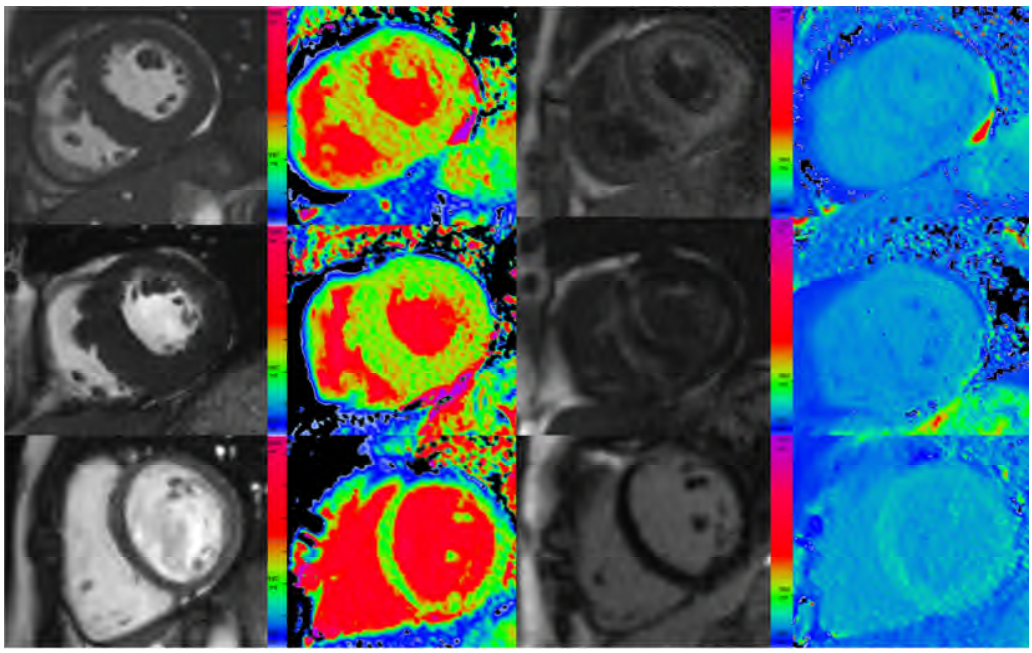

Figure 20. Characteristic example CMRs in AL, ATTR patients and healthy volunteer.

Characteristic examples from CMR scans in (upper, mid, lower panels) definite AL, definite ATTR patient and healthy volunteer. CMR end-diastolic cine still (left panel); ShMOLLI native T1 map (center left); late gadolinium enhancement (LGE) (middle right) and ShMOLLI T1 map at equilibrium.

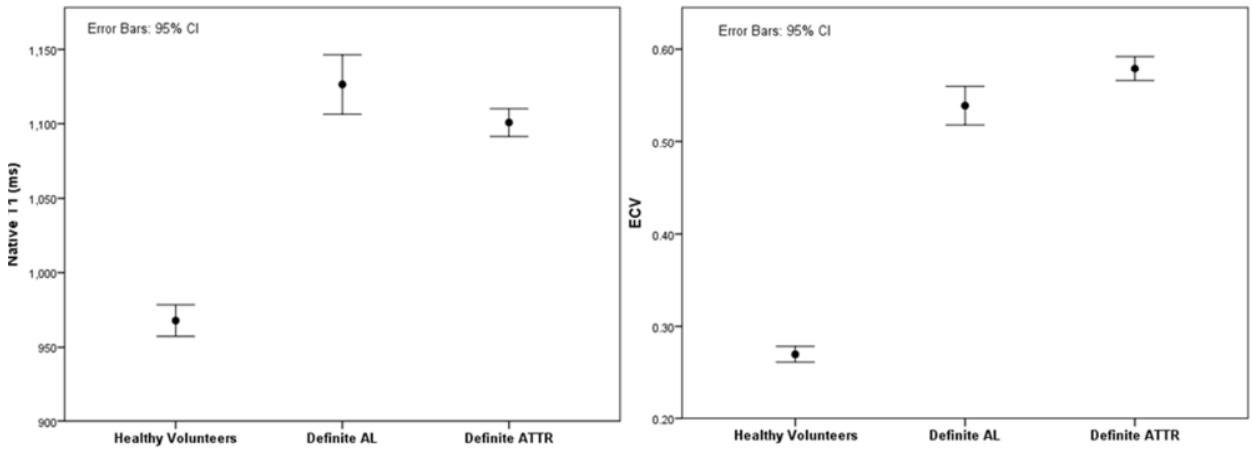

Figure 21. Native T1 and ECV in healthy volunteers, definite AL and definite ATTR.

Native T1 is higher in AL than ATTR – whereas ECV is higher in ATTR than AL. This discordance suggests an additional process is causing native T1 elevation in AL – potentially edema.

The extent of the elevation was discordant between AL and TTR: the ECV and Total Amyloid Volume were higher in ATTR (ECV 0.58±0.06 vs 0.54±0.07, p=0.001; Total Amyloid Volume 74±19ml/m^2 vs 54±15ml/m^2, p<0.0001), whereas native T1 was higher in AL (1126±70ms vs 1101±46ms, p<0.05) (Figure 21 and 22). ATTR had a higher Total Cell Volume than normal subjects (53±12ml/m^2 vs 45±11ml/m^2, p=0.001), but the Total Cell Volume in AL was unchanged (47±17ml/m^2 vs 45±11ml/m^2, p=1) (Figure 22).

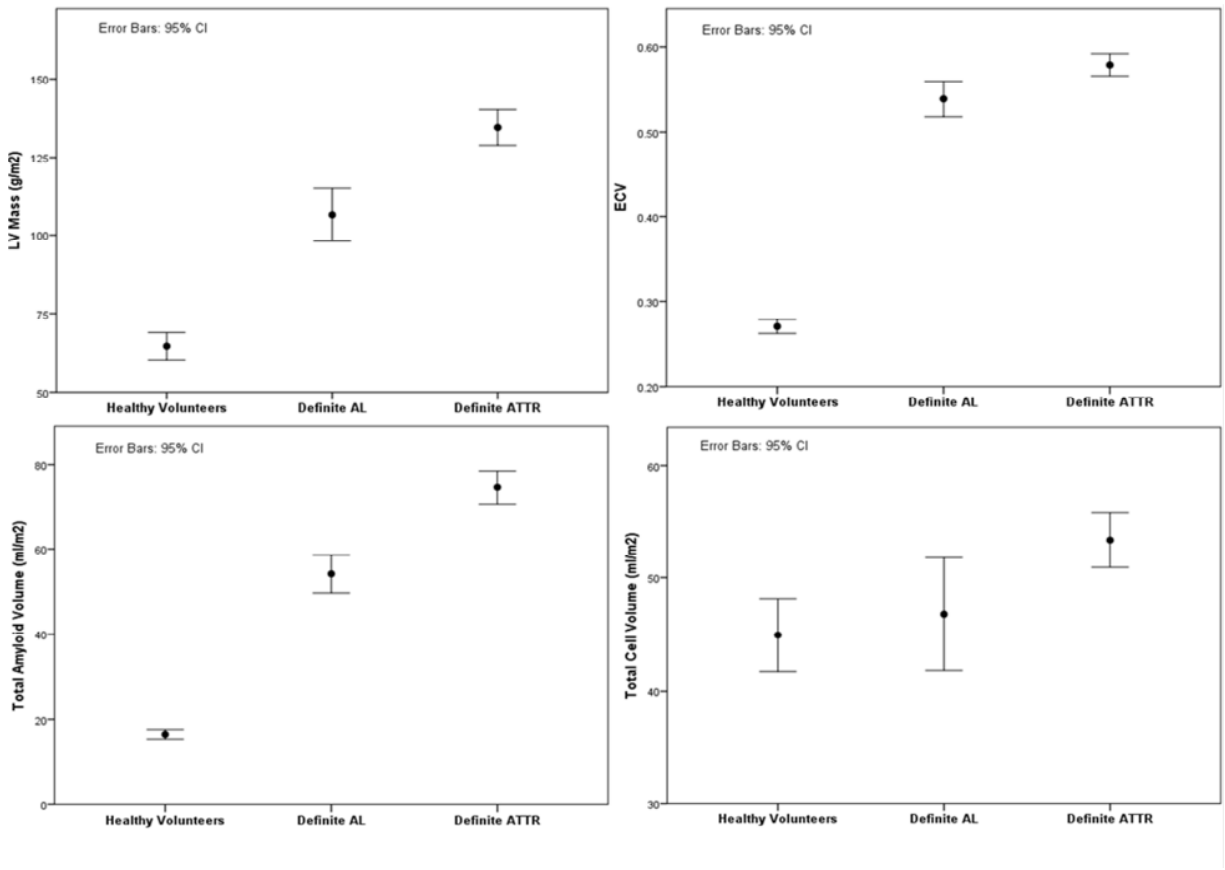

Figure 22. LV mass indexed, ECV, Total Amyloid Volume, Total Cell Volume in healthy volunteers, definite AL and definite ATTR.

LV mass indexed (left upper panel), ECV (right upper panel), Total Amyloid Volume (left lower panel), Total Cell Volume (right lower panel) in healthy controls subjects, definite AL cardiac amyloidosis and patients with definite ATTR cardiac amyloidosis.

ECV AND TOTAL CELL VOLUME ACCORDING TO THE DEGREE OF CARDIAC INVOLVEMENT

When AL and ATTR patients were divided according to the degree of cardiac involvement in three categories (no, possible and definite cardiac involvement) ECV increased between groups in both AL and ATTR (AL: 0.30±0.6 vs 0.40±0.07 vs 0.54±0.07, for all $p<0.0001$ ATTR: 0.27±0.03 vs 0.36±0.08 vs 0.58±0.06, for all $p<0.001$), (Figure 23).

The Total Cell Volume was discordant in AL and ATTR, as the total cell volume did not increase between groups in AL patients but increased in ATTR patients (AL: 47±14 vs 45±14 vs 47±17, p=1 for all; ATTR: 42±9 vs 44±10 vs 53±12, no cardiac involvement vs definite p<0.05, possible vs definite cardiac involvement p<0.05, other comparisons not significant), (Figure 23).

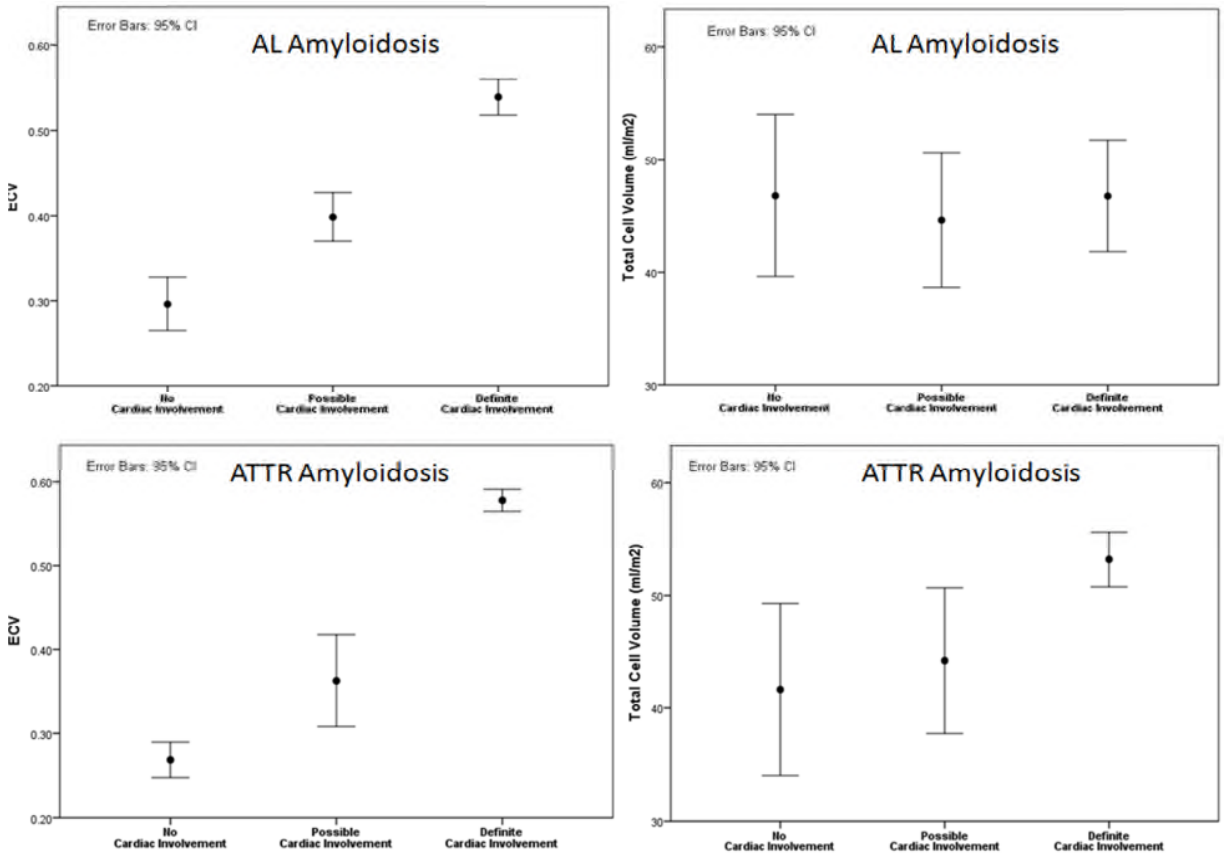

Figure 23. ECV and Total Cell Volume in AL and ATTR patients divided according to the degree of cardiac involvement.

ECV in AL (left upper panel), Total Cell Volume in AL (right upper panel), ECV in ATTR (left lower panel), Total Cell Volume in ATTR (right lower panel). * P< 0.01 level; †P<0.05.

T1 AND ECV AND CARDIAC FUNCTION, BIOMARKERS, ECG AND 6 MWT

Correlations were similar for T1 and ECV in AL and ATTR patients (Table 5). They correlated with indices of systolic and diastolic function, indexed LV mass and known prognostic biomarkers. All the correlations were stronger with ECV than native T1.

	T1 AL patients (R)	T1 ATTR patients (R)	ECV AL patients (R)	ECV ATTR patients (R)
LV structure by CMR				
LV mass$_i$, g/m^2	0.378*	0.617*	0.400*	0.699*
LA area$_i$,cm^2/m^2	0.076	0.303*	0.278†	0.427*
LV systolic function by CMR				
LVEF, %	-0.350*	-0.269*	-0.472*	-0.534*
SV$_i$,ml/m^2	-0.279*	-0.233†	-0.305*	-0.428*
LV diastolic function by echo				
E/E'	-0.258†	0.461*	0.306*	0.543*
E-deceleration time, ms	-0.255†	-0.54	-0.262†	-0.192†
6 minutes walking test, meters	-0.014	-0.295*	0.050	-0.387*
Biomarkers				
NT-proBNP, pmol/L	0.528*	0.571*	0.631*	0.795*
Troponin T, pmol/L	0.344†	0.508*	0.497*	0.688*
ECG				
PR, ms	0.137	0.377*	0.226	0.495*
QRS, ms	0.163	0.227†	0.199	0.240†
ECG limb lead mean voltage	-0.347*	-0.182	-0.407*	-0.275*

Table 5. Correlations between native T1 and ECV with cardiac function, biomarkers, ECG and 6 MWT.

R = Pearson correlation coefficient; AL, light-chain amyloidosis; ATTR, transthyretin amyloidosis; NT-proBNP, N-terminal pro-brain natriuretic peptide; CMR, cardiovascular magnetic resonance; EDV$_i$, end diastolic volume indexed; ESV$_i$ end systolic volume indexed; LVEF, left ventricular ejection fraction; SV$_i$, stroke volume indexed; LV, left ventricular; LAA$_i$ left atrial area indexed. * P< 0.01 level; †P<0.05.

11.5 DISCUSSION

AL and ATTR amyloidosis have a different natural history and prognosis, but in both, cardiac involvement is the main driver of prognosis. Amyloidosis is used as the exemplar of an interstitial disease - whilst the quantity of amyloid expanding the body's extracellular space varies substantially, it can exceed kilograms in some patients. We report here a comparison of AL and ATTR amyloidosis combined measurements of amyloid burden (the ECV and Total Amyloid Volume, estimates respectively of the amyloid fraction and amyloid volume) but also the ICV (a measure of the myocyte volume fraction), along with native T1 signal, a composite from both myocytes and interstitium, which is mainly driven by the amount of water in the tissue. Both ECV and Total Amyloid Volume, i.e. the amyloid burden, are very elevated in ATTR amyloidosis and to a significantly greater degree than in AL patients. The greater amyloid burden in ATTR patients is also associated with an increased myocyte volume suggesting a compensatory myocyte hypertrophy response in this type of amyloidosis, which may favorably influence clinical outcome. However, in AL amyloidosis there no net differences in myocardial cell volume compared with healthy volunteers, suggesting AL in general either has no myocyte hypertrophy or any such hypertrophy is balanced by myocyte loss. Intriguingly and importantly, the greater elevation in T1 signal in AL patients compared with ATTR in the presence of a smaller amyloid burden points to an additional process, the most likely explanation being myocardial edema (158). This hypothesis is plausible and compatible with hypertrophy balanced by myocyte loss – a scenario that would fits with more myocardial damage in AL as evidenced by greater troponin release than occurs in ATTR type, although debate

continues as to whether this may result from light chain/AL fibril toxicity or differing rates of amyloid deposition (4,153). If amyloidosis is considered solely as an infiltrative myocardial disease, the higher ECV in ATTR compared to AL is paradoxical as ATTR has a more benign prognosis (4). A protective hypertrophic response in ATTR may be part of the explanation. When a third parameter, native T1 is added, this paradoxical difference can be explained by edema in AL and a further refinement of a model comes into view with, in AL, a hypertrophic response balanced by myocyte loss and associated edema. The results also add nuance to the debate of nomenclature for the wall thickening found in amyloid: the findings suggest that “hypertrophy” is appropriate for ATTR, whereas in AL the situation remains more complex.

These results and methodologies deepen our understanding of cardiac amyloid by firstly quantifying amyloid deposition, but secondly providing insights into myocyte response which is different in ATTR and AL. Further work is needed to explore these models - and they generate testable hypotheses: for example, the above model suggests in AL that very high T1 might be associated with a) troponin release and b) T2, the traditional myocardial parameter used to image edema. Furthermore, if light chains are “switched off” using chemotherapy, T1 may be expected to fall faster than ECV changes and track troponin and BNP reduction. Other explanations are, however, possible. The ECV is fundamentally tracking extracellular water. Collagen deposition or the hydration of collagen, possibly reflecting maturity of amyloid, may be different between AL and ATTR. The T1 is measuring both extracellular and intracellular signal so either AL myocytes or amyloid could have higher native T1 or ATTR amyloid and myocytes could have lower native T1.

Other as yet unknown factors in addition to collagen, amyloid and edema could change this – known examples are iron or fat infiltration, although neither is likely in amyloid.

Despite these limitations, overall, these findings support the concept that cardiac amyloid is not a disease of solely infiltration but of *compensated* infiltration and with superimposed toxicity and eventual failure of compensation - which is measurably more prominent in AL compared to ATTR (153,159). This different mechanism of myocardial damage and different myocardial response could have important implications in terms of future therapeutic targets. Furthermore the ability of measuring treatment response not only in terms of neurohormonal activation, but also in terms of structural changes is important in the process of drug development. More specifically, with T1 mapping by cardiac CMR we will be able to measure the effect of treatment at 3 different levels, i.e. infiltration (amyloid burden, ECV), edema (native T1) and myocyte response (intracellular volume), providing a richer understanding of the pathophysiological mechanism.

Although this series represents the largest prospective CMR study of the AL and ATTR amyloid (until my later studies – see next chapter) with the use of innovative techniques further work is needed. A limitation of this study is the lack of histological validation. There was no biopsy evidence of amyloid in 30% of ATTR patients – but this cohort of patients was fully characterized with all other clinical investigative techniques currently available including DPD scanning. This composite diagnostic pathway is known to provide high diagnostic accuracy. No follow-up was imaging was performed and therefore change over time was not tracked. Despite this, these results set the scene for a more sophisticated approach to cardiac amyloidosis, refocusing on the myocyte.

12. RESULTS: PROGNOSTIC VALUE OF LATE GADOLINIUM ENHANCEMENT CARDIOVASCULAR MAGNETIC RESONANCE IN CARDIAC AMYLOIDOSIS

With the work described in this chapter I was shortlisted for the Early Career Award (clinical translational) at SCMR 2015 and for the Melvin Judkins Young Investigator Award 2014.

This chapter is based on the publication below.

Fontana M, Pica S, Reant P, Abdel-Gadir A, Treibel TA, Banypersad SM, Maestrini V, Barcella W, Rosmini S, Bulluck H, Sayed RH, Patel K, Mahmood S, Bucciarelli-Ducci C, Whelan CJ, Herrey AS, Lachmann HJ, Wechalekar AD, Manisty CH, Schelbert EB, Kellman P, Gillmore JD, Hawkins PN, Moon JC. Circulation. 2015 Sep 11. pii:

My contribution was recruiting, consenting and performing the scans of all the ATTR patients and 70% of AL. I have analysed all the data as first operator, done the statistical analysis and wrote the paper.

12.1 INTRODUCTION

The prognosis of immunoglobulin AL and ATTR amyloidosis is substantially influenced by the presence and severity of cardiac involvement which then governs therapeutic strategies.(4,160) Although blood biomarkers are useful guides for risk stratification,(7) they are not specific for cardiac involvement, and current strategies do not ascertain all patients at risk. Mortality, despite treatment progress, remains high.(9,35,161,162) Over the last decade, new chemotherapy regimens and stem cell transplantation have been associated with improved survival in patients with AL amyloidosis, but the prognosis remains poor in those with cardiac involvement, which also contributes substantially to treatment related morbidity and mortality. There remains much unmet need for improved

non-invasive criteria to stratify risk in selecting optimal therapy whilst avoiding serious toxicities.

Cardiac amyloid deposition represents a key process in amyloid pathophysiology.(45,163) CMR with LGE identifies myocardial infiltration: after the administration of contrast, CMR shows a characteristic pattern of global subendocardial LGE coupled with abnormal myocardial and blood-pool gadolinium kinetics.(138,164) However, despite excellent diagnostic accuracy for the presence of amyloid, conflicting results have been reported regarding the prognostic impact AL amyloidosis, and no studies have been published in ATTR amyloidosis.(149,165-171) Newer techniques, particularly phase sensitive inversion recovery, an LGE image reconstruction technique that is less sensitive to operator choice of null point and renders signal intensity truly T1 weighted, may better reflect extent of cardiac involvement(172) and thereby improve risk stratification.

We report here a prospective CMR study conducted in amyloidosis, in which we investigated the prognostic value of LGE in 250 consecutive CMR-eligible subjects.

The aims of the study were to assess: 1- patterns of LGE and the benefit of new more robust approaches (PSIR); 2- correlation with the cardiac amyloid burden; 3- the prognostic impact of LGE in both AL and ATTR cardiac amyloidosis.

12.2 METHOD

AMYLOIDOSIS PATIENTS

A total of 250 patients were categorized into 3 groups: Outcome (dead/alive) was ascertained using death certificates

SUBJECTS WITH AL AMYLOID

119 patients with biopsy proven systemic AL amyloid (77 male, 65%; age 62±10 years), with biopsies from the myocardium (n=7, 6%) or other tissues (n=112, 94%).

SUBJECTS WITH ATTR AMYLOID

122 consecutive, consenting patients with ATTR amyloidosis (101 male, 83%; age 71±11years) were recruited. 69 percent (n=84) had histological proof of ATTR amyloidosis by Congo red and immunohistochemical staining of myocardial (n=35, 29%) or other tissues (n=49, 40%). The presence of cardiac amyloid was defined by presence of ATTR amyloid in a myocardial biopsy or positive technetium-labelled bone scintigraphy using 3,3-diphosphono-1,2-propanodicarboxylicacid (DPD scintigraphy). All subjects underwent sequencing of exons 2, 3, and 4 of the *TTR* gene.

TTR GENE MUTATION CARRIERS

In addition, there were 9 subjects with amyloidogenic *TTR* gene mutations (3 male, 33%; age 47±6 years) defined as individuals with no evidence of clinical disease (no cardiac

uptake on DPD scintigraphy and normal echocardiography, CMR, N-terminal pro-brain natriuretic peptide [NT-proBNP] and Troponin T).

CMR IMAGE ACQUISITION

CMR was standard volumes and LGE with PSIR in 43% of patients. T1 mapping was ShMOLLI with regions of interest drawn in the 4 chamber view at the level of the basal and mid inferoseptum (2 segments, large region of interest).(157)

CMR LGE INTERPRETATION

During interpretation, prior to our adoption of PSIR for all amyloidosis patients, because myocardial nulling can be difficult in the presence of amyloid, any confusion with MAG-IR images was resolved by selecting the images that most matched the post contrast T1 maps – with “bright” LGE expected to correlate with areas with the lowest post contrast T1 (i.e. the highest gadolinium concentration, the highest interstitial expansion).

The LGE pattern was classified by 2 different observers (MF and SP) into 3 groups according to the degree of transmurality: 1-no LGE; 2-subendocardial LGE (when there was global subendocardial involvement but no transmural LGE); 3-transmural LGE (when the LGE was extending transmurally), (Figure 24). Thus a patient with basal transmural LGE but apical subendocardial LGE would be classified as “transmural LGE”.

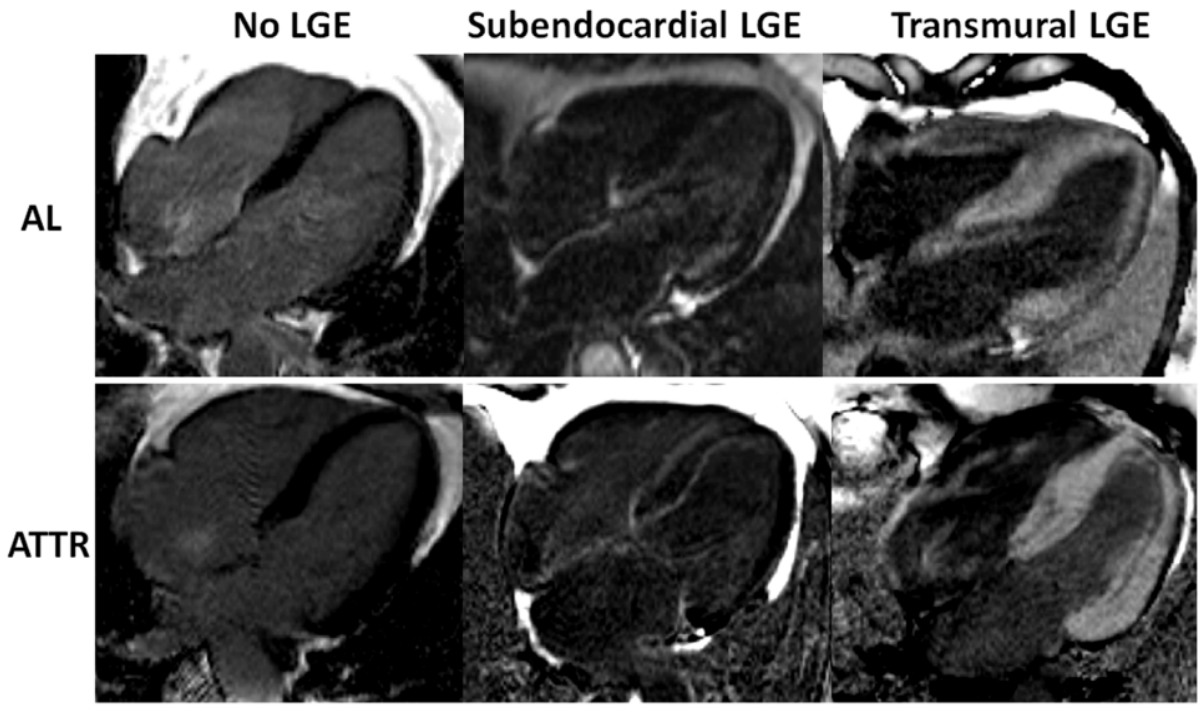

Figure 24. Characteristic PSIR LGE patterns in 3 AL and 3 ATTR patients.

No gadolinium enhancement (LGE) (left panels); Subendocardial LGE (middle); transmural LGE (left panels).

CMR PSIR VERSUS MAG-IR

A sample of 100 images (50 PSIR, 50 MAG-IR reconstruction) was analyzed for concordance or discordance with the post-contrast T1 maps which were used as the truth standard (Figure 25). We considered that nulled tissue should be the tissue with the least contrast (longest T1 on post contrast T1 map). This means that a normal subject should have nulled myocardium; a high infiltration amyloid patient bright myocardium (transmural) and nulled blood, and the possibility of intermediate blood and myocardium nulling concurrently (typically with “bright” endocardium). This is discussed further in the figure legends and discussion.

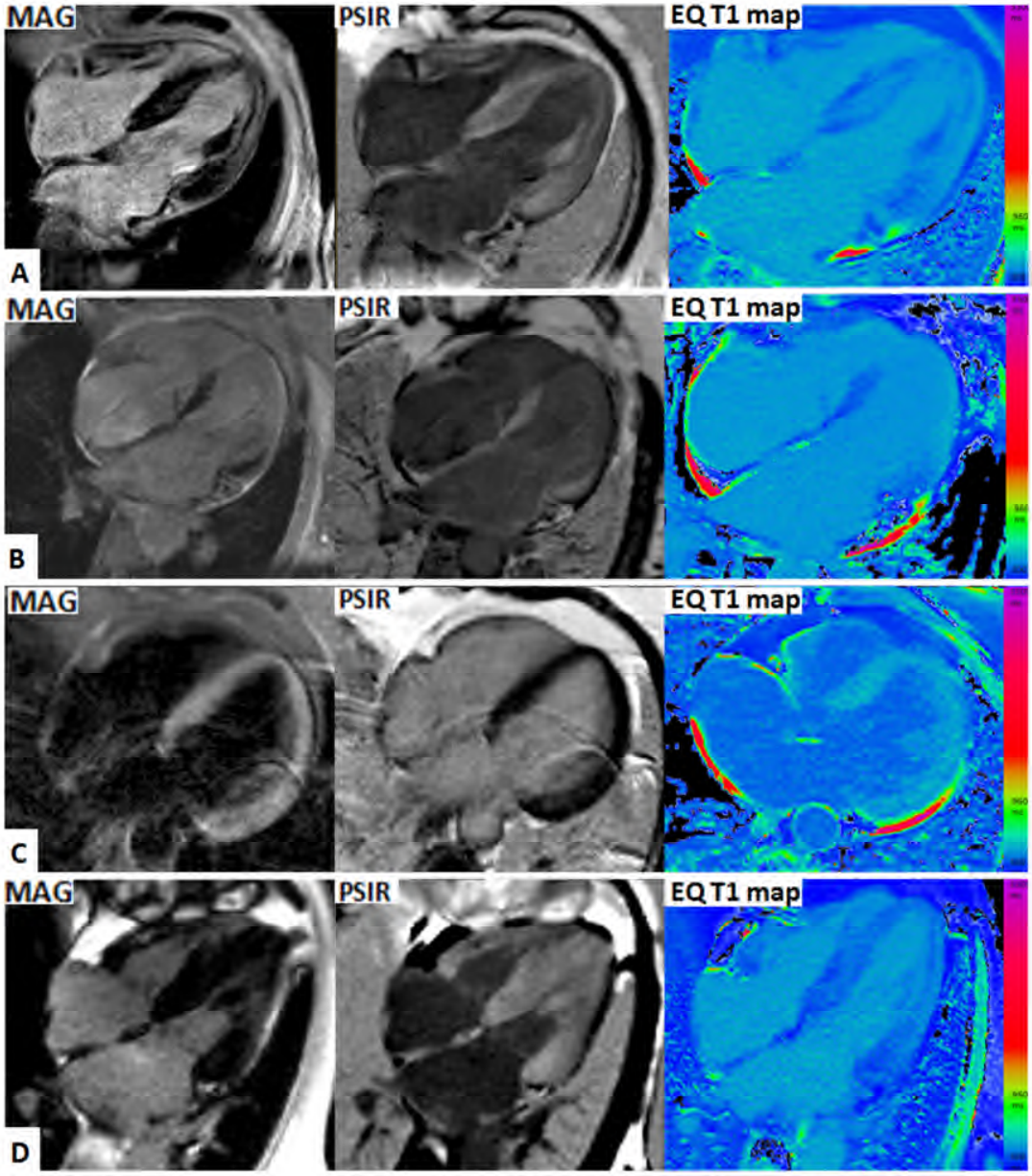

Figure 25. Characteristic CMRs in 4 different patients.

LGE with magnitude reconstruction (left); LGE with PSIR (middle) and post contrast ShMOLLI T1 maps (right). On PSIR, there is 100% concordance between myocardial T1 and LGE: firstly areas of low T1 (darkest blue) and focal areas of LGE; secondly where myocardial T1 is lower than blood T1, global LGE is demonstrated and thirdly, where myocardial T1 is higher than blood T1, no LGE is demonstrated. On MAG-IR images, discordance is present in all 4 of these cases: mid myocardial rather than subendocardial (Panel A); apical rather than basal (panel B), transmural LGE rather than normal (panel C) and normal rather than transmural (panel D).

. STATISTICAL ANALYSIS

See methods. In addition, survival was evaluated using Cox proportional hazards regression analysis, providing estimated hazard ratios (HR) with 95% confidence intervals (CI) and Kaplan Meier curves. Variables selected *a priori* for the clinical relevance and first explored with univariate Cox regression were entered in the multivariable models. Multivariable models evaluated the independent predictive value of LGE above other clinically and statistically significant covariates. Harrell's C statistic was calculated for the different models.

12.3 RESULTS

STUDY POPULATION

The details of the 250 subjects are shown in table 1. At the time of scanning, the AL amyloidosis cohort had 46 new untreated (to date) patients; 21 patients undergoing second or third line therapy and 52 stable patients (complete or very good response 80%; stable partial response 20%). UK first line therapy at the time of this study was typically Cyclophosphamide, Thalidomide and Dexamethasone (CTD) or Cyclophosphamide, Bortezomib and Dexamethasone (CVD). Relapse therapy was typically CVD or a Lenalidomide-containing regimen. The TTR mutations were: V122I [n = 23], T60A [n = 13], V30M [n = 10], E54G [n = 2], S77Y [n = 2], E89K [n = 2] and D38Y, G47V, E89K, I84S, I107F and L12P in one case each. Of the 9 asymptomatic individuals with TTR mutations, 5 had *TTR* V30M and 3 T60A and 1 S77Y.

	All Patients	AL patients∞			ATTR patients		
	n=250	No LGE n=37	Subendocardial LGE n=42	Transmural LGE n=30	No LGE n=17	Subendocardial LGE n=31	Transmural LGE n=83
Age, y	67±12	63±10	61±11	60±12	55±14	74±10	73±9‡
Hypertension, %	20	35	12	3†	17	35	18
eGFR, ml/min/1.73 m²	67±22	72±26	74±19	73±22	80±13	63±21	57±20‡
Systolic BP, mmHg	123±19	138±20	121±19	112±16‡	128±20	133±16	118±15‡
Diastolic BP, mmHg	74±12	81±11	73±11	71±11‡	76±10	77±11	72±11
NT-proBNP, pmol/L	210 (71-446)	29 (9.5-75)	134 (84-370)	319 (186-823) ‡	8 (4-12)	196 (89-359)	412 (245-629) ‡
6 MWT, meters	318±135	284±126	301±125	274±148	500±71	328±138	305±120‡
PR, ms	188±51	157±25	180±45	186±46*	154±40	188±34	222±58‡
QRS, ms	107±26	95±16	101±24	103±19	90±9	114±29	120±29‡
Sum limb leads voltage, mm	31±15	37±15	30±14	23±16‡	39±11	35±15	28±14†
E wave, cm/sec	0.79±0.19	0.67±0.21	0.81±0.20	0.84±0.22†	0.73±0.13	0.85±0.18	0.80±0.17
A, cm/sec	0.61±0.25	0.78±0.18	0.72±0.23	0.57±0.25†	0.65±0.16	0.61±018	0.41±0.20‡
E/A	1.59±0.92	0.89±0.33	1.27±0.64	1.80±0.92‡	1.12±0.28	1.52±0.85	2.3±1.05‡
Average E', cm/s	0.06±0.03	0.08±0.02	0.07±0.03	0.06±0.02†	0.11±0.04	0.06±0.02	0.05±0.01‡
E/E'	14±7	10±6	13±6	18±9‡	7±3	15±4	17±6‡
E wave deceleration time, ms	183±61	212±62	190±51	173±54*	194±73	200±81	162±50*

Table 6. Main Clinical Characteristics, echocardiographic and ECG findings in patients with AL and ATTR amyloidosis according to the LGE pattern.

∞less 10 patients with non-diagnostic MAG-IR LGE images. p-values: * p<0.05, † p<0.01, ‡ p<0.001 for trend across different pattern of LGE.

MAG-IR VERSUS PSIR

MAG-IR LGE and T1 maps were discordant in 57% (where the operator was selecting the inversion time according to his/her best judgment) meaning that operator TI selection was mainly incorrect. Ten patients with MAG-IR only had not one LGE images that matched the T1 mapping for classification (implying the operator systematically kept the TI incorrect for the whole scan). All patients with PSIR LGE had diagnostic images. PSIR LGE and T1 maps were never (0%) discordant, Figures 25 and 26. MAG-IR could be incorrect in three ways: inappropriately nulling global LGE, Figure 25D, particularly the highest ECV cases; to get the incorrect distribution (especially making LGE apical rather than basal, Figure

25A and B; or creating transmural LGE where there should be global nulling (and the ECV was low), Figure 25C. With PSIR, the longest T1 tissue after windowing is always nulled.

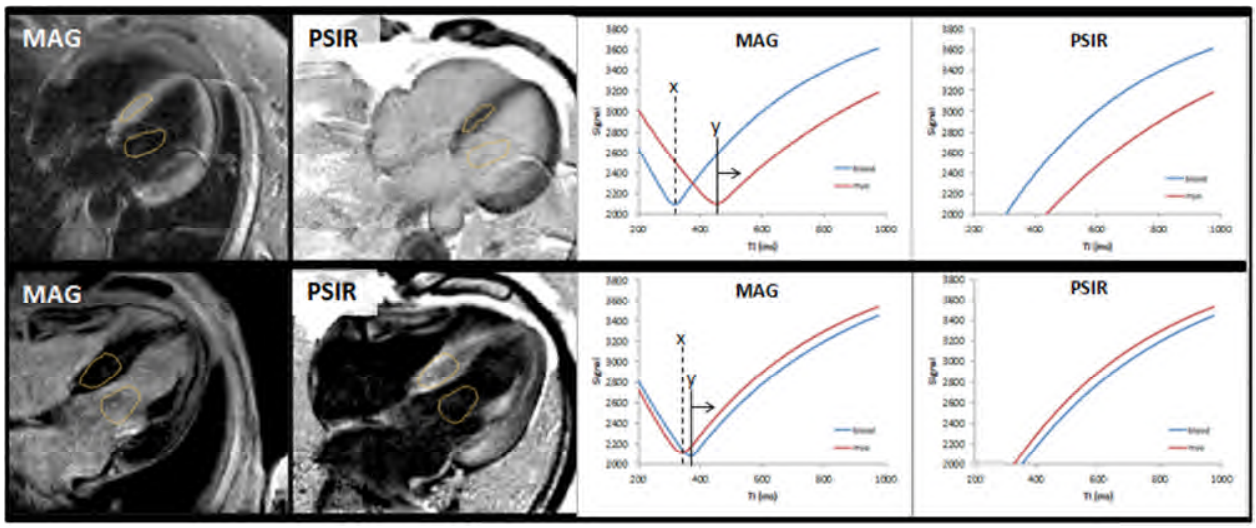

Figure 26. Two patients with MAG and PSIR LGE reconstruction images.

Two patients (top and bottom) with MAG and PSIR LGE reconstruction images (left). In both patients, the MAG and PSIR are discordant with opposite LGE patterns. Only one can be correct. The tissue to null is the one with the slowest T1 recovery (i.e. the least gadolinium). On the right are the signal intensity curves as the TI varies for MAG and PSIR. How the operator sets the TI matters in MAG imaging – but not in PSIR. The operator set the TI for both patients at X, nulling the wrong tissue. Only had they set the TI greater than Y would the image have been correct. With PSIR, the TI could have been set anywhere and the tissue with the least gadolinium has lower signal and will be nulled after windowing.

LGE PATTERN AND CORRELATION WITH ECV

Three patterns of LGE are observed: no LGE; subendocardial LGE and transmural LGE, Figure 24. There was good agreement in the assignment of these patterns between two observers (ICC 0.97, 95%CI 0.97-0.98). All patterns were present in AL and ATTR cardiac amyloidosis (Figure 27) but to different extents, with subendocardial LGE being more prevalent in AL (39% in AL vs 24% in ATTR, $p<0.05$) and transmural LGE more prevalent in ATTR (27% in AL vs 63%, $p<0.0001$), Figure 27.

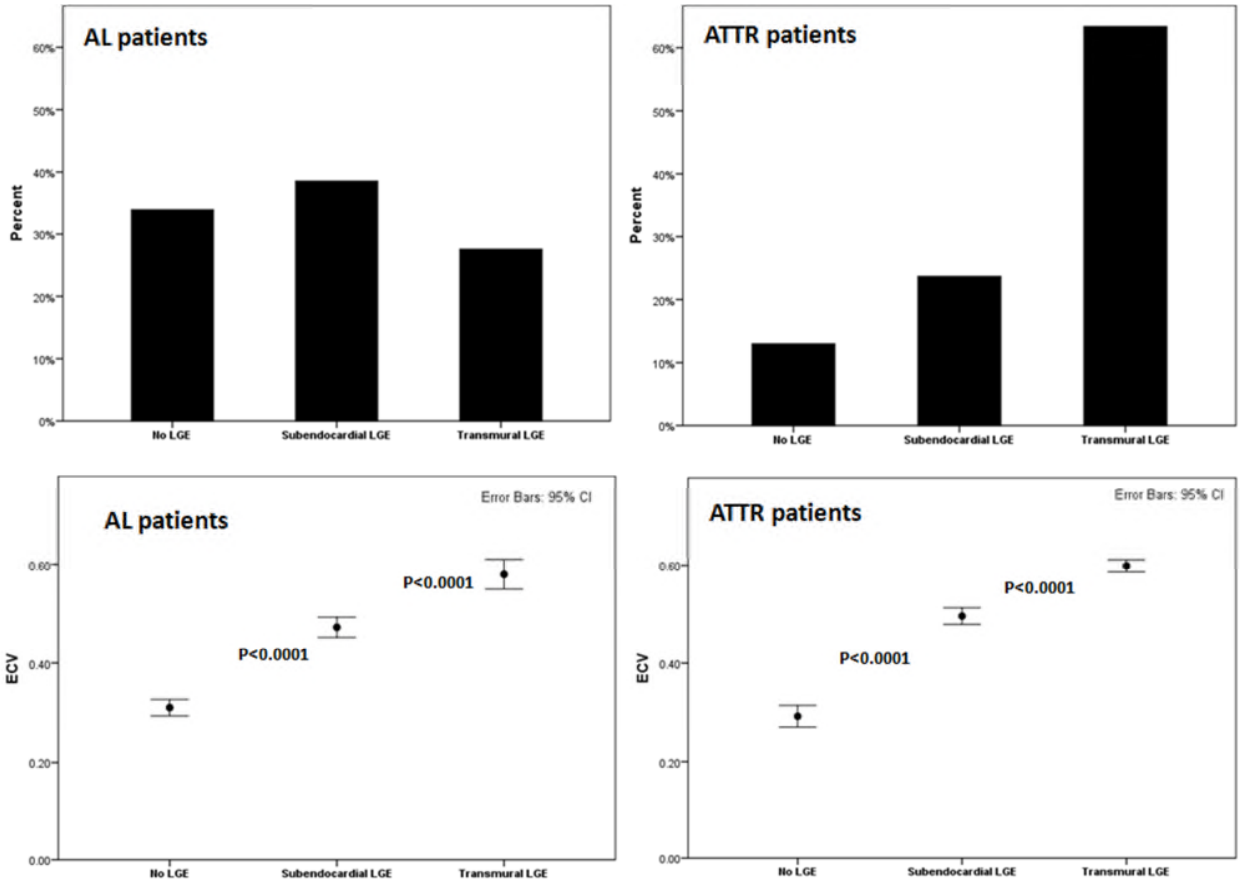

Figure 27. LGE patterns correlation with amyloid burden.

Histograms showing the prevalence of the different LGE patterns (upper panels) in AL and ATTR patients; correlation with the amyloid burden (lower panels), measured as extracellular volume (ECV) in AL and ATTR patients. Bonferroni-adjustment was applied.

Increasing LGE (none, subendocardial, transmural) was associated with increasing ECV (AL: 0.31±0.04, 0.47±0.06, 0.58±0.07; ATTR: 0.29±0.04, 0.50±0.05, 0.60±0.05, for both p<0.0001), Figure 27. In ATTR, this correlated also with DPD grade (p<0.0001). Apparent transitions are evident with subendocardial LGE appearing at an ECV of 0.40-0.43 for AL and 0.39-0.40 for ATTR and transmural at 0.48-0.55 for AL and 0.47-0.59 for ATTR. However 39% of the no LGE patients had ECV elevation as compared to normal range

(ECV elevation between 0.32 and 0.40). Of the patients with no LGE and increased ECV, 4 patients had mutant ATTR (DPD grade 1 in 3; grade 0 in one) and 17 patients had AL.

Increasing LGE (none, subendocardial, transmural) was associated in both AL and ATTR with lower systolic blood pressure, ECG changes (prolonged PR interval, prolonged QRS in ATTR), increased NT-proBNP, structural and functional changes (increased LV mass, increased end systolic volume, decreased stroke volume, decreased ejection fraction, left atrial dilatation), increasingly abnormal tissue characterisation (elevated native T1 and ECV, Table 2) and more severe echo diastolic dysfunction. In ATTR, increasing LGE was also associated with decreased functional capacity (6 minute walk test).

	All patients	AL patients∞			ATTR patients		
	n=250	No LGE n=37	Subendocardial LGE n=42	Transmural LGE n=30	No LGE n=17	Subendocardial LGE n=31	Transmural LGE n=83
LV mass, g	203±77	140±45	170±60	204±56‡	109±25	208±58	266±60‡
LV massi, g/m²	108±39	78±29	88±28	108±25‡	61±12	110±26	139±28‡
Maximal IVS, mm	15±4	11±2	14±3	16±3	10±2	17±3	19±3*
EDV, mL	125±30	118±29	123±32	114±28	119±25	121±26	138±31†
EDVi, mL/m²	67±16	64±17	65±16	61±16	67±12	64±11	73±16*
ESV, mL	52±27	35±18	42±22	50±21*	38±19	43±21	71±28‡
ESVi, mL/m²	27±14	18±11	22±12	27±12*	21±9	23±10	38±15‡
SV,ml	74±20	83±20	81±21	64±17‡	81±16	78±18	67±18‡
SVi,ml/m²	39±10	45±9	43±11	35±9‡	46±8	41±9	35±9‡
LVEF, %	60±14	72±9	67±12	57±11‡	69±11	65±12	49±13‡
LA area,cm²	27±7	23±6	25±6	26±5*	22±3	31±7	32±5‡
LA areai,cm²/m²	15±3	13±4	13±3	14±2	12±2	16±3	17±1‡
RA area,cm²	25±8	21±5	22±6	24±7	20±3	26±8	30±8‡
RA areai,cm²/m²	13±4	12±3	12±3	13±3	11±2	14±4	16±4‡
MAPSE, mm	9±4	12±4	9±4	6±3‡	14±2	9±2	7±2‡
TAPSE, mm	15±6	21±3	17±5	12±5‡	23±3	15±5	12±4‡
Precontrast T1, ms	1082±75	993±46	1100±58	1150±68‡	968±41	1073±34	1113±47‡
ECV, %	0.50±0.12	0.31±0.04	0.47±0.06	0.58±0.07‡	0.29±0.04	0.50±0.05	0.60±0.05‡

Table 7. CMR findings in patients with AL and ATTR amyloidosis according to the LGE pattern.

∞less 10 patients with non-diagnostic MAG-IR LGE images. p-values: * p<0.05, † p<0.01, ‡ p<0.001 for trend (one-way analysis of variance) in AL and ATTR patients across different pattern of LGE.

LGE PATTERN AND PROGNOSIS

At follow up (mean 24±13 months), 67 (27%) of 250 patients had died. Transmural LGE was a significant predictor of mortality in the overall population (HR 5.4, 95% CI: 2.1-13.7, P<0.0001) (Figure 28).

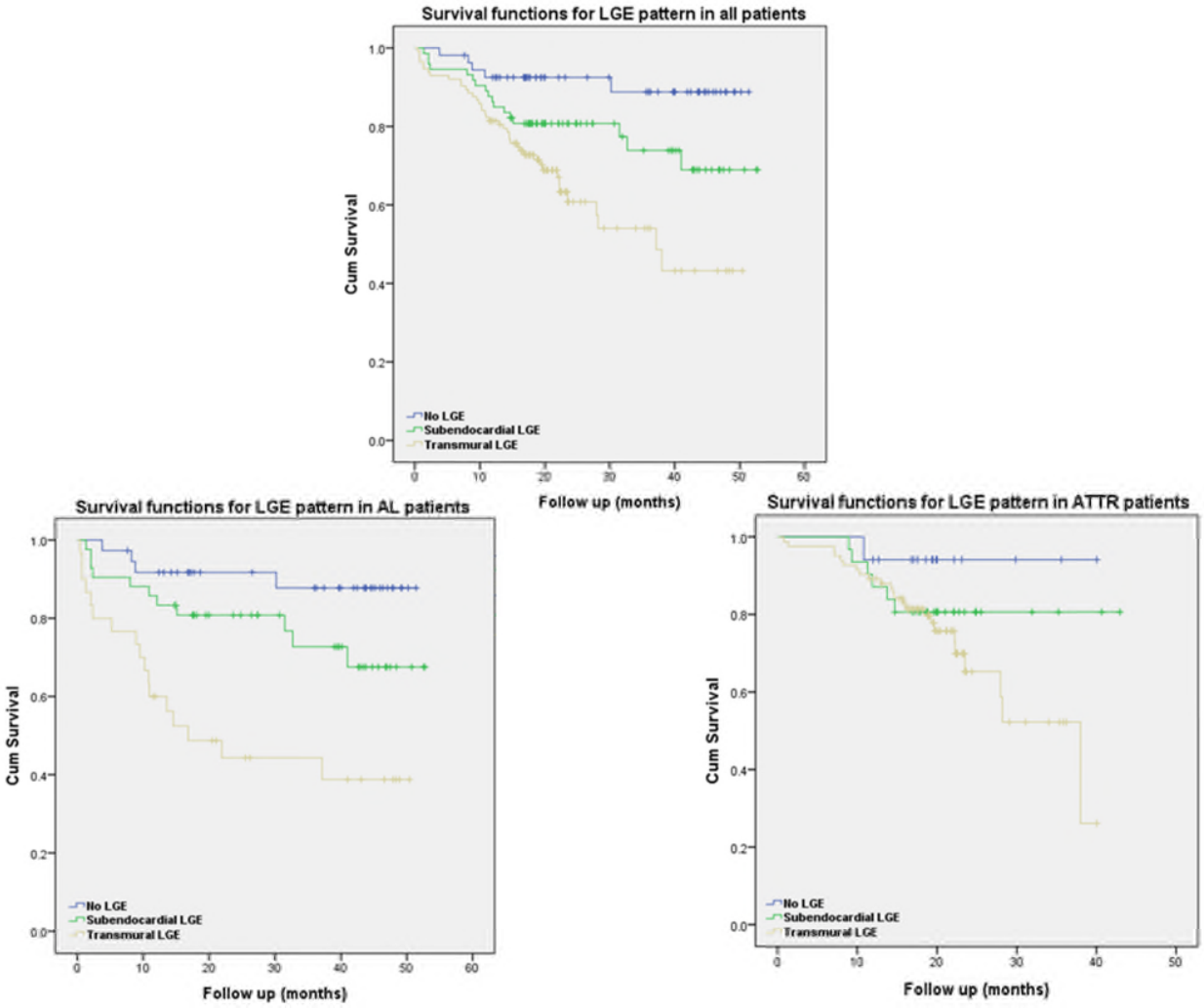

Figure 28. Kaplan Meier curves for late gadolinium enhancement.

Kaplan Meier curves for late gadolinium enhancement patterns in all patients (upper panel), AL (left lower panel) and ATTR patients (right lower panel).

The survival curves indicates that there is an approximately 92% chance of survival at 24 months in patients with a no LGE (92% in AL 94% in ATTR) compared to 81% for patients with subendocardial LGE (81% in AL 81% in ATTR) and 61% with transmural LGE (45% in AL 65% in ATTR). The median survival in patients with transmural LGE was 17 months in AL and 38 months in ATTR. Transmural LGE was significantly associated with mortality (HR = 4.1, 95% CI: 1.3-13.1, $p<0.05$) in multivariable Cox models that included NT-proBNP, ejection fraction, stroke volume indexed, E/E', left ventricular mass indexed (Troponin results were not available in all patients). NT-ProBNP and stroke volume indexed also remained independently predictive (Table 3). Harrel C statistics for this model was 0.72.

The Harrel C statistics of a comparable preCMR-model including demographics, systolic and diastolic function parameters and biomarkers (Age, EF, EE, BNP, interventricular septal wall thickness) was 0.67.

12.4 DISCUSSION

Cardiac infiltration is the chief driver of prognosis in systemic amyloidosis, and stratification of patients is essential for prognosis and optimal management, including selection of patients to receive aggressive higher risk therapies and to minimise cardiac toxicities. Echocardiography, once the gold standard cardiac investigation in amyloidosis, has limited sensitivity and specificity, and risk stratification is currently places great emphasis on blood biomarkers. However, these strategies do not identify all amyloidosis patients at risk, and the findings of studies on evaluation of cardiac involvement by CMR

have been conflicting.[4-7, 19] Recently, considerable interest has emerged in using LGE to improve the risk stratification model,(149,165-171) but studies in AL cardiac amyloidosis have been few, mostly small, retrospective and have employed non-standardized LGE approaches, and have produced inconsistent results(138,165,166,168,169,171). No studies have been published in ATTR amyloidosis.

In the present study, the largest CMR study in amyloidosis to date, we showed that misleading results using the MAG-IR LGE technique was likely to account for the conflicting finding that have previously been published. By convention, LGE should display containing the most contrast (i.e. shortest T1 on T1 maps). For amyloidosis, myocardium can contain more gadolinium than blood – under those circumstances, myocardium should appear globally bright (transmural LGE). It is a property of MAG imaging that signal is highly dependent and non-linear with user defined choice of the TI (time to null), Figure 26, and images can be “inverted” with the wrong TI choice. When all of the myocardium is abnormal (frequent in cardiac amyloidosis), the abnormal myocardium could be wrongly nulled, as the MAG-IR relies on ‘nulling’ what is perceived to be normal myocardium. This limitation was quantified in our study by comparison with a true standard of post contrast T1. More importantly, this problem does not occur with the PSIR approach. PSIR substantially removes the issue of operator selected inversion time and completely removes the potential for a “mirror image”. On a PSIR reconstruction when windowed by the operator, the tissue with the longest T1 (least gadolinium - blood or myocardium), after windowing, is always nulled. The practical result is this: a) if myocardium is globally nulled by PSIR, the ECV is less than blood and <0.4-0.43: any amyloid present (detectable by an

ECV>0.32), is not extensive. b) above this, LGE areas appear particularly in the sub endocardium. PSIR LGE areas are the areas of most amyloid deposition in the heart; c) above an ECV of 0.47-0.59, blood has less gadolinium than myocardium and blood is nulled – myocardium appears uniformly bright – heterogeneity is present but it is swamped by all the myocardium becoming bright. Examples of MAG-IR errors are in Figure 25: mid myocardial rather than subendocardial (Figure 25 panel A); apical rather than basal (Figure 25 panel B), transmural LGE rather than normal (Figure 25 panel C) and normal rather than transmural (Figure 25 panel D).(172,173) Accordingly, we believe that PSIR should be universally adopted for amyloid LGE imaging – particularly as PSIR-LGE is easily available from all scanner manufacturers (whereas T1 mapping is not yet).

Using PSIR, three patterns were relatively easy to determine, and the previously frequently described LGE pattern of “patchy” LGE was not evident using PSIR – many of these on PSIR appeared to have transmural LGE. A key insight is that amyloid cardiac involvement is not dichotomous, but a continuum from no LGE to subendocardial to transmural tracking increasing ECV (Figure 29).(70,174) Transmural LGE appears to be the pattern that carries the most adverse prognosis – it is an important marker of all-cause mortality, after adjustment for other relevant disease variables and regardless of treatment status (indeed irrespective of whether patients are presenting at diagnosis or years into the disease process). Indeed, in ATTR, the majority of the deaths are in patients with transmural LGE (no LGE, subendocardial LGE, transmural: 1,6,24 deaths respectively).

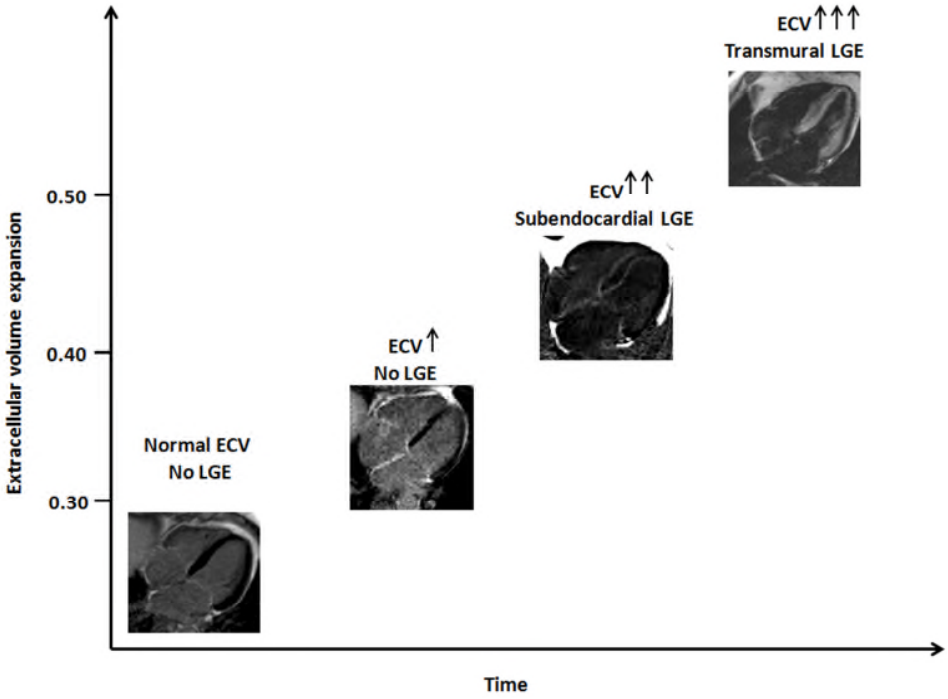

Figure 29. Hypothesized cardiac amyloid progression across time.

When amyloid starts to accumulate 3 steps can be identified; 1-No evidence of LGE but increase in native T1 and extracellular volume (ECV); 2-Further increase in T1 and ECV and appearance of subendocardial LGE; 3-Further increase in native T1 and ECV and progression to transmural LGE.

Within this spectrum, the degree of involvement is important, and with transmural LGE defining the high risk group. The prevalence of patients in the different stages of disease progression (Figure 29) is different in AL and ATTR. 39% of the no LGE patients had ECVs in the 0.32 to 0.4 range, particularly AL amyloidosis. It is expected that ATTR patient must pass through this phase, but it is not clinically recognised. Early cardiac involvement in AL is detected through cardiac screening of AL patients presenting with extracardiac disease. The majority of ATTR patients (wild type ATTR and mutant ATTR associated with the variant V122I) present with heart failure symptoms that appear only when advanced (LGE is invariably present, mostly transmural). This has potential treatment

implications. Currently, patients with subendocardial LGE may be classified as “cardiac involvement” and denied therapies, which are known to improve long term survival – but which are contraindicated in “cardiac involvement” – such as stem cell transplants (AL), some chemotherapy regimens (AL) and liver transplants (ATTR). More data is needed and consideration of cardiac involvement as a continuum should provide the insights into the impact of different degrees of cardiac infiltration and possibly changing the current therapeutic approach. Within the transmural pattern, the median survival is significantly different in the two amyloid types, 17 months for AL and 38 months for ATTR. These findings support the concept that cardiac amyloid is not a disease of solely infiltration but may have with superimposed toxicity (AL > ATTR) or that the rate of accumulation is myotoxic, a contributor to different prognosis between AL and ATTR despite ATTR higher degrees of LVH, cardiac dysfunction and amyloid burden (175). T1 mapping techniques provide new insights into this, being able to follow the disease at three different levels, i.e. infiltration (amyloid burden, ECV), edema (native T1) and myocyte response (intracellular volume) and providing new prognostic markers.(77) These new biomarkers may aid diagnosis, risk stratifications and act as surrogate end points in clinical trials. However the current limited availability, the technical challenges related to sequence and vendor specific differences limit the role of T1 mapping in routine clinical practice. The common use of the LGE technique in all clinical CMR scans and the availability of PSIR reconstruction on all different vendor platforms make LGE a robust and reliable approach for routine risk stratification of patients with cardiac amyloidosis.

Limitations of the study are that patients are at different treatment stages, with treatment reflecting current UK practice. Cardiac biopsy is present only in a minority of patients, but this cohort of patients was fully characterized with all other clinical investigative techniques currently available including DPD scanning. This composite diagnostic pathway is known to provide high diagnostic accuracy. The causes of death are not known as patients die locally and the National Amyloidosis centre only receives notification of death rather than cause of death. Although this study highlights the prognostic role of transmural LGE for risk stratification of patients with cardiac amyloidosis, further studies are needed to assess the direct correlation between patterns of LGE and treatment related mortality.

13. DISCUSSION AND CONCLUSION

13.1 BACKGROUND AND HYPOTHESES EXPLORED:

Cardiac amyloidosis remains challenging to diagnose and to treat. Key 'red-flags' that should raise suspicion include clinical features indicating multisystem disease and concentric LV thickening on echocardiography in the absence of increased voltage on ECG. The pattern of gadolinium enhancement on CMR appears to be very characteristic. Confirmation of amyloid type is now possible in most cases through a combination of immunohistochemistry, DNA analysis and proteomics.

But whilst developments in chemotherapy have improved the outlook in AL amyloidosis, the prognosis of patients with cardiac involvement remains very poor. Senile cardiac amyloidosis is probably greatly under-diagnosed. The inability to reconcile advances in treatment strategies with improved outcomes reflects our incomplete understanding of the biology of the disease process. This is likely because no technique has been thus far able to feasibly image or quantify the amyloid burden and understand the myocyte response. Being able to do so would undoubtedly improve our knowledge of the differences between amyloid types and may allow therapy to be better targeted. Recently, CMR with T1 mapping has been shown to measure the ECV and cardiac amyloid burden. Furthermore ECV have been shown in AL to be an independent prognostic marker and non-contrast CMR with native T1 to be a potentially useful tool for the diagnosis of cardiac amyloid infiltration in AL patients.

As a result of the work during my PhD:

1) I have refined the technique as described in chapter 8 to make T1 measurement and ECV faster, more robust and therefore clinically more applicable.

2) I then explored, in chapter 9, the ability of native T1 measurement to detect cardiac infiltration in patients with both AL and ATTR cardiac amyloidosis, providing a new clinical test that can be used in patients with contraindication to gadolinium.

3) Using contrast to measure the ECV and combining this information with the myocardial mass and native T1, I was able, as described in chapter 10, to non-invasively and directly measure the amyloid burden and myocyte response, gaining unique insight in the pathophysiology of cardiac amyloidosis.

4) In chapter 11 I have finally shown that LGE measured with PSIR is a robust, now widely available technique that can be used for better patient stratification.

13.2 Refining Clinical Applicability of ECV measurement

Before the work in this thesis, measurement of the ECV required with the FLASH IR method, required 9 breath-holds before and after contrast administration, each lasting around 14 seconds to acquire a single slice. This technique was very sentive to cardiac arrhytmias and could not be used in patients with ectopics or atrial fibrillation.

In the first part of my PhD I compared the accuracy of the ECV measured using the multibreath-hold T1 pulse sequence to the ECV measured with ShMOLLI, a new, faster sequence of T1 mapping.

ShMOLLI allows a T1 map of a selected slice to be generated in a single breath-hold over 9 heart beats. We found it to be faster and more reproducible than the the FLASH IR method in amyloidosis. In chapter 8 I showed that that more patients were able to perform ShMOLLI than the multibreath-hold technique, that ECV calculated by multibreath-hold T1 and ShMOLLI showed strong correlation, little bias and good agreement. ECV correlated with histological collagen volume fraction by multibreath-hold ECV but better by ShMOLLI ECV. Inter-study reproducibility demonstrated that ShMOLLI ECV trended towards greater reproducibility than the multibreath-hold ECV.

In conclusion I showed that ECV quantification by single breath-hold ShMOLLI T1 mapping can measure ECV by EQ-CMR across the spectrum of interstitial expansion, it is procedurally better tolerated, slightly more reproducible and better correlates with histology compared to the older multibreath-hold FLASH techniques.

These advances have made the assessment of ECV a much simpler “add on” to a clincal CMR scan, only requiring in addition, a haematocrit measurement.

13.3 NATIVE T1 IN ATTR AMYLOIDOSIS

Before my work, in ATTR cardiac amyloidosis only contrast CMR could detect non invasivly cardiac involvement. However, administration of gadolinium chelates is contraindicated in patients with severe kindey failure.

My work demonstrated the ability of native T1 measured with ShMOLLI to detect cardiac infiltration in both types of cardiac amyloidosis. In chapter 9 I showed that T1 was elevated in ATTR patients compared to patients with HCM and normal subjects. In

established cardiac ATTR amyloidosis, T1 elevation was not as high as in AL amyloidosis. Diagnostic performance was similar for AL and ATTR amyloid and T1 tracked cardiac amyloid burden as determined semi-quantitatively by DPD scintigraphy. T1 was not elevated in mutation carriers but was in isolated DPD grade 1.

These advances have provided a new diagnostic tool for the diagnosis of cardiac infiltration in ATTR amyloidosis in patients with renal failure. A weakness persists that we don't have reference ranges (if needed) for subjects in end stage renal failure. The possibility that their native T1 is elevated by ESRF is not yet explored.

13.4 DIFFERENTIAL MYOCYTE RESPONSE IN AL AND ATTR CARDIAC AMYLOIDOSIS

Prior to my work, the pathophysiological understanding of the mechanisms of cardiac response to amyloid infiltration was very limited.

My work has provided unique insight in the pathophysiology of cardiac amyloidosis. In chapter 10 I showed that that both the LV $mass_i$ and ECV were markedly elevated in amyloidosis, but the Total Cell Volume was normal in AL, but significantly elevated in ATTR. The result is that all the increase in LV mass in AL is extracellular volume, whereas the increase in ATTR is extracellular but within addition, an 18% increase in the intra-cellular space.

These findings shows that cardiac amyloid deposits seem more extensive in ATTR than in AL type, but that ATTR type is uniquely associated with myocyte hypertrophy. Compensatory myocyte hypertrophy may contribute to the superior clinical outcome of

ATTR amyloidosis. These results have provided unique understanding of the pathophysiological mechanism behind the differences between ATTR and AL amyloidosis.

13.5 Prognostic value of LGE

Prior to my work, the potential of LGE for risk stratification of patients with cardiac amyloidosis was unknown.

In chapter 11, I showed that LGE in patients with amyloidosis could be classified into 3 different patterns: none, subendocardial and transmural, which were associated with increasing amyloid burden as defined by ECV. Transmural LGE predicted death and remained independent after adjusting for NT-proBNP, ejection fraction, stroke volume index, E/E' and left ventricular mass index.

These results showed that there is a continuum of cardiac involvement in systemic AL and ATTR amyloidosis. Transmural LGE is determined reliably by PSIR and represents advanced cardiac amyloidosis. The PSIR technique provides incremental information on outcome even after adjusting for known prognostic factors.

These findings have provided a widely available prognostic marker for better risk stratification of patients with AL and ATTR cardiac amyloidosis.

13.6 Clinical Insights and Potential

Cardiac infiltration is the chief driver of prognosis in systemic amyloidosis. Its assessment aids patient selection to receive (or not) aggressive chemotherapy, stem cell therapy and newer therapies. Currently, stratification uses blood biomarkers and echocardiography -

but echocardiography has limited sensitivity and specificity particularly in apparently early disease and where confounders are present (such as hypertension). Cardiovascular Magnetic Resonance shows promise with T1 mapping and Late Gadolinium Enhancement (LGE) technique to visualise infiltration.

T1 mapping, now with new, faster and more robust sequences, is a useful diagnostic tool to quantify amyloid infiltration and diagnose cardiac amyloidosis also in patients with kidney failure. With the administration of the contrast, throughout the measurement of ECV and myocyte volume, provide unique insights in the pathophysiology of cardiac amyloidosis: the disease is not only about amyloid infiltration, the myocyte response is essential to understand the differences in natural history and prognosis between the types. Finally LGE with PSIR is a robust widely available technique that can be used both for diagnosis and better risk stratification of patients with cardiac amyloidosis. This could potentially save patient lives not only from the disease itself, but possibly even reduce some of the treatment-related mortality.

However, it is important to balance this with recognition of the current limitations. I have not been able to histologically validate the technique so the technique cannot yet be deemed to be a true non-invasive quantifier of cardiac amyloid burden.

Furthermore, although LGE has emerged as independently predictive of survival in multivariate analysis, it is unclear how much this will impact on and change current clinical management which relies heavily on Troponin T and NT-pro BNP; if one considers LGE as a biomarker, it is more expensive than Troponin T and NT-pro BNP although if one

considers the additional information gained from cardiac MRI as a whole, this may represent a more cost-effective strategy overall – further studies are needed.

There are also standardisation challenges yet to be addressed across different centres with MRI.

FUTURE WORK:

This thesis has looked at the diverse uses of CMR T1 mapping based methodology to assess systemic amyloidosis.

Work is needed to establish histological validation of ECV with cardiac histology. This is challenging not only because of the obvious invasive nature of biopsy, but also because of the need to correlate the timing of biopsy within an acceptable time-frame of the EQ-CMR scan, something which is not easy when patients live so far away. The ideal staining method to differentiate amyloid from fibrosis in a manner which is still quantifiable by computer software remains an ongoing challenge too.

ECV measurements in extracardiac organs also requires standardising. The ideal method of T1 mapping the liver and spleen remains undetermined and where to draw ROIs in the liver requires universal agreeement. Further work is also needed in evaluating the role of ECV and T1 in ATTR amyloidosis – this is already work in progress.

From an MRI perspective, the T1 mapping sequences are constantly improving e.g. the ShMOLLI sequence currently does not correct for any motion artefacts which makes it more likely to result in partial voluming with blood at the edges of a myocardial ROI – such

sequences are work in progress.[204] There has also been very little work comparing the reproducibility T1 and ECV across multiple sites and using MRI equipment from differing vendors.

From a more general perspective, myocardial T1 and ECV assessment is a new field and there is little agreement between groups as to what terminology should be used e.g. extracellular volume (ECV), extracellular volume fraction (ECVF), myocardial volume of distribution ($Vd_{(m)}$) have all been used by different groups to describe the same thing over the last 2-3 years. An initiative from this hospital (Prof. James Moon) has therefore set up a T1 mapping development group which has now met 7 times and published a consensus statement for everyone in the field to use as a baseline guide.

My work has triggered a number of key changes and progressions, specifically:

1. The NAC now routinely transfers patients to the Heart Hospital for CMR scanning and T1 mapping to calculate ECV which was not previously the case.
2. ECV results now play a key role in the weekly MDT meetings when determining the timing and choice of treatment.
3. My work comparing ECV to SAP scanning in AL amyloidosis has laid the groundwork for similar research in comparing ECV with DPD scanning in ATTR amyloidosis. This work has already begun and the preliminary findings were shortlisted at the Young Investigator Awards at the 2014 AHA scientific sessions in Chicago, USA.

4. My work with ECV in the liver and spleen in AL amyloidosis has attracted the attention of the pharmaceutical industry who are now using ECV of the liver and spleen as an endpoint for their first in man study of therapy in systemic AL amyloidosis, following my *presentation of this data at the International Amyloidosis Symposium in 2012.* The first paper by GSK is published in NEJM

5. National commissioning is centrally funding 500 amyloid scans a year for the NAC

6. The National Amyloid Centre is installing a dedicated CMR department with 50% time for amyloid. The magnet is delivered second week in October. The advert for lead of the department is out and I am short-listed for interview in October.

13.7 CONCLUSION:

This thesis has provided further insight into the field of cardiac amyloidosis. CMR with T1 mapping and LGE has unique ability to show and quantify amyloid infiltration. My thesis shows the huge potential of these techniques and lays a path for future work in the field to ultimately benefit and improve patient outcomes from this rare but fatal disease.

14. PUBLICATIONS

14.1 PRIZES

1. **Finalist: Early Career Award** (clinical translational) SCMR 2015, Nice

LGE-PSIR is an independent predictor of mortality in cardiac amyloidosis: a 250 patient prospective study**.** Fontana M, Pica S, Reant P, Abdel-Gadir A, Treibel TA, Banypersad SM, Maestrini V, Bulluck H, Lane TL, Lachmann H, Whelan CJ, Wechalekar AD, Manisty CH, Herrey AS, Kellman P, Hawkins PN, Moon JC.

2. **Winner of a travel scholarship**, Nice 2015

3. **Finalist: Melvin Judkins Young Investigator Award**, AHA 2014 Chicago

Cardiovascular Magnetic Resonance in Cardiac amyloidosis: a 242 patient prospective study. Fontana M, Pica S, Reant P, Abdel-Gadir A, Treibel TA, Banypersad SM, Maestrini V, Lane TL, Lachmann H, Whelan CJ, Wechalekar AD, Manisty CH, Herrey AS, Hawkins PN, Moon JC.

4. **Winner of a UCL scholarship** for the EUREKA course in Translational Medicine

5. **Early Career Award** (clinical translational) at SCMR 2014, New Orleans,

Native T1 mapping in ATTR cardiac amyloidosis – comparison with AL cardiac amyloidosis- a 200 patient study". Fontana M , Banypersad SM, Treibel TA, Maestrini V, Sado D, White SK, Castelletti S, Herrey AS, Hawkins PN, Moon JC.

14.2 PAPERS

1 Sayed RH, Wechalekar AD, Gilbertson JA, Bass P, Mahmood S, Sachchithanantham S, **Fontana M**, Patel K, Whelan CJ, Lachmann HJ, Hawkins PN, Gillmore JD. Natural history and outcome of light chain deposition disease. **Blood**. 2015 Sep 21, pii.

2 **Fontana M**, Pica S, Reant P, Abdel-Gadir A, Treibel TA, Banypersad SM, Maestrini V, Barcella W, Rosmini S, Bulluck H, Sayed RH, Patel K, Mamhood S, Bucciarelli-Ducci C, Whelan CJ, Herrey AS, Lachmann HJ , Wechalekar AD, Manisty CH, Schelbert EB, Kellman P, Gillmore JD, Hawkins PN, Moon JC. Prognostic Value of Late Gadolinium Enhancement Cardiovascular Magnetic Resonance in Cardiac Amyloidosis. **Circulation**. 2015 Sep 11,pii.

3 Bulluck H, White SK, Rosmini S, Bhuva A, Treibel TA, **Fontana M**, Abdel-Gadir A, Herrey A, Manisty C, Wan SM, Groves A, Menezes L, Moon JC, Hausenloy DJ. T1 mapping and T2 mapping at 3T for quantifying the area-at-risk in reperfused STEMI patients. **J Cardiovasc Magn Reson**. 2015 Aug 12;17(1):73.

4 Richards DB, Cookson LM, Berges AC, Barton SV, Lane T, Ritter JM, **Fontana M**, Moon JC, Pinzani M, Gillmore JD, Hawkins PN, Pepys MB. Therapeutic Clearance of Amyloid by Antibodies to Serum Amyloid P Component. **N Engl J Med**. 2015 Jul 15.

5 Treibel TA, Bandula S, **Fontana M**, White SK, Gilbertson JA, Herrey AS, Gillmore JD, Punwani S, Hawkins PN, Taylor SA, Moon JC. Extracellular volume quantification by dynamic equilibrium cardiac computed tomography in cardiac amyloidosis. **J Cardiovasc Comput Tomogr**. 2015 Jul 10.

6 Sayed RH, Rogers D, Khan F, Wechalekar AD, Lachmann HJ**,** **Fontana M**, Mahmood S, Sachchithanantham S, Patel K, Hawkins PN, Whelan CJ, Gillmore JD. A study of implanted cardiac rhythm recorders in advanced cardiac AL amyloidosis. **Eur Heart J**. 2015 May 7;36(18):1098-105.

7 **Fontana M**, Banypersad SM, Treibel TA, Abdel-Gadir A, Maestrini V, Lane T, Gilbertson JA, Hutt DF, Lachmann HJ, Whelan CJ, Wechalekar AD, Herrey AS, Gillmore JD, Hawkins PN, Moon JC. Differential Myocyte Responses in Patients with Cardiac Transthyretin Amyloidosis and Light-Chain Amyloidosis: A Cardiac MR Imaging Study. **Radiology**. 2015 May 21:141744.

8 McColgan P, Viegas S, Gandhi S, Bull K, Tudor R, Sheikh F, Pinney J, **Fontana M**, Rowczenio D, Gillmore JD, Gilbertson JA, Whelan CJ, Shah S, Jaunmuktane Z, Holton

JL, Schott JM, Werring DJ, Hawkins PN, Reilly MM. Oculoleptomeningeal Amyloidosis associated with transthyretin Leu12Pro in an African patient. **J Neurol**. 2015 Jan;262(1):228-34.

9 Flett AS, Maestrini V, Milliken D, **Fontana M**, Treibel TA, Harb R, Sado DM, Quarta G, Herrey A, Sneddon J, Elliott P, McKenna W, Moon JC. Diagnosis of apical hypertrophic cardiomyopathy: T-wave inversion and relative but not absoluteapical left ventricular hypetrophy. **Int J Cardiol**. 2015 Mar 15;183:143-8.

10 **Fontana M**, Chung R, Hawkins PN, Moon JC. Cardiovascular magnetic resonance for amyloidosis. **Heart Fail Rev**. 2015 Mar;20(2):133-44.

11 Pica S, Sado DM, Maestrini V, **Fontana M**, White SK, Treibel T, Captur G, Anderson S, Piechnik SK, Robson MD, Lachmann RH, Murphy E, Mehta A, Hughes D, Kellman P, Elliott PM, Herrey AS, Moon JC. Reproducibility of native myocardial T1 mapping in the assessment of Fabry disease and its role in early detection of cardiac involvement by cardiovascular magnetic resonance. **J Cardiovasc Magn Reson**. 2014 Dec 5;16:99.

12 Bhuva AN, Treibel TA, **Fontana M**, Herrey AS, Manisty CH, Moon JC. T1 mapping: non-invasive evaluation of myocardial tissue composition by cardiovascular magnetic resonance. **Expert Rev Cardiovasc Ther**. 2014 Dec;12(12):1455-64.

13 Banypersad SM, **Fontana M**, Maestrini V, Sado DM, Captur G, Petrie A, Piechnik SK, Whelan CJ, Herrey AS, Gillmore JD, Lachmann HJ, Wechalekar AD, Hawkins PN, Moon JC. T1 mapping and survival in systemic light-chain amyloidosis. **Eur Heart J**. 2015 Jan 21;36(4):244-51.

14 White SK, Frohlich GM, Sado DM, Maestrini V, **Fontana M**, Treibel TA, Tehrani S, Flett AS, Meier P, Ariti C, Davies JR, Moon JC, Yellon DM, Hausenloy DJ. Remote Ischemic Conditioning Reduces Myocardial Infarct Size and Edema in Patients With ST-Segment Elevation Myocardial Infarction. **JACC Cardiovasc Interv**. 2015 Jan;8(1 Pt B):178-88.

15 Maestrini V, Treibel TA, White SK, **Fontana M**, Moon JC. T1 Mapping for Characterization of Intracellular and Extracellular Myocardial Diseases in Heart Failure. **Curr Cardiovasc Imaging Rep**. 2014;7:9287.

16 Sado DM, **Fontana M**, Moon JC. Heart muscle disease and cardiovascular magnetic resonance imaging. **Br J Hosp Med (Lond)**. 2014 Jul;75(7):384-90.

17 White SK, **Fontana M**, Moon JC. Reply: myocardial extracellular volume measurement by cardiac magnetic resonance. **JACC Cardiovasc Imaging**. 2014 Jan;7(1):107-8.

18 **Fontana M**, Banypersad SM, Treibel TA, Maestrini V, Sado DM, White SK, Pica S, Castelletti S, Piechnik SK, Robson MD , Gilbertson JA, Rowczenio D, Hutt DF, Lachmann HJ, Wechalekar AD, Whelan CJ, Gillmore JD, Hawkins PN, Moon JC. Native myocardial T1 mapping in transthyretin amyloidosis. **JACC Cardiovasc Imaging**. 2014 Feb;7(2):157-65.

19 White SK, Sado DM, **Fontana** M, Banypersad SM, Maestrini V, Flett AS, Piechnik SK, Robson MD, Hausenloy DJ, Sheikh AM, Hawkins PN, Moon JC.T1 Mapping for Myocardial Extracellular Volume Measurement by CMR: Bolus Only Versus Primed Infusion Technique. **JACC Cardiovasc Imaging**. 2013 Sept; 6(9):955-62.

20 Sado DM, White SK, Piechnik SK, Banypersad SM, Treibel T, Captur G, **Fontana M**, Maestrini V, Flett AS, Robson MD, Lachmann RH, Murphy E, Mehta A, Hughes D, Neubauer S, Elliott PM, Moon JC. Identification and assessment of anderson-fabry disease by cardiovascular magnetic resonance noncontrast myocardial t1 mapping. **Circ Cardiovasc Imaging**. 2013 May 1;6(3):392-8.

21 Karamitsos TD, Piechnik SK, Banypersad SM, **Fontana M**, Ntusi NB, Ferreira VM, Whelan CJ, Myerson SG, Robson MD, Hawkins PN, Neubauer S, Moon JC. Noncontrast T1 mapping for the diagnosis of cardiac amyloidosis. **JACC Cardiovasc Imaging**. 2013 Apr;6(4):488-97.

22 Banypersad SM, Sado DM, Flett AS, Gibbs SD, Pinney JH, Maestrini V, Cox AT, **Fontana M**, Whelan CJ, Wechalekar AD, Hawkins PN, Moon JC.Quantification of myocardial extracellular volume fraction in systemic Al amyloidosis: an equilibrium contrast cardiovascular magnetic resonance study. **Circ Cardiovasc Imaging**. 2013 Jan 1;6(1):34-9.

23 **Fontana M,** White SK, Banypersad SM, Sado DM, Maestrini V, Flett AS, Piechnik SK, Neubauer S, Roberts N, Moon JC. Comparison of T1 mapping techniques for ECV quantification. Histological validation and reproducibility of ShMOLLI versus multibreath-hold T1 quantification equilibrium contrast CMR. **J Cardiovasc Magn Reson**. 2012 Dec 28;14(1):88.

14.3 ORAL PRESENTATIONS:

1 LGE-PSIR is an independent predictor of mortality in cardiac amyloidosis: a 250 patient prospective study**.** Fontana M, Pica S, Reant P, Abdel-Gadir A, Treibel TA, Banypersad SM, Maestrini V, Bulluck H, Lane TL, Lachmann H, Whelan CJ, Wechalekar AD, Manisty CH, Herrey AS, Kellman P, Hawkins PN, Moon JC. Finalist Early Career Award clinical SCMR 2015, Nice.

2 Cardiovascular Magnetic Resonance in Cardiac amyloidosis: a 242 patient prospective study. Fontana M, Pica S, Reant P, Abdel-Gadir A, Treibel TA, Banypersad SM, Maestrini V, Lane TL, Lachmann H, Whelan CJ, Wechalekar AD, Manisty CH, Herrey AS, Hawkins PN, Moon JC. Finalist, Melvin Judkins Young Investigator Award, AHA 2014 Chicago

3 The additive value of T1 mapping in differentiating the hypertrophic phenotype in cardiomyopathy, invited lecture, plenary session, SCMR 2015, Nice, France

4 A test to measure cardiac amyloid burden in AL and TTR cardiac amyloidosis using Cardiac MRI. Fontana M, Banypersad SM, Treibel T, Sado DM, Castelletti S, Hutt D, Wechalekar AD, Lachmann HJ, Whelan CJ, Gillmore JD, Hawkins PN, Moon JC. Research Retreat. London. May 2013.

6. Trials and Tribulations of T1 mapping: clinical trials and follow-up studies. Heart Hospital early experience. 5th T1 Mapping Development group meeting – invited lecture. EuroCMR. May 2013, Florence.

7. A test to diagnose and measure cardiac amyloid in AL and ATTR amyloidosis using non-contrast cardiac MRI. Fontana M, Banypersad SM, Hutt DF, Lane T, Wechalekar AD, Whelan CJ, Gillmore JD, Hawkins PN, Moon JC. FAP Congress, Rio De Janeiro. November 2013.

8. We need contrast for T1 mapping. 6thT1 Mapping Development group meeting. Debate – invited lecture. SCMR 2014, New Orleans.

9. Native T1 mapping in ATTR cardiac amyloidosis – comparison with AL cardiac amyloidosis- a 200 patient study. Fontana M, Banypersad SM, Treibel TA, Maestrini V, Sado D, White SK, Castelletti S, Herrey AS, Hawkins PN, Moon JC. SCMR, New Orleans, January 2014, Shortlisted and winner, Early Career Award clinical.

15. BIBLIOGRAPHY

1. Westermark P, Benson MD, Buxbaum JN et al. A primer of amyloid nomenclature. Amyloid : the international journal of experimental and clinical investigation : the official journal of the International Society of Amyloidosis 2007;14:179-83.
2. Kisilevsky R. The relation of proteoglycans, serum amyloid P and apo E to amyloidosis current status, 2000. Amyloid : the international journal of experimental and clinical investigation : the official journal of the International Society of Amyloidosis 2000;7:23-5.
3. Jahn TR, Radford SE. Folding versus aggregation: polypeptide conformations on competing pathways. Archives of biochemistry and biophysics 2008;469:100-17.
4. Rapezzi C, Merlini G, Quarta CC et al. Systemic cardiac amyloidoses: disease profiles and clinical courses of the 3 main types. Circulation 2009;120:1203-12.
5. Falk RH. Diagnosis and management of the cardiac amyloidoses. Circulation 2005;112:2047-60.
6. Merlini G, Stone MJ. Dangerous small B-cell clones. Blood 2006;108:2520-2530.
7. Dispenzieri A, Gertz MA, Kyle RA et al. Serum cardiac troponins and N-terminal pro-brain natriuretic peptide: a staging system for primary systemic amyloidosis. Journal of clinical oncology : official journal of the American Society of Clinical Oncology 2004;22:3751-7.
8. Merlini G, Bellotti V. Molecular mechanisms of amyloidosis. The New England journal of medicine 2003;349:583-96.
9. Dubrey SW, Cha K, Skinner M, LaValley M, Falk RH. Familial and primary (AL) cardiac amyloidosis: echocardiographically similar diseases with distinctly different clinical outcomes. Heart 1997;78:74-82.
10. Connors LH, Prokaeva T, Lim A et al. Cardiac amyloidosis in African Americans: comparison of clinical and laboratory features of transthyretin V122I amyloidosis and immunoglobulin light chain amyloidosis. American heart journal 2009;158:607-14.
11. Falk RH. The neglected entity of familial cardiac amyloidosis in African Americans. Ethnicity & disease 2002;12:141-3.
12. Westermark P, Sletten K, Johansson B, Cornwell GG, 3rd. Fibril in senile systemic amyloidosis is derived from normal transthyretin. Proceedings of the National Academy of Sciences of the United States of America 1990;87:2843-5.
13. Ng B, Connors LH, Davidoff R, Skinner M, Falk RH. Senile systemic amyloidosis presenting with heart failure: a comparison with light chain-associated amyloidosis. Archives of internal medicine 2005;165:1425-9.

14. Connors LH, Lim A, Prokaeva T, Roskens VA, Costello CE. Tabulation of human transthyretin (TTR) variants, 2003. Amyloid : the international journal of experimental and clinical investigation : the official journal of the International Society of Amyloidosis 2003;10:160-84.

15. Dubrey SW, Falk RH. Amyloid heart disease. British journal of hospital medicine 2010;71:76-82.

16. Falk RH, Dubrey SW. Amyloid heart disease. Progress in cardiovascular diseases 2010;52:347-61.

17. Cheng ZW, Tian Z, Kang L et al. [Electrocardiographic and echocardiographic features of patients with primary cardiac amyloidosis]. Zhonghua Xin Xue Guan Bing Za Zhi 2010;38:606-609.

18. Murtagh B, Hammill SC, Gertz MA, Kyle RA, Tajik AJ, Grogan M. Electrocardiographic findings in primary systemic amyloidosis and biopsy-proven cardiac involvement. The American journal of cardiology 2005;95:535-7.

19. Dungu J, Sattianayagam PT, Whelan CJ et al. The electrocardiographic features associated with cardiac amyloidosis of variant transthyretin isoleucine 122 type in Afro-Caribbean patients. Am Heart J 2012;164:72-9.

20. Dubrey SW, Cha K, Anderson J et al. The clinical features of immunoglobulin light-chain (AL) amyloidosis with heart involvement. QJM 1998;91:141-57.

21. Takigawa M, Hashimura K, Ishibashi-Ueda H et al. Annual electrocardiograms consistent with silent progression of cardiac involvement in sporadic familial amyloid polyneuropathy: a case report. Intern Med 2010;49:139-44.

22. Pinney J GJ, Lachmann H, Wechalekar A, Gibbs S, Banypersad SM, Dungu J, Rannigan L, Collins E, McCarthy C, Hawkins P, Whelan C. Disturbances of Cardiac Rhythm in AL Amyloidosis. 13th International Myeloma Workshop 2011:426.

23. Kristen AV, Perz JB, Schonland SO et al. Rapid progression of left ventricular wall thickness predicts mortality in cardiac light-chain amyloidosis. J Heart Lung Transplant 2007;26:1313-9.

24. Koyama J, Falk RH. Prognostic significance of strain Doppler imaging in light-chain amyloidosis. JACC Cardiovasc Imaging 2010;3:333-42.

25. Migrino RQ, Mareedu RK, Eastwood D, Bowers M, Harmann L, Hari P. Left ventricular ejection time on echocardiography predicts long-term mortality in light chain amyloidosis. J Am Soc Echocardiogr 2009;22:1396-402.

26. Patel AR, Dubrey SW, Mendes LA et al. Right ventricular dilation in primary amyloidosis: an independent predictor of survival. Am J Cardiol 1997;80:486-92.

27. Porciani MC, Lilli A, Perfetto F et al. Tissue Doppler and strain imaging: a new tool for early detection of cardiac amyloidosis. Amyloid 2009;16:63-70.

28. Tsang W, Lang RM. Echocardiographic evaluation of cardiac amyloid. Current cardiology reports 2010;12:272-6.

29. Bellavia D, Pellikka PA, Abraham TP et al. Evidence of impaired left ventricular systolic function by Doppler myocardial imaging in patients with systemic amyloidosis and no evidence of cardiac involvement by standard two-dimensional and Doppler echocardiography. Am J Cardiol 2008;101:1039-45.

30. Park SJ, Miyazaki C, Bruce CJ, Ommen S, Miller FA, Oh JK. Left ventricular torsion by two-dimensional speckle tracking echocardiography in patients with diastolic dysfunction and normal ejection fraction. J Am Soc Echocardiogr 2008;21:1129-37.

31. Porciani MC, Cappelli F, Perfetto F et al. Rotational mechanics of the left ventricle in AL amyloidosis. Echocardiography 2010;27:1061-8.

32. Kusunose K, Yamada H, Iwase T et al. Images in cardiovascular medicine. Cardiac magnetic resonance imaging and 2-dimensional speckle tracking echocardiography in secondary cardiac amyloidosis. Circ J 2010;74:1494-6.

33. Sun JP, Stewart WJ, Yang XS et al. Differentiation of hypertrophic cardiomyopathy and cardiac amyloidosis from other causes of ventricular wall thickening by two-dimensional strain imaging echocardiography. Am J Cardiol 2009;103:411-5.

34. Quarta CC, Solomon SD, Uraizee I et al. Left ventricular structure and function in transthyretin-related versus light-chain cardiac amyloidosis. Circulation 2014;129:1840-9.

35. Palladini G, Campana C, Klersy C et al. Serum N-terminal pro-brain natriuretic peptide is a sensitive marker of myocardial dysfunction in AL amyloidosis. Circulation 2003;107:2440-5.

36. Wechalekar AD, Gillmore JD, Wassef N, Lachmann HJ, Whelan C, Hawkins PN. Abnormal N-terminal fragment of brain natriuretic peptide in patients with light chain amyloidosis without cardiac involvement at presentation is a risk factor for development of cardiac amyloidosis. Haematologica 2011.

37. Dispenzieri A, Kyle RA, Gertz MA et al. Survival in patients with primary systemic amyloidosis and raised serum cardiac troponins. Lancet 2003;361:1787-9.

38. Kristen AV, Giannitsis E, Lehrke S et al. Assessment of disease severity and outcome in patients with systemic light-chain amyloidosis by the high-sensitivity troponin T assay. Blood 2010;116:2455-61.

39. Palladini G, Barassi A, Klersy C et al. The combination of high-sensitivity cardiac troponin T (hs-cTnT) at presentation and changes in N-terminal natriuretic peptide type B (NT-proBNP) after chemotherapy best predicts survival in AL amyloidosis. Blood 2010;116:3426-30.

40. Dispenzieri A, Gertz MA, Kyle RA et al. Prognostication of survival using cardiac troponins and N-terminal pro-brain natriuretic peptide in patients with primary

systemic amyloidosis undergoing peripheral blood stem cell transplantation. Blood 2004;104:1881-7.

41. Palladini G, Russo P, Nuvolone M et al. Treatment with oral melphalan plus dexamethasone produces long-term remissions in AL amyloidosis. Blood 2007;110:787-8.

42. Palladini G, Dispenzieri A, Gertz MA et al. New criteria for response to treatment in immunoglobulin light chain amyloidosis based on free light chain measurement and cardiac biomarkers: impact on survival outcomes. Journal of clinical oncology : official journal of the American Society of Clinical Oncology 2012;30:4541-9.

43. Tapan U, Seldin DC, Finn KT et al. Increases in B-type natriuretic peptide (BNP) during treatment with lenalidomide in AL amyloidosis. Blood 2010;116:5071-2.

44. Dispenzieri A, Dingli D, Kumar SK et al. Discordance between serum cardiac biomarker and immunoglobulin-free light-chain response in patients with immunoglobulin light-chain amyloidosis treated with immune modulatory drugs. Am J Hematol 2010;85:757-9.

45. Hawkins PN, Lavender JP, Pepys MB. Evaluation of systemic amyloidosis by scintigraphy with 123I-labeled serum amyloid P component. The New England journal of medicine 1990;323:508-13.

46. Minutoli F GM, Di Bella G, Crisafulli C, Murè G, Militano V, Brancati M, Di Leo R, Mazzeo A, Baldari S. Cardiac involvement in transthyretin familial amyloid polyneuropathy - comparison between 99mTc-DPD SPECT and magnetic resonance imaging. European Association of Nuclear Medicine 2010:252.

47. Perugini E, Guidalotti PL, Salvi F et al. Noninvasive etiologic diagnosis of cardiac amyloidosis using 99mTc-3,3-diphosphono-1,2-propanodicarboxylic acid scintigraphy. Journal of the American College of Cardiology 2005;46:1076-84.

48. Antoni G, Lubberink M, Estrada S et al. In vivo visualization of amyloid deposits in the heart with 11C-PIB and PET. J Nucl Med 2013;54:213-20.

49. Pozo E, Kanwar A, Deochand R et al. Cardiac magnetic resonance evaluation of left ventricular remodelling distribution in cardiac amyloidosis. Heart 2014;epub 2014 Jul 10.

50. Bogaert J, Taylor AM. Non-ischemic myocardial disease. In: Bogaert J DS, Taylor AM, editor Clinical Cardiac MRI. New York: Springer Verlag, 2005:234-7.

51. White SK, Sado D, Fontana M et al. T1 mapping for myocardial extracellular volume measurement by CMR: bolus only versus primed infusion technique. JACC Cardiovasc Imaging 2013;6:955-62.

52. Maceira AM, Joshi J, Prasad SK et al. Cardiovascular magnetic resonance in cardiac amyloidosis. Circulation 2005;111:186-93.

53. Syed IS, Glockner JF, Feng D et al. Role of cardiac magnetic resonance imaging in the detection of cardiac amyloidosis. JACC Cardiovasc Imaging 2010;3:155-64.

54. Austin BA, Tang WH, Rodriguez ER et al. Delayed hyper-enhancement magnetic resonance imaging provides incremental diagnostic and prognostic utility in suspected cardiac amyloidosis. JACC Cardiovasc Imaging 2009;2:1369-77.

55. Ruberg FL, Appelbaum E, Davidoff R et al. Diagnostic and prognostic utility of cardiovascular magnetic resonance imaging in light-chain cardiac amyloidosis. Am J Cardiol 2009;103:544-9.

56. Vogelsberg H, Mahrholdt H, Deluigi CC et al. Cardiovascular magnetic resonance in clinically suspected cardiac amyloidosis: noninvasive imaging compared to endomyocardial biopsy. J Am Coll Cardiol 2008;51:1022-30.

57. Aquaro GD, Pugliese NR, Perfetto F et al. Myocardial signal intensity decay after gadolinium injection: a fast and effective method for the diagnosis of cardiac amyloidosis. The international journal of cardiovascular imaging 2014;30:1105-15.

58. Dungu JN, Valencia O, Pinney JH et al. CMR-based differentiation of AL and ATTR cardiac amyloidosis. JACC Cardiovasc Imaging 2014;7:133-42.

59. Perugini E, Guidalotti PL, Salvi F et al. Non-invasive Etiologic diagnosis of cardiac amyloidosis using 99mTC-3,3-Diphophono-1,2-Propanodicarboxylic acid scintography. J Am Coll Cardiol 2005;46:1076-84.

60. Kellman P, Arai AE, McVeigh ER, Aletras AH. Phase-sensitive inversion recovery for detecting myocardial infarction using gadolinium-delayed hyperenhancement. Magn Reson Med 2002;47:372-83.

61. Kellman P, Hansen M. T1-mapping in the heart: accuracy and precision. J Cardiovasc Magn Reson 2014;16:2-20.

62. Sado DM, Maestrini V, Piechnik SK et al. Noncontrast myocardial T(1) mapping using cardiovascular magnetic resonance for iron overload. J Magn Reson Imaging 2014;epub 2014 Aug 8.

63. Sado DM, White SK, Piechnik SK et al. Identification and assessment of Anderson-Fabry disease by cardiovascular magnetic resonance noncontrast myocardial T1 mapping. Circ Cardiovasc Imaging 2013;6:392-8.

64. Thompson RB, Chow K, Khan A et al. T_1 mapping with cardiovascular MRI is highly sensitive for Fabry disease independent of hypertrophy and sex. Circ Cardiovasc Imaging 2013;6:637-45.

65. Banypersad SM, Sado DN, Flett AS et al. Quantification of myocardial extracellular volume fraction in systemic AL amyloidosis: an equilibrium contrast cardiovascular magnetic resonance study. Circ Cardiovasc Imaging 2013;6:34-9.

66. Karamitsos TD, Piechnik SK, Banypersad SM et al. Noncontrast T1 mapping for the diagnosis of cardiac amyloidosis. JACC Cardiovasc Imaging 2013;6:488-97.

67. Moon JC, Messroghli DR, Kellman P et al. Society for Cardiovascular Magnetic Resonance Imaging; Cardiovascular Magnetic Resonance Working Group of the

European Society of Cardiology. Myocardial T1 mapping and extracellular volume quantification: a Society for Cardiovascular Magnetic Resonance (SCMR) and CMR Working Group of the European Society of Cardiology consensus statement. J Cardiovasc Magn Reson 2013;15:92.

68. Lee JJ, Liu S, Nacif MS et al. Myocardial T1 and extracellular volume fraction mapping at 3 tesla. J Cardiovasc Magn Reson 2011;13:75-85.

69. Roujol S, Weingärtner S, Foppa M et al. Accuracy, Precision, and Reproducibility of Four T1 Mapping Sequences: A Head-to-Head Comparison of MOLLI, ShMOLLI, SASHA, and SAPPHIRE. Radiology 2014;4:140296.

70. Mongeon FP, Jerosch-Herold M, Coelho-Filho OR, Blankstein R, Falk RH, Kwong RY. Quantification of extracellular matrix expansion by CMR in infiltrative heart disease. JACC Cardiovascular imaging 2012;5:897-907.

71. Quarta CC, Guldalotti PL, Longhi S et al. Defining the diagnosis in echocardiographically suspected senile systemic amyloidosis. J Am Coll Cardiol Imaging 2012;5:755-8.

72. Koyama J, Falk RH. Prognostic significance of strain Doppler imaging in light-chain amyloidosis. JACC Cardiovasc Imaging 2010;3:333-42.

73. Palka P, Lange A, Fleming AD et al. Differences in myocardial velocity gradient measured throughout the cardiac cycle in patients with hypertrophic cardiomyopathy, athletes and patients with left ventricular hypertrophy due to hypertension. J Am Coll Cardiol 1997;30:760-8.

74. Biagini E, Spirito P, Rocchi G et al. Prognostic implications of the Doppler restrictive filling pattern in hypertrophic cardiomyopathy. Am J Cardiol 2009;104:1727-31.

75. Kwong RY, Falk RH. Cardioavascular magnetic resonance in cardiac amyloidosis. Circulation 2005;111:122-4.

76. White JA, Kim HW, Shah D et al. CMR imaging with rapid visual T1 assessment predicts mortality in patients suspected of cardiac amyloidosis. JACC Cardiovasc Imaging 2014;7:143-56.

77. Banypersad SM, Fontana M, Maestrini V et al. T1 mapping and survival in systemic light-chain amyloidosis. European heart journal 2015;36:244-51.

78. Alnylam. Phase 2 Study to Evaluate ALN-TTRSC in Patients With Transthyretin (TTR) Cardiac Amyloidosis. 2013.

79. GlaxoSmithKline. A Study to Evaluate the Safety of GSK2398852 When Co-administered With GSK2315698 in Patients With Systemic Amyloidosis. 2013.

80. Rubinow A, Skinner M, Cohen AS. Digoxin sensitivity in amyloid cardiomyopathy. Circulation 1981;63:1285-8.

81. Gertz MA, Skinner M, Connors LH, Falk RH, Cohen AS, Kyle RA. Selective binding of nifedipine to amyloid fibrils. Am J Cardiol 1985;55:1646.

82. Pollak A, Falk RH. Left ventricular systolic dysfunction precipitated by verapamil in cardiac amyloidosis. Chest 1993;104:618-20.

83. Kristen AV, Dengler TJ, Hegenbart U et al. Prophylactic implantation of cardioverter-defibrillator in patients with severe cardiac amyloidosis and high risk for sudden cardiac death. Heart Rhythm 2008;5:235-40.

84. Sayed RH, Rogers D, Khan F et al. A study of implanted cardiac rhythm recorders in advanced cardiac AL amyloidosis. European heart journal 2015;36:1098-105.

85. Seethala S, Jain S, Ohori NP et al. Focal monomorphic ventricular tachycardia as the first manifestation of amyloid cardiomyopathy. Indian Pacing Electrophysiol J 2010;10:143-147.

86. Dhoble A, Khasnis A, Olomu A, Thakur R. Cardiac amyloidosis treated with an implantable cardioverter defibrillator and subcutaneous array lead system: report of a case and literature review. Clin Cardiol 2009;32:E63-5.

87. Bellavia D, Pellikka PA, Abraham TP et al. 'Hypersynchronisation' by tissue velocity imaging in patients with cardiac amyloidosis. Heart 2009;95:234-240.

88. Sattianayagam PT, Gibbs SD, Pinney JH et al. Solid organ transplantation in AL amyloidosis. American journal of transplantation : official journal of the American Society of Transplantation and the American Society of Transplant Surgeons 2010;10:2124-31.

89. Gillmore JD, Goodman HJ, Lachmann HJ et al. Sequential heart and autologous stem cell transplantation for systemic AL amyloidosis. Blood 2006;107:1227-9.

90. Mignot A, Varnous S, Redonnet M et al. Heart transplantation in systemic (AL) amyloidosis: a retrospective study of eight French patients. Arch Cardiovasc Dis 2008;101:523-32.

91. Sack FU, Kristen A, Goldschmidt H et al. Treatment options for severe cardiac amyloidosis: heart transplantation combined with chemotherapy and stem cell transplantation for patients with AL-amyloidosis and heart and liver transplantation for patients with ATTR-amyloidosis. Eur J Cardiothorac Surg 2008;33:257-62.

92. Dey BR, Chung SS, Spitzer TR et al. Cardiac transplantation followed by dose-intensive melphalan and autologous stem-cell transplantation for light chain amyloidosis and heart failure. Transplantation 2010;90:905-11.

93. Barreiros AP, Post F, Hoppe-Lotichius M et al. Liver transplantation and combined liver-heart transplantation in patients with familial amyloid polyneuropathy: a single-center experience. Liver Transpl 2010;16:314-23.

94. Hamour IM, Lachmann HJ, Goodman HJ et al. Heart transplantation for homozygous familial transthyretin (TTR) V122I cardiac amyloidosis. Am J Transplant 2008;8:1056-9.

95. Gertz MA, Lacy MQ, Dispenzieri A et al. Effect of hematologic response on outcome of patients undergoing transplantation for primary amyloidosis: importance of achieving a complete response. Haematologica 2007;92:1415-8.

96. Wechalekar AD, Gillmore JD, Wassef N, Lachmann HJ, Whelan C, Hawkins PN. Abnormal N-terminal fragment of brain natriuretic peptide in patients with light chain amyloidosis without cardiac involvement at presentation is a risk factor for development of cardiac amyloidosis. Haematologica 2011;96:1079-80.

97. Merlini G, Seldin DC, Gertz MA. Amyloidosis: pathogenesis and new therapeutic options. Journal of clinical oncology : official journal of the American Society of Clinical Oncology 2011;29:1924-33.

98. Skinner M, Sanchorawala V, Seldin DC et al. High-dose melphalan and autologous stem-cell transplantation in patients with AL amyloidosis: an 8-year study. Annals of internal medicine 2004;140:85-93.

99. Cibeira MT, Sanchorawala V, Seldin DC et al. Outcome of AL amyloidosis after high-dose melphalan and autologous stem cell transplantation: long-term results in a series of 421 patients. Blood 2011;118:4346-52.

100. Gertz MA, Lacy MQ, Dispenzieri A et al. Refinement in patient selection to reduce treatment-related mortality from autologous stem cell transplantation in amyloidosis. Bone marrow transplantation 2013;48:557-61.

101. Ihse E, Suhr OB, Hellman U, Westermark P. Variation in amount of wild-type transthyretin in different fibril and tissue types in ATTR amyloidosis. J Mol Med 2011;89:171-80.

102. Tomas MT, Santa-Clara H, Bruno PM et al. The impact of exercise training on liver transplanted familial amyloidotic polyneuropathy (FAP) patients. Transplantation 2013;95:372-7.

103. Benson MD, Kluve-Beckerman B, Zeldenrust SR et al. Targeted suppression of an amyloidogenic transthyretin with antisense oligonucleotides. Muscle Nerve 2006;33:609-18.

104. Phipps JE, Kestler DP, Foster JS et al. Inhibition of pathologic immunoglobulin-free light chain production by small interfering RNA molecules. Experimental hematology 2010;38:1006-13.

105. Coelho T, Adams D, Silva A et al. Safety and efficacy of RNAi therapy for transthyretin amyloidosis. The New England journal of medicine 2013;369:819-29.

106. Sekijima Y, Dendle MA, Kelly JW. Orally administered diflunisal stabilizes transthyretin against dissociation required for amyloidogenesis. Amyloid 2006;13:236-49.

107. Tojo K, Sekijima Y, Kelly JW, Ikeda S. Diflunisal stabilizes familial amyloid polyneuropathy-associated transthyretin variant tetramers in serum against dissociation required for amyloidogenesis. Neurosci Res 2006;56:441-9.

108. Berk JL, Suhr OB, Obici L et al. Repurposing diflunisal for familial amyloid polyneuropathy: a randomized clinical trial. JAMA : the journal of the American Medical Association 2013;310:2658-67.

109. Maurer MS, Grogan DR, Judge DP et al. Tafamidis in transthyretin amyloid cardiomyopathy: effects on transthyretin stabilization and clinical outcomes. Circulation Heart failure 2015;8:519-26.

110. Kolstoe SE, Mangione PP, Bellotti V et al. Trapping of palindromic ligands within native transthyretin prevents amyloid formation. Proc Natl Acad Sci U S A 2010;107:20483-8.

111. Bodin K, Ellmerich S, Kahan MC et al. Antibodies to human serum amyloid P component eliminate visceral amyloid deposits. Nature 2010;468:93-7.

112. Richards DB, Cookson LM, Berges AC et al. Therapeutic Clearance of Amyloid by Antibodies to Serum Amyloid P Component. The New England journal of medicine 2015;373:1106-14.

113. Gertz MA, Comenzo R, Falk RH et al. Definition of organ involvement and treatment response in immunoglobulin light chain amyloidosis (AL): a consensus opinion from the 10th International Symposium on Amyloid and Amyloidosis, Tours, France, 18-22 April 2004. American journal of hematology 2005;79:319-28.

114. Moon JC, Messroghli DR, Kellman P et al. Myocardial T1 mapping and extracellular volume quantification: a Society for Cardiovascular Magnetic Resonance (SCMR) and CMR Working Group of the European Society of Cardiology consensus statement. Journal of cardiovascular magnetic resonance : official journal of the Society for Cardiovascular Magnetic Resonance 2013;15:92.

115. ATS statement: guidelines for the six-minute walk test. Am J Respir Crit Care Med 2002;166:111-7.

116. Borg GA. Psychophysical bases of perceived exertion. Med Sci Sports Exerc 1982;14:377-81.

117. Nagueh SF, Appleton CP, Gillebert TC et al. Recommendations for the evaluation of left ventricular diastolic function by echocardiography. J Am Soc Echocardiogr 2009;22:107-33.

118. Hundley WG, Bluemke D, Bogaert JG et al. Society for Cardiovascular Magnetic Resonance guidelines for reporting cardiovascular magnetic resonance examinations. J Cardiovasc Magn Reson 2009;11:5.

119. Arheden H, Saeed M, Higgins CB et al. Measurement of the distribution volume of gadopentetate dimeglumine at echo-planar MR imaging to quantify myocardial infarction: comparison with 99mTc-DTPA autoradiography in rats. Radiology 1999;211:698-708.

120. Schelbert EB, Testa SM, Meier CG et al. Myocardial extravascular extracellular volume fraction measurement by gadolinium cardiovascular magnetic resonance in

humans: slow infusion versus bolus. Journal of cardiovascular magnetic resonance : official journal of the Society for Cardiovascular Magnetic Resonance 2011;13:16.

121. Flett AS, Hayward MP, Ashworth MT et al. Equilibrium contrast cardiovascular magnetic resonance for the measurement of diffuse myocardial fibrosis: preliminary validation in humans. Circulation 2010;122:138-44.

122. White SK, Sado DM, Flett AS, Moon JC. Characterising the myocardial interstitial space: the clinical relevance of non-invasive imaging. Heart 2012;98:773-9.

123. Messroghli DR, Radjenovic A, Kozerke S, Higgins DM, Sivananthan MU, Ridgway JP. Modified Look-Locker inversion recovery (MOLLI) for high-resolution T1 mapping of the heart. Magnetic resonance in medicine : official journal of the Society of Magnetic Resonance in Medicine / Society of Magnetic Resonance in Medicine 2004;52:141-6.

124. Piechnik SK, Ferreira VM, Dall'Armellina E et al. Shortened Modified Look-Locker Inversion recovery (ShMOLLI) for clinical myocardial T1-mapping at 1.5 and 3 T within a 9 heartbeat breathhold. Journal of cardiovascular magnetic resonance : official journal of the Society for Cardiovascular Magnetic Resonance 2010;12:69.

125. Siebers A, Oberg U, Skargren E. The effect of modified constraint-induced movement therapy on spasticity and motor function of the affected arm in patients with chronic stroke. Physiotherapy Canada Physiotherapie Canada 2010;62:388-96.

126. Messroghli DR, Rudolph A, Abdel-Aty H et al. An open-source software tool for the generation of relaxation time maps in magnetic resonance imaging. BMC medical imaging 2010;10:16.

127. Lee JJ, Liu S, Nacif MS et al. Myocardial T1 and extracellular volume fraction mapping at 3 tesla. Journal of cardiovascular magnetic resonance : official journal of the Society for Cardiovascular Magnetic Resonance 2011;13:75.

128. Xue H, Shah S, Greiser A et al. Motion correction for myocardial T1 mapping using image registration with synthetic image estimation. Magnetic resonance in medicine : official journal of the Society of Magnetic Resonance in Medicine / Society of Magnetic Resonance in Medicine 2012;67:1644-55.

129. Kawel N, Nacif M, Zavodni A et al. T1 mapping of the myocardium: intra-individual assessment of the effect of field strength, cardiac cycle and variation by myocardial region. Journal of cardiovascular magnetic resonance : official journal of the Society for Cardiovascular Magnetic Resonance 2012;14:27.

130. Kawel N, Nacif M, Zavodni A et al. T1 mapping of the myocardium: intra-individual assessment of post-contrast T1 time evolution and extracellular volume fraction at 3T for Gd-DTPA and Gd-BOPTA. Journal of cardiovascular magnetic resonance : official journal of the Society for Cardiovascular Magnetic Resonance 2012;14:26.

131. Cornwell GG, 3rd, Murdoch WL, Kyle RA, Westermark P, Pitkanen P. Frequency and distribution of senile cardiovascular amyloid. A clinicopathologic correlation. Am J Med 1983;75:618-623.

132. Yamashita T, Asl KH, Yazaki M, Benson MD. A prospective evaluation of the transthyretin Ile122 allele frequency in an African-American population. Amyloid : the international journal of experimental and clinical investigation : the official journal of the International Society of Amyloidosis 2005;12:127-130.

133. Buxbaum J, Jacobson DR, Tagoe C et al. Transthyretin V122I in African Americans with congestive heart failure. Journal of the American College of Cardiology 2006;47:1724-5.

134. Jacobson DR, Pastore RD, Yaghoubian R et al. Variant-sequence transthyretin (isoleucine 122) in late-onset cardiac amyloidosis in black Americans. The New England journal of medicine 1997;336:466-73.

135. Pinney JH, Whelan CJ, Petrie A et al. Senile systemic amyloidosis: clinical features at presentation and outcome. Journal of the American Heart Association 2013;2:e000098.

136. Pinney JH, Smith CJ, Taube JB et al. Systemic amyloidosis in England: an epidemiological study. British journal of haematology 2013;161:525-32.

137. Ruberg FL, Berk JL. Transthyretin (TTR) Cardiac Amyloidosis. Circulation 2012;126:1286-1300.

138. Maceira AM, Joshi J, Prasad SK et al. Cardiovascular magnetic resonance in cardiac amyloidosis. Circulation 2005;111:186-93.

139. Di Bella G, Minutoli F, Mazzeo A et al. MRI of cardiac involvement in transthyretin familial amyloid polyneuropathy. AJR American journal of roentgenology 2010;195:W394-9.

140. Karamitsos TD, Piechnik SK, Banypersad SM et al. Noncontrast T1 mapping for the diagnosis of cardiac amyloidosis. JACC Cardiovascular imaging 2013;6:488-97.

141. Elliott P, Andersson B, Arbustini E et al. Classification of the cardiomyopathies: a position statement from the European Society Of Cardiology Working Group on Myocardial and Pericardial Diseases. Eur Heart J 2008;29:270-6.

142. Kramer CM, Barkhausen J, Flamm SD, Kim RJ, Nagel E, Society for Cardiovascular Magnetic Resonance Board of Trustees Task Force on Standardized P. Standardized cardiovascular magnetic resonance imaging (CMR) protocols, society for cardiovascular magnetic resonance: board of trustees task force on standardized protocols. Journal of cardiovascular magnetic resonance : official journal of the Society for Cardiovascular Magnetic Resonance 2008;10:35.

143. Ruberg FL. T1 mapping in cardiac amyloidosis: can we get there from here? JACC Cardiovascular imaging 2013;6:498-500.

144. Banypersad SM, Sado DM, Flett AS et al. Quantification of myocardial extracellular volume fraction in systemic AL amyloidosis: an equilibrium contrast cardiovascular magnetic resonance study. Circulation Cardiovascular imaging 2013;6:34-9.

145. Shi J, Guan J, Jiang B et al. Amyloidogenic light chains induce cardiomyocyte contractile dysfunction and apoptosis via a non-canonical p38alpha MAPK pathway. Proceedings of the National Academy of Sciences of the United States of America 2010;107:4188-93.

146. Rapezzi C, Quarta CC, Guidalotti PL et al. Role of (99m)Tc-DPD scintigraphy in diagnosis and prognosis of hereditary transthyretin-related cardiac amyloidosis. JACC Cardiovascular imaging 2011;4:659-70.

147. Liu CY, Liu YC, Wu C et al. Evaluation of Age-Related Interstitial Myocardial Fibrosis With Cardiac Magnetic Resonance Contrast-Enhanced T1 Mapping: MESA (Multi-Ethnic Study of Atherosclerosis). Journal of the American College of Cardiology 2013;62:1280-7.

148. Piechnik SK, Ferreira VM, Lewandowski AJ et al. Normal variation of magnetic resonance T1 relaxation times in the human population at 1.5 T using ShMOLLI. Journal of cardiovascular magnetic resonance : official journal of the Society for Cardiovascular Magnetic Resonance 2013;15:13.

149. Syed IS, Glockner JF, Feng D et al. Role of cardiac magnetic resonance imaging in the detection of cardiac amyloidosis. JACC Cardiovascular imaging 2010;3:155-64.

150. Perugini E, Rapezzi C, Piva T et al. Non-invasive evaluation of the myocardial substrate of cardiac amyloidosis by gadolinium cardiac magnetic resonance. Heart 2006;92:343-9.

151. Dungu JN VO, Pinney JH, Gibbs SDJ, Rowczenio D, Gilbertson JA, Lachmann HJ, Wechalekar A, Gillmore JD, Whelan CJ, Hawkins PN, Anderson LJ. Cardiac magnetic resonance (CMR) for the differentiation of AL and ATTR cardiac amyloidosis. JACC Cardiovascular imaging 2014;In press.

152. Suhr OB, Anan I, Backman C et al. Do troponin and B-natriuretic peptide detect cardiomyopathy in transthyretin amyloidosis? Journal of internal medicine 2008;263:294-301.

153. Brenner DA, Jain M, Pimentel DR et al. Human amyloidogenic light chains directly impair cardiomyocyte function through an increase in cellular oxidant stress. Circulation research 2004;94:1008-10.

154. Banypersad SM, Moon JC, Whelan C, Hawkins PN, Wechalekar AD. Updates in cardiac amyloidosis: a review. Journal of the American Heart Association 2012;1:e000364.

155. Bull S, White SK, Piechnik SK et al. Human non-contrast T1 values and correlation with histology in diffuse fibrosis. Heart 2013;99:932-7.

156. Ferreira VM, Piechnik SK, Dall'Armellina E et al. T(1) mapping for the diagnosis of acute myocarditis using CMR: comparison to T2-weighted and late gadolinium enhanced imaging. JACC Cardiovascular imaging 2013;6:1048-58.

157. Fontana M, White SK, Banypersad SM et al. Comparison of T1 mapping techniques for ECV quantification. Histological validation and reproducibility of ShMOLLI versus multibreath-hold T1 quantification equilibrium contrast CMR. Journal of cardiovascular magnetic resonance : official journal of the Society for Cardiovascular Magnetic Resonance 2012;14:88.

158. Ferreira VM, Piechnik SK, Dall'Armellina E et al. Non-contrast T1-mapping detects acute myocardial edema with high diagnostic accuracy: a comparison to T2-weighted cardiovascular magnetic resonance. Journal of cardiovascular magnetic resonance : official journal of the Society for Cardiovascular Magnetic Resonance 2012;14:42.

159. Lachmann HJ, Gallimore R, Gillmore JD et al. Outcome in systemic AL amyloidosis in relation to changes in concentration of circulating free immunoglobulin light chains following chemotherapy. British journal of haematology 2003;122:78-84.

160. Falk RH, Comenzo RL, Skinner M. The systemic amyloidoses. The New England journal of medicine 1997;337:898-909.

161. Wechalekar AD, Schonland SO, Kastritis E et al. A European collaborative study of treatment outcomes in 346 patients with cardiac stage III AL amyloidosis. Blood 2013;121:3420-7.

162. Sayed RH, Rogers D, Khan F et al. A study of implanted cardiac rhythm recorders in advanced cardiac AL amyloidosis. European heart journal 2014.

163. Kwong RY, Jerosch-Herold M. CMR and amyloid cardiomyopathy: are we getting closer to the biology? JACC Cardiovascular imaging 2014;7:166-8.

164. Kwong RY, Falk RH. Cardiovascular magnetic resonance in cardiac amyloidosis. Circulation 2005;111:122-4.

165. Dungu JN, Valencia O, Pinney JH et al. CMR-based differentiation of AL and ATTR cardiac amyloidosis. JACC Cardiovascular imaging 2014;7:133-42.

166. Vogelsberg H, Mahrholdt H, Deluigi CC et al. Cardiovascular magnetic resonance in clinically suspected cardiac amyloidosis: noninvasive imaging compared to endomyocardial biopsy. Journal of the American College of Cardiology 2008;51:1022-30.

167. Maceira AM, Prasad SK, Hawkins PN, Roughton M, Pennell DJ. Cardiovascular magnetic resonance and prognosis in cardiac amyloidosis. Journal of cardiovascular magnetic resonance : official journal of the Society for Cardiovascular Magnetic Resonance 2008;10:54.

168. Austin BA, Tang WH, Rodriguez ER et al. Delayed hyper-enhancement magnetic resonance imaging provides incremental diagnostic and prognostic utility in suspected cardiac amyloidosis. JACC Cardiovascular imaging 2009;2:1369-77.

169. Ruberg FL, Appelbaum E, Davidoff R et al. Diagnostic and prognostic utility of cardiovascular magnetic resonance imaging in light-chain cardiac amyloidosis. The American journal of cardiology 2009;103:544-9.

170. Mekinian A, Lions C, Leleu X et al. Prognosis assessment of cardiac involvement in systemic AL amyloidosis by magnetic resonance imaging. The American journal of medicine 2010;123:864-8.

171. White JA, Kim HW, Shah D et al. CMR imaging with rapid visual T1 assessment predicts mortality in patients suspected of cardiac amyloidosis. JACC Cardiovascular imaging 2014;7:143-56.

172. Kellman P, Arai AE, McVeigh ER, Aletras AH. Phase-sensitive inversion recovery for detecting myocardial infarction using gadolinium-delayed hyperenhancement. Magnetic resonance in medicine : official journal of the Society of Magnetic Resonance in Medicine / Society of Magnetic Resonance in Medicine 2002;47:372-83.

173. Kellman P, Arai AE. Cardiac imaging techniques for physicians: late enhancement. Journal of magnetic resonance imaging : JMRI 2012;36:529-42.

174. Barison A, Aquaro GD, Pugliese NR et al. Measurement of myocardial amyloid deposition in systemic amyloidosis: insights from cardiovascular magnetic resonance imaging. Journal of internal medicine 2014.

175. Fontana M, Banypersad SM, Treibel TA et al. Differential Myocyte Responses in Patients with Cardiac Transthyretin Amyloidosis and Light-Chain Amyloidosis: A Cardiac MR Imaging Study. Radiology 2015:141744.